Dissertation der Fakultät für Biologie

der Ludwig-Maximilian-Universität München

# The role of the herpesviral proteins LMP2A, K1, and K15 during oncogenic transformation of primary B cells


Lisa Steinbrück

Die Dissertation wurde am 24.11.2011 zur Beurteilung eingereicht.

| | |
|---|---|
| Erstgutachter: | Prof. Dr. Dirk Eick |
| Zweitgutachter: | Prof. Dr. Michael Boshart |
| Weitere Gutachter: | Prof. Dr. Heinrich Leonhardt |
| | Prof. Dr. Bettina Kempkes |
| | Dr. Josef Mautner |
| | Prof. Dr. Thomas Cremer |

Tag der mündlichen Prüfung: 22.02.2012

# Erklärung

Hiermit erkläre ich, dass die vorliegende Arbeit mit dem Titel

„The role of the herpesviral proteins LMP2A, K1, and K15 during oncogenic transformation of primary B cells“

von mir selbstständig und ohne unerlaubte Hilfsmittel angefertigt wurde, und ich mich dabei nur der ausdrücklich bezeichneten Quellen und Hilfsmittel bedient habe. Die Arbeit wurde weder in der jetzigen noch in einer abgewandelten Form einer anderen Prüfungskommission vorgelegt.

München, 24. November 2011

Lisa Steinbrück

# Content

**1 Introduction ..... 5**
**1.1 The Immune system ..... 5**
1.1.1 The innate immune system ..... 5
1.1.2 The adaptive immune system ..... 6
**1.2 B cells and their B cell receptor (BCR) ..... 7**
1.2.1 The BCR ..... 7
1.2.2 B cell development ..... 8
1.2.3 The BCR complex ..... 12
1.2.4 BCR signaling ..... 13
1.2.4.1 The PI3K/Akt signaling pathway ..... 13
1.2.4.2 The PLCγ2 pathway induces calcium signaling ..... 14
1.2.4.3 Tonic BCR signaling ..... 16
1.2.5 Studying BCR's function – the quasi-monoclonal mouse ..... 17
**1.3 The Epstein-Barr virus (EBV) ..... 19**
1.3.1 General facts ..... 19
1.3.2 Infection of B cells by EBV – the latency programs ..... 20
1.3.3 EBV-associated lymphoma ..... 22
1.3.4 The latent membrane protein 2A (LMP2A) ..... 24
1.3.4.1 Composition of the LMP2A gene locus ..... 24
1.3.4.2 LMP2A signaling ..... 25
1.3.4.3 Studying LMP2A's function – the LMP2A:mCD69 construct ..... 25
**1.4 The Kaposi's sarcoma-associated herpes virus (KSHV) ..... 26**
1.4.1 General facts ..... 26
1.4.2 KSHV genes expressed during the latent phase ..... 26
1.4.3 K1 ..... 28
1.4.4 K15 ..... 29
**2 Objectives ..... 31**
**3 Materials ..... 33**
**3.1 Plasmids and bacteria strain ..... 33**
3.1.1 Maxi-EBV plasmids ..... 33
3.1.2 High-copy plasmids ..... 34
**3.2 Bacteria media and selection plates ..... 34**

**3.3 Primary eukaryotic cells ..... 35**
**3.4 Eukaryotic cell lines ..... 35**
**3.5 Cell culture media for eukaryotic cells ..... 37**
**3.6 Antibodies ..... 37**
3.6.1 Antibodies and staining reagents for flow cytometry ..... 37
3.6.2 Antibodies for cell sorting ..... 37
3.6.3 Antibodies and NP-antigen for cell stimulation ..... 38
3.6.4 Phosphospecific antibodies ..... 38
3.6.5 Antibodies for Western Blot analysis ..... 38
**3.7 Kits ..... 38**
**3.8 Stock solutions and buffers ..... 39**
3.8.1 Plasmid DNA preparation from bacteria ..... 39
3.8.2 Agarose gel electrophoresis ..... 39
3.8.3 Flow cytometry ..... 39
3.8.4 Cell lysis ..... 40
3.8.5 SDS-polyacrylamide gel electrophoresis (PAGE) ..... 40
3.8.6 Western Blot analysis ..... 40
**3.9 Primer-pairs for quantitative real-time PCR (qRT-PCR) ..... 41**
**3.10 Enzymes and Chemicals ..... 41**
**3.11 Consumables and Devices ..... 41**
**3.12 Software ..... 42**
**4 Methods ..... 43**
**4.1 Cloning with the Maxi-EBV system ..... 43**
4.1.1 Preparation of the *galK* cassette ..... 45
4.1.2 Production of heat-shocked sw105 electro-competent bacteria ..... 46
4.1.3 Electroporation of the *galK* cassette into electro-competent sw105 bacteria and subsequent positive selection ..... 46
4.1.4 Electroporation of the DNA cassette into electro-competent sw105 bacteria for reversion of *galK* followed by selection on DOG plates ..... 47
4.1.5 Verification of the new maxi-EBV by restriction enzyme digestion and agarose gel electrophoresis ..... 47
4.1.6 Storage and cultivation of bacteria for DNA preparation ..... 48
4.1.7 Preparation of maxi-EBV DNA using CsCl-gradient centrifugation ..... 48
**4.2 Cell culture techniques ..... 50**
4.2.1 Cultivation of cell lines ..... 50

4.2.2 Storage of cells ..... 50
4.2.3 Establishment of stable virus producing HEK293 cell lines ..... 51
4.2.4 Induction of virus production in stably transfected HEK293 cell lines ..... 51
4.2.5 Determination of virus titer ..... 52
4.2.6 Concentration of virus supernatant by ultra centrifugation ..... 52
4.2.7 Preparation of primary human B cells from adenoids ..... 53
4.2.8 Infection and outgrowth of adenoid B cells ..... 53
4.2.9 Determination of cell doubling time ..... 53
**4.3 Flow cytometric methods ..... 54**
4.3.1 Detection of surface molecules ..... 54
4.3.2 Cell sorting of BCR-negative B cells ..... 54
4.3.3 Phosphospecific flow cytometry ..... 55
4.3.4 Cytokine release assay ..... 55
4.3.5 Calcium flux analysis ..... 56
**4.4 Protein analytic techniques ..... 57**
4.4.1 Cell lysis and determination of protein concentration ..... 57
4.4.2 SDS-PAGE ..... 57
4.4.3 Western Blot analysis ..... 57
**4.5 DNA/RNA analytic techniques ..... 58**
4.5.1 Extraction of cellular RNA ..... 58
4.5.2 Reverse transcription of RNA into cDNA ..... 58
4.5.3 qRT-PCR ..... 58
**5 Results ..... 60**
**5.1 Establishment of a sorting protocol of BCR-negative primary human B cells ..... 60**
5.1.1 Sorting protocol ..... 60
5.1.2 Analysis of BCR-negative sorted cells ..... 62
5.1.3 Analysis of infected cells ..... 64
**5.2 Comparison of BCR and LMP2A signaling shortly after infection ..... 65**
5.2.1 Replacement of LMP2A by an inducible LMP2A:mCD69 chimera or NP-specific murine IgM (NP-mIgM) ..... 65
5.2.1.1 Expression and functionality of LMP2A:mCD69 in LCLs ..... 68
5.2.1.2 Strategy of NP-mIgM expression in EBV-infected B cells ..... 72
5.2.1.3 Expression of the NP-mIgM in LCLs ..... 73
5.2.1.4 Signaling capacity of the NP-mIgM in LCLs compared to splenic B cells from the quasi-monoclonal mouse ..... 78

5.2.2 LMP2A:mCD69 but not NP-mIgM rescued BCR-negative B cells from apoptosis ..... 80
**5.3 Comparison of EBV's LMP2A to K1 and K15 from KSHV ..... 89**
5.3.1 Construction of K1 and K15 mutant EBVs ..... 89
5.3.2 Expression of K1 and K15 in LCLs ..... 90
5.3.3 Comparison of LMP2A, K1, and K15 shortly after infection ..... 91
5.3.3.1 Rescue of BCR-negative B cells from apoptosis ..... 92
5.3.3.2 Basal Syk phosphorylation levels ..... 94
5.3.3.3 Activation of B cell markers ..... 96
5.3.3.4 Cytokine production ..... 98
5.3.4 BCR signaling in the presence of LMP2A, K1, and K15 ..... 100
**6 Discussion ..... 103**
**6.1 Functionally impeded LMP2A:mCD69 and NP-mIgM mutant EBVs ..... 103**
6.1.1 The LMP2A:mCD69 EBV ..... 105
6.1.2 The NP-mIgM EBV ..... 107
**6.2 K1 and K15 can partially replace LMP2A functions ..... 111**
**7 Summary ..... 120**
**8 Abbreviations ..... 122**
**9 References ..... 126**
**10 Acknowledgements ..... 137**

# 1 Introduction

## 1.1 The Immune system

During our entire life microorganisms surround us. Some of them are beneficial e.g. intestinal bacteria, which hinder pathogenic bacteria to colonize the gut by competing for space and food, but many pathogens are harmful and can lead to severe diseases. To protect the body from these aggressors our immune system has evolved during evolution. It can be divided into two basic parts: the innate immune system, reacting nonspecifically but immediately against a subset of pathogens such as bacteria and the adaptive immune system reacting more slowly but against nearly all foreign substances, compounds, and molecules. Both systems rely on white blood cells, called leukocytes.

### 1.1.1 The innate immune system

The innate immune system reacts against common features of pathogens and leads to a generic reaction independent of the type of microorganisms it is confronted with eliminating the majority of pathogens. If it fails, the innate immune system attempts to hold the invader in check until the adaptive immune system is able to mount a pathogen-specific response.

The first barrier against infections is the epithelial layer of the body. During breathing and ingestion pathogens are always taken up. To impair their entry to the inner body, the skin, the gastrointestinal tract, the respiratory tract, as well as the urogenital tract are lined by tightly packed epithelial cells, often being covered by mucus. The mucus hinders the pathogen to attach to the cells and also guides the invader out of the body. Besides this physical barrier epithelial cells also produce chemical substances like the antibacterial lysozyme in the eye. Also, the low pH in the stomach reduces pathogen survival and proliferation.

Specific leukocytes, the phagocytes, which recognize the invader by pattern recognition receptors, often eliminate pathogenic microbes if they overcome the epithelial barrier. Pattern recognition receptors react against common components of microorganisms like

lipopolysaccharide (LPS) or DNA of many bacteria. As a consequence phagocytes either kill the pathogen by phagocytosis or attract additional immune cells to the side of infection.

A third barrier of the innate immune system is the complement system. It consists of a number of plasma proteins, which recognize common surface structures on pathogens. The binding of complement factors (i) marks the pathogen so that it is taken up and destroyed by phagocytes (called opsonization), (ii) attracts other immune cells for help, (iii) induces pores in the membrane of certain microorganisms, and (iv) activates the adaptive immune system.

### 1.1.2 The adaptive immune system

During evolution pathogens have developed mechanisms to overcome the innate immune system, which presumably led to the development of the adaptive immune system in vertebrates. The adaptive immune system needs four to eight days before it can fully react to an infection. Despite this reaction in time, it is able to recognize and eliminate nearly all foreign structures, which are recognizes as antigens, and establishes an immunological memory, which can quickly reactivate antigen-specific effector cells.

The main players of the adaptive immune system are lymphocytes, which can be divided into B and T cells developing from a common lymphoid precursor in the bone marrow. The abbreviation “B” from B cells comes from the Latin word *Bursa fabricii*, a lymphatic organ of birds, where B cell development was first described. In contrast to B cells, which develop and differentiate in the bone marrow of mammalians, T cells infiltrate the thymus for further development. The site of maturation gave T (thymus) cells their names and defined the bone marrow and thymus as two primary lymphoid organs. Mature B and T cells enter the bloodstream and circulate through secondary lymphoid organs like spleen and lymph nodes. Using the lymph system they reenter the bloodstream leading to a continuous circulation of lymphocytes.

B and T cells recognize foreign structures *via* cellular surface receptors, which bind to so-called antigens or epitopes, respectively. B cells express a B cell receptor (BCR) and,

accordingly, T cells a T cell receptor (TCR). Each B or T cell expresses many copies of a single receptor, which binds a single antigen or epitope, only. Clonal B and T cell receptors develop from a nearly infinite repertoire of specificities in complex differentiation and maturation steps (see below). Ligand binding of B or T cell receptors leads to the activation of the lymphocyte and its strong proliferation, called clonal expansion. It ensures the presence of sufficient numbers of clonal cells, termed effector cells, to fight the antigen. To become effector cells B cells differentiate into plasma cells or memory B cells. Plasma cells release soluble antigen receptors, called antibodies. They can bind to the antigen (i) preventing its binding to target structures, a process called neutralization, (ii) mark it for opsonization, and (iii) activate the complement system. Likewise, T cells differentiate into cytotoxic T cells, which kill virus-infected cells, or into T helper cells, which help to activate B cells or macrophages. If the antigen is successfully eliminated, most of the effector cells undergo apoptosis. Only a small subset survives, which constitutes the long-lived immunological memory.

## 1.2 B cells and their B cell receptor (BCR)

### 1.2.1 The BCR

The BCR complex consists of two major components: the immunoglobulin (Ig) chains and the Ig-α and Ig-β heterodimer. An Ig can be a soluble antibody or attached to the plasma membrane as part of the BCR. Immunoglobulins are Y-shaped (Figure 1-1) and consist of two heavy and two light chains. The two arms of the "Y" contain two pairs of variable regions, which bind the antigen. The "stem of the Y" is the constant region, which either anchors the Ig to the B cell membrane or defines the effector function of the soluble Ig.

The Ig-α and Ig-β chains are associated with the BCR. When the BCR binds its cognate antigen, it senses this contact and transmits signals into the cells, which the Ig-α and Ig-β chains convey. Both Ig-α and Ig-β contain immunoreceptor tyrosine-based activation motifs (ITAM) in their cytoplasmic tails (Reth, 1989). The ITAM consists of the amino acid sequence D/ExxYxxLx($_{6-10}$)YxxL/I where x can be any amino acid (Reth, 1989). When an antigen binds, the Ig-α/β chains of the BCR change their conformation and the

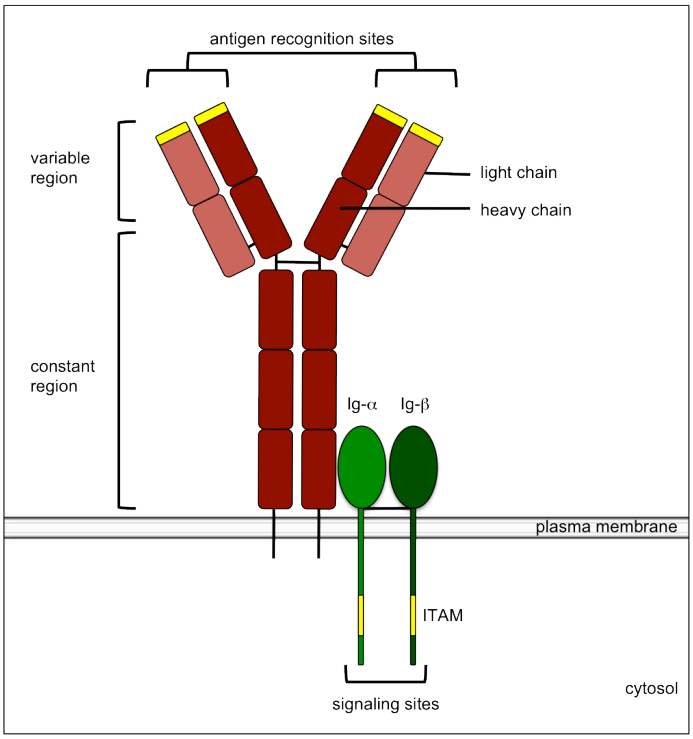


**Figure 1-1: The B cell receptor (BCR)**
The B cell receptor consists of a membrane bound immunoglobulin (Ig, red) at the cell surface and a heterodimer, consisting of the subunits Ig-α and Ig-β (green) as the receptor-signaling moiety. The Ig consists of two heavy chains and two light chains, which are connected via disulfide bonds. The membrane distal part, the variable region, is responsible for antigen binding. It harbors the antigen recognition sites (yellow), which are unique to a given B cell clone, but show a high diversity among BCRs of different B cells. The membrane proximal part, the constant region, determines the effector function of the soluble Ig. Its isotype can be IgM (as depicted here), IgD, IgG, IgA, or IgE. The function of the BCR is to bind its cognate antigen. Since the membrane bound Ig cannot transmit signals into the cell, it is associated with the Ig-α/β heterodimer. This dimer comprises two immunoreceptor tyrosine-based activation motifs (ITAMs), which transmit signals into the cell upon antigen encounter of the Ig part of the BCR. The Ig-α/β heterodimer is also linked via a disulfide bond.

tyrosines (Y) of the ITAMs are phosphorylated by recruited kinases, which are membrane proximal signaling mediators. Phosphorylation of the ITAMs is the initial step towards BCR signaling and induces B cell survival, proliferation, and differentiation. To ensure that a B cell expresses a functional and antigen-specific BCR, the B cell passes through different signaling checkpoints during its differentiation, which are described in the next section.

### 1.2.2 B cell development

B cells are generated from hematopoietic stem cells (HSC) and develop in the bone marrow. After several maturation steps they migrate into the bloodstream and reach peripheral lymphoid organs. Figure 1-2 shows a simplified model of the hematopoietic

differentiation starting from the HSC (Nagasawa, 2006). The HSC is pluripotent, has self-renewal potential, and can differentiate into a common lymphoid progenitor cell (CLP) and the common myeloid progenitor cell (CMP). The CMP gives rise to macrophages, granulocytes, erythrocytes, and megakaryocytes (which later develop into platelets). The CLPs express the interleukin 7 receptor (IL7R) and have the potential to differentiate into T cells, B cells, natural killer cells (NK cells), and dentritic cells (Nagasawa, 2006). The many different steps in B cell development can be divided into several stages based on the status of Ig rearrangement and the expression of certain characteristic cell surface markers.

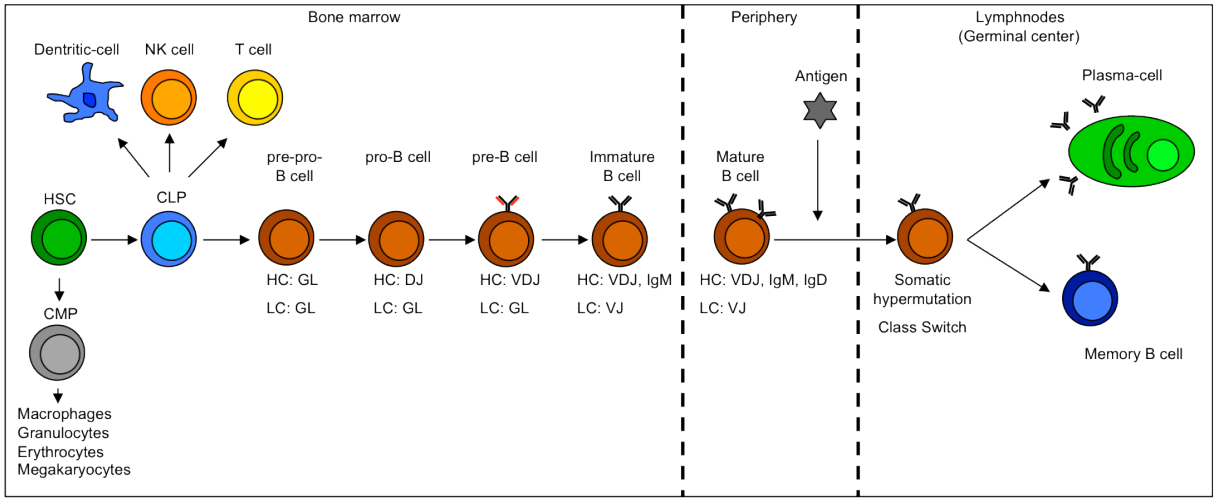


**Figure 1-2: B cell development**
B cells develop in the bone marrow until they express a functional BCR. Subsequently, they leave the bone marrow and travel through the periphery where they come in contact with antigen leading to their activation and further differentiation. B cells originate from the hematopoietic stem cell (HSC), which can differentiate into the common myeloid progenitor (CMP) and the common lymphoid progenitor (CLP) cells. The CLP differentiate into dentritic cells, natural killer (NK) cells, T cells, and B cells. In pre-pro B cells the genetic loci of the Ig heavy (HC) and light chains (LC) are still in germ line (GL) configuration but pro-B cells start DJ-rearrangement of the HC locus. Pre-B cells have finished the HC rearrangement and express a pre-BCR on their surface, which consists of the HC and a surrogate light chain. If the pre-BCR proves to be functional, LC rearrangement is induced. Immature B cells, which are able to express a functional BCR, leave the bone marrow, and travel through the periphery. When they encounter their cognate antigen, they proliferate and form germinal centers in the lymph node or spleen. In these germinal centers somatic hypermutation and class switch recombination (CSR) take place. During somatic hypermutation the affinity of the BCR to the antigen is increased. During CSR the constant region of the immunoglobulin (Ig) can switch from IgM or IgD to IgG, IgA, or IgE determining the effector function of the Ig. Finally, B cells can differentiate into plasma cells, which secrete soluble Igs or into memory B cells, which are long-lived and able to react fast on a second infection with the same antigen.

The genes coding for the variable region of the heavy ($_H$) and light ($_L$) chains are arranged in different clusters. The light chain locus comprises a variable (V) and a joining (J) cluster, the heavy chain has an additional diversity (D) cluster. Each cluster

contains several segments. During B cell development one segment of each cluster is chosen and linked to one segment of a neighboring cluster building a VJ light chain exon and a VDJ heavy chain exon. Selection and linkage of Ig gene cassettes occurs at the level of genomic DNA, a process, which is called somatic recombination. After transcription, these exons are spliced to a constant segment of the Ig genes forming complete heavy and light chains.

The earliest pre-pro-B cells have the Ig heavy and the Ig light chain still in germ line configuration but start to express recombination-activating genes (RAG). During development to the pro-B cell stage the cells express Ig-α and Ig-β as well as λ5, and VpreB, which are the components of the surrogate light chain (SLC) of the BCR. Pro-B cells are large and mitotically active. They have finished the $DJ_H$ rearrangement, but their light chain gene configuration is still in germ line state. $VDJ_H$ rearrangement is completed during development to the pre-B cell stage, and the newly synthesized heavy chain has to be tested for its function. Towards this end, the SLC (as a simplified model of the rearranged light chain, which is used later) must bind to the heavy chain, and both are expressed on the cell surface as the pre-BCR (Kurosaki *et al.*, 2009). The expression of the pre-BCR signals the cell that the formed heavy chain is complete, that further rearrangements at the heavy chain locus of the second allele has to be suppressed (allelic exclusion), and that the cell can continue its differentiation. At this point, the survival of the cell does not only depend on intrinsic signals but also upon extrinsic factors including interleukin (IL) 7, which, in combination with the pro-BCR, leads to a high proliferation.

After the functional Ig heavy chain is approved, pre-B cells stop to express the SLC, become immature B cells, and start to rearrange the light chain locus. These cells are smaller than pre-B cells and finally express the newly synthesized light chain together with the IgM heavy chain as the new BCR on their surface. Now the cells can leave the bone marrow unless the BCR is autoreactive, a state that can cause receptor editing or lead to apoptosis. Non-autoreactive cells migrate via the bloodstream into the spleen, where they differentiate into mature B cells expressing IgM and IgD on their cell surface.

Now, the B cell is ready to bind its specific antigen and to produce high amounts of antibodies, which constitute the humoral arm of the immune response.

A B cell is activated if it encounters its antigen. The BCR-antigen complex is internalized by endocytosis, the antigen is proteolytically processed and presented on MHC (major histocompatibility complex) class II molecules on the cell surface. CD4 (cluster of differentiation 4) positive T cells recognize the MHC II bound antigen with their TCR and react with an upregulation of their CD40 ligand (CD40L) (Bryant & Ploegh, 2004). CD40L expressed on T cells binds to the CD40 receptor on B cells providing an important second stimulatory signal to induce clonal expansion of the B cell and germinal center (GC) formation. During the GC reaction the affinity and the effector function of the BCR towards its antigen is optimized. If the BCR recognizes its antigen, but the B cell does not receive the essential CD40 signal, the cell enters an anergic state, during which it looses its responsiveness entirely (Cambier *et al.*, 2007). The anergic state ensures that a B cell, which reacts to self-antigen, is not activated because the corresponding and self-reactive T cell does not exist. The mechanism of B cell activation depends on two independent signals to prevent the expansion of auto-reactive B cells and the induction of autoimmune diseases.

Mutations are randomly inserted into the Ig genes of naive B cells during the GC reaction of somatic hypermutation. The purpose of this process is to improve the affinity of the BCR to its antigen. Most of the inserted mutations lead to a decreased BCR affinity or even to the functional disruption of the Ig gene. B cells that are incapable of expressing a functional, high affinity BCR undergo apoptosis because they lack strong and necessary survival signals from a high affinity BCR. Only if a cell expresses a high affinity BCR, the constant region of the BCR can be switched (called class switch) from the IgM type to IgG, IgA, or IgE, which have different effector functions. Post-GC B cells can differentiate into two B cell classes, namely plasma and memory B cells. Plasma cells are short-lived, secrete soluble high affinity Igs, and constitute the humoral immune response whereas memory B cells have a long life expectancy. Upon a second exposure to the same antigen, their antigen-optimized, high affinity BCR induces a rapid proliferation and

differentiation of memory B cells into plasma cells, which quickly secrete high affinity antibodies.

Many different B cells provide a high diversity of BCRs to the organism, to be capable to recognize nearly all foreign structures that might be harmful for the host. This is ensured by four main mechanisms. (i) Each heavy and light chain cluster is divided in sub-clusters coding for several V, D (only heavy chain), J segments (called combinatorial diversity). (ii) During segment linkage random nucleotides are inserted between the segments (called junctional diversity). (iii) There are two different light chain gene clusters, the λ and κ light chain cluster, which can pair with a heavy chain. (iv) During somatic hypermutation the affinity of the BCR is increased by random insertion of single or extended mutations into the Ig gene.

### 1.2.3 The BCR complex

BCR signaling is induced by antigen binding. It leads to tyrosine phosphorylation of the ITAMs of the Ig-α and -β chains and the activation of protein-tyrosine kinases (Ptks). How the BCR discriminates between its antigen-bound and -unbound forms is still under investigation. For example, it is not clear whether the BCR is a monomer in the antigen-free form and clusters upon antigen binding or if a BCR complex is formed in absence of antigen.

Antigen binding induces a conformational change of Ig-α/β to an open conformation (Figure 1-3) as observed by fluorescence resonance energy transfer (FRET) (Tolar *et al.*, 2005). At the same time the Ptk Lyn phosphorylates the ITAMs, a process which might stabilize the open conformation, and additional signaling molecules are recruited (Tolar *et al.*, 2008). Opening of the cytoplasmic BCR domains might be induced by the localization to lipid rafts, which have other physical properties than the normal fluidic membrane. They are thicker and have a stronger curvature (Tolar *et al.*, 2008), which might induce conformational changes in the Ig-α/β chains. Upon antigen binding, clustering of BCRs starts and CD19 (cluster of differentiation 19), which is a member of the co-receptor complex, enhances the BCR signal by spreading it throughout the plasma

membrane. CD19 might also regulate changes in the cytoskeleton after BCR activation (Harwood & Batista, 2010) to induce BCR-microcluster formation.

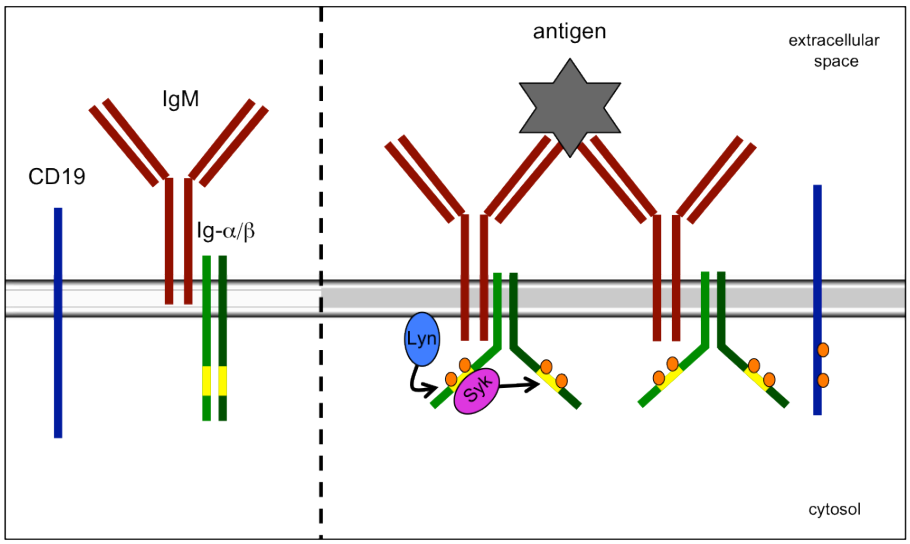


**Figure 1-3: The BCR complex and its activation**
The BCR complex consists of the immunoglobulin (Ig, red), the Ig-α/β heterodimer (green), and the co-receptor CD19 (blue). In the absence of an antigen, the Ig-α/β heterodimer is in a closed conformation and the ITAMs (yellow) are unphosphorylated. Upon antigen binding, the Ig locates to lipid rafts (grey). Translocation leads to the association with the tyrosine-kinase Lyn and the conformation of the Ig-α/β heterodimer changes to an open state. Lyn phosphorylates the ITAMs (orange dots) of Ig-α/β forming binding sites for the protein-tyrosine kinase Syk. Syk phosphorylates adjacent ITAMs as well as CD19, which spreads the signal and leads to an activation of additional signaling cascades.

Proteins with a SRC homology 2 (SH2)-domain can bind to the phosphorylated tyrosines of the ITAMs. The most important member is the spleen tyrosine kinase (Syk). Syk has a tandem SH2-domain with, which it can specifically bind the two phosphorylated tyrosines of the ITAM leading to a conformational change in the Syk protein and causing its activation (Kulathu *et al.*, 2009). Active Syk phosphorylates additional ITAMs of neighboring BCRs spreading and enhancing the BCR signal. There are two major downstream BCR signaling cascades, the phosphoinositide 3-kinase (PI3K) and the phospholipase C γ2 (PLCγ2) pathway (Kurosaki, 2011).

### 1.2.4 BCR signaling

#### *1.2.4.1 The PI3K/Akt signaling pathway*

CD19, the co-receptor of the BCR, plays an important role in the PI3K/Akt signaling pathway (Figure 1-4). Upon BCR stimulation, tyrosine residues of the cytosolic domain

of CD19 are phosphorylated by Lyn. PI3K binds via BCAP (B cell adaptor for PI3K) to the phosphorylated CD19 molecule and is thereby recruited to the plasma membrane. The activated PI3K starts to phosphorylate the plasma membrane component phosphatidylinositol-bisphosphate ($PIP_2$) to phosphatidylinositol-trisphosphate ($PIP_3$) (Kurosaki, 2011). The serine/threonine kinase Akt and the phosphoinositide-dependent protein kinase (PDK) bind to $PIP_3$, and PDK1 activates Akt by phosphorylation (Manning & Cantley, 2007). Akt is a key player in lymphocyte survival and maturation (Calamito *et al.*, 2009) as it activates several downstream cascades.

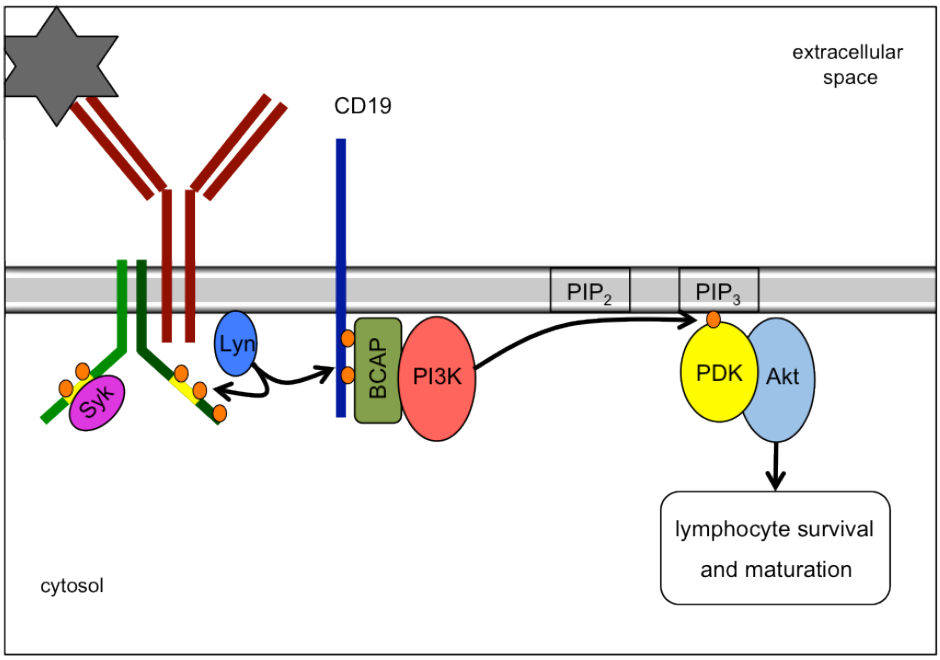


**Figure 1-4: The PI3 kinase (PI3K) signaling pathway**
Antigen (grey) binding to the Ig (dark red) leads to the phosphorylation (orange) of the Ig-α/β heterodimer (dark green) and CD19 by the tyrosine-kinase Lyn. The B cell adaptor for PI3K (BCAP) recruits PI3K to the plasma membrane where it phosphorylates the plasma membrane component phosphatidylinositol-bisphosphate ($PIP_2$) to phosphatidylinositol-trisphosphate ($PIP_3$). The phosphoinositide-dependent protein kinase (PDK) and the serine/threonine kinase Akt bind to $PIP_3$. Akt is activated by PDK1 and induces several signaling cascades, which regulate lymphocyte survival and maturation.

### *1.2.4.2 The PLCγ2 pathway induces calcium signaling*

Upon antigen binding, Lyn and Syk phosphorylate the ITAMs of Ig-α/β. The B cell linker protein (BLNK) binds to a phosphorylated tyrosine adjacent to the ITAM of Ig-α/β with its SH2-binding site (Engels *et al.*, 2001) and is phosphorylated by Syk (Figure 1-5). Phosphorylated BLNK forms a platform recruiting PLCγ2 and Bruton's tyrosine kinase (Btk), which, in close proximity to the plasma membrane, controls phospholipid

metabolism and calcium influx (Kelly & Chan, 2000). Syk phosphorylates PLCγ2, which then hydrolyzes $PIP_2$ to diacylglycerol (DAG) and inositol-trisphosphate ($IP_3$). $IP_3$ binds to its receptor ($IP_3R$) in the endoplasmic reticulum (ER) membrane resulting in a fast release of calcium from the ER into the cytosol (Kurosaki *et al.*, 2009). The ER membrane protein STIM1 senses the decreased calcium level in the ER and activates

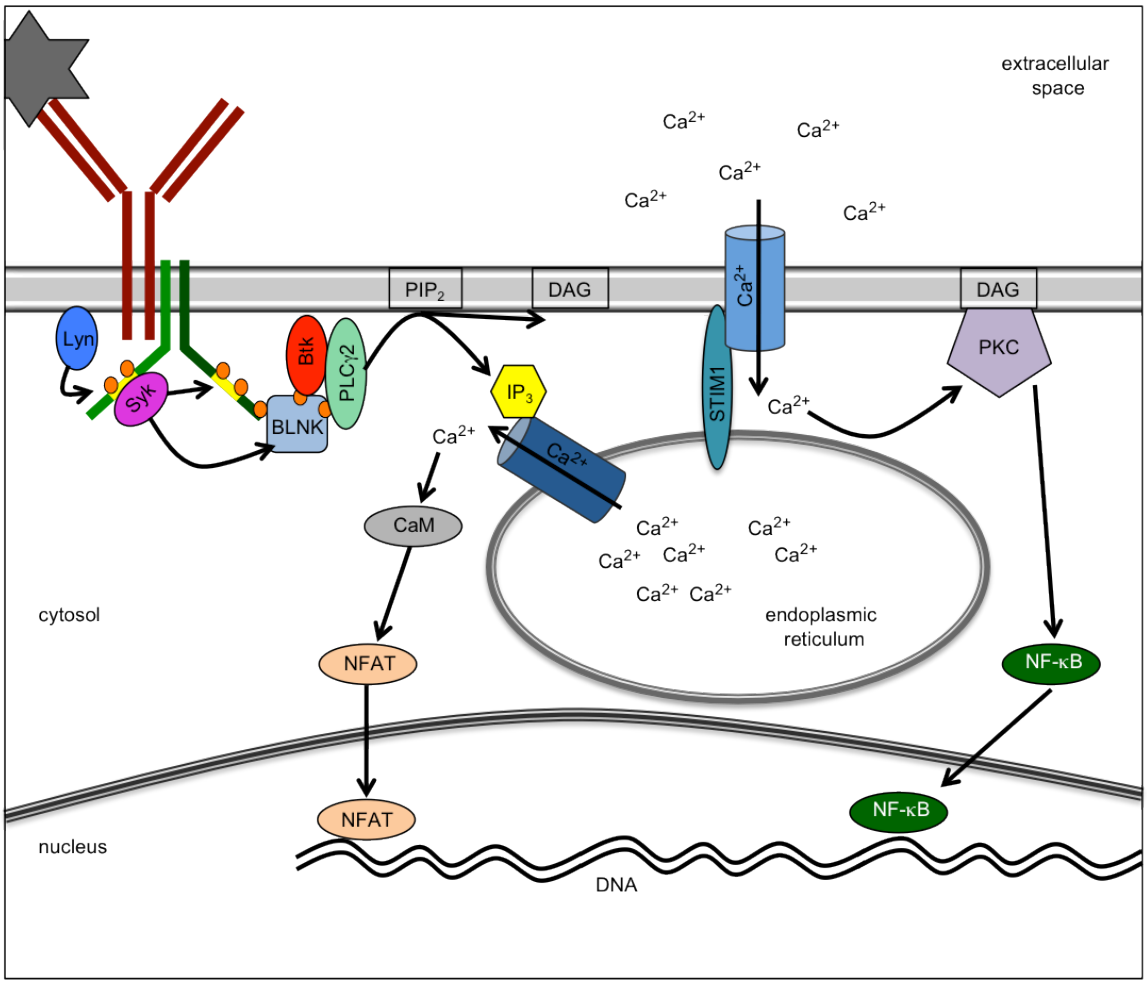


**Figure 1-5: The phospholipase γ2 (PLC γ2) signaling pathway**
Upon antigen binding (grey star) to the Ig (dark red), Lyn phosphorylates the ITAMs (yellow) of the Ig-α/β heterodimer (dark green). Syk can bind to the phosphorylated ITAMs and phosphorylates Ig-α/β inside and outside the ITAMs. The B cell linker protein (BLNK) binds to the Ig-α/β dimer and builds a binding platform for Bruton's tyrosine kinase (Btk) as well as PLCγ2 that controls lipid metabolism and calcium (Ca) signaling. PLCγ2 hydrolyzes the plasma membrane component phosphatidylinositol-bisphosphate ($PIP_2$) to diacylglycerol (DAG) and inositol-trisphosphate ($IP_3$). $IP_3$ binds to Ca-channels (dark blue) in the endoplasmic reticulum (ER) leading to an influx of calcium ions ($Ca^{2+}$) into the cytosol. The decreased $Ca^{2+}$ level in the ER is sensed by STIM1 that activates $Ca^{2+}$ channels in the plasma membrane leading to an increased influx of $Ca^{2+}$ into the cell. $Ca^{2+}$ binding activates calmodulin (CaM) that induces the translocation of the transcription factor NFAT (nuclear factor of activated T cells) from the cytosol to the nucleus. $Ca^{2+}$ together with DAG activates protein kinase C (PKC), which itself activates the transcription factor NF-κB (nuclear factor-κB). NFAT and NF-κB activate genes that are involved in B cell development, survival and activation.

calcium release-activated calcium (CRAC) channels in the plasma membrane (Hogan *et al.*, 2010). Open CRAC channels permit the influx of calcium from the extracellular space into the cell, which the calcium-binding protein calmodulin (CaM) senses and induces different pathways (Hogan *et al.*, 2010). One of them leads to the dephosphorylation of the transcription factor NFAT (nuclear factor of activated T cells), which translocates to the nucleus. NFAT plays a central role in the development of B cells from the immature to the mature, immunoglobulin expressing B cell (Feske, 2007). Calcium together with DAG can also directly activate protein kinase C (PKC), which in turn activates the transcription factor nuclear factor-κB (NF-κB) important for B cell survival and activation (Guo *et al.*, 2004).

Taken together, phosphorylation of signaling molecules like Syk and PLCγ2 as well as an increase of calcium ions in the cytosol are hallmarks of BCR activation.

#### *1.2.4.3 Tonic BCR signaling*

Survival of mature B cells in the periphery depends on two signals from the BCR and the B cell activating factor (BAFF). The function of the BCR is to sense antigen binding, whereas BAFF is a cytokine, which is secreted by B cells. It binds to the BAFF receptor on B cells and stimulates B cell survival. The BAFF receptor senses the density of neighboring B cells by the amount of released BAFF and controls B cell numbers (Srinivasan *et al.*, 2009). Depletion of the BCR signaling unit Ig-α/β or the BAFF receptor leads to apoptosis in mature B cells (Lam *et al.*, 1997; Batten *et al.*, 2000) indicating that a constant "tonic" signaling level of the BCR (in the absence of antigen) as well as of BAFF is needed for B cell survival (Cancro, 2009). Recently, it was found that mature BCR-negative B cells can be rescued from apoptosis by induction of the PI3K pathway (Srinivasan *et al.*, 2009). Antigen binding induces PI3K signaling via ITAM phosphorylation, CD19, and BCAP. In the absence of antigen and tonic signaling, PI3K is directly recruited to the non-phosphorylated ITAMs via the GTPase (guanosine triphosphate hydrolyzing enzyme) TC21 (Delgado *et al.*, 2009) conveying signals independent of antigen binding. Since the ITAMs of the BCR complex as well as CD19 are not phosphorylated, the BCR signal is not extrapolated to other BCR complexes keeping the signal strength low.

How the BCR initiates tonic signaling in mature resting B cells is under investigation. Recently, Treanor *et al*. could show that two BCR populations with different dynamics exist. BCRs with a high diffusion coefficient were found in actin-poor areas, whereas BCRs with a low diffusion coefficient were present in actin- and ezrin-rich areas (Treanor *et al.*, 2010). Ezrin is a linker between the plasma membrane and the cytoskeleton. Slow movement in actin/ezrin-rich regions was controlled by Ig-β, and treatment of cells with different drugs led to an alteration in the cytoskeleton and induced BCR signaling (measured by calcium-flux and Akt phosphorylation) independent of antigen engagement. Accordingly, the authors suggested that the tonic signaling is maintained by the organization of the cytoskeleton, which either concentrates signaling activators or excludes signaling inhibitors from the BCR (Pierce & Liu, 2010). Due to restricted diffusion and fixation of the BCR in actin-rich areas, the tonic signal cannot spread or become amplified.

Upon antigen binding, the cytoskeleton architecture changes, which leads to BCR microcluster formation and full BCR signaling (Pierce & Liu, 2010). Thus, cytoskeleton formation plays an important role in controlling BCR dynamics and signaling intensity.

### 1.2.5 Studying BCR's function – the quasi-monoclonal mouse

To study BCR's function, signaling can be induced by two means: adding the antigen or cross-linking the BCR with an α-Ig antibody. Since the antigen specificity of the BCR is generally unknown, α-Ig antibodies are preferentially used. Another advantage of α-Ig antibodies is their ability to cross-link BCRs of many different antigen specificities presented in the highly diverse B cell population.

BCR signaling is a tightly regulated process, controlled by the inhibitory molecules CD22 and CD72 among others (Nitschke & Tsubata, 2004). Both molecules contain an IT<u>I</u>M (immunoreceptor tyrosine-based inhibition motif), which is also phosphorylated by Lyn upon antigen binding to the BCR. The phosphorylated IT<u>I</u>Ms recruit the SH2-containing protein tyrosine phosphatase-1 (SHP-1), which in turn dephosphorylates the IT<u>A</u>M of Ig-α/β thereby controlling the duration of a BCR signal (Nitschke & Tsubata, 2004). This

type of feedback regulation is important to prevent uncontrolled B cell activation and cellular proliferation, which could lead to leukemia, eventually.

The BCR transmits different and distinct signals upon antigen binding or α-Ig cross-linking. Antigen-mediated BCR activation leads to phosphorylation of CD22 and CD72 and recruitment of SHP-1 (Hokazono *et al.*, 2003), but cells only proliferate and survive the stimulus if the CD40 receptor was cross-linked with α-CD40 antibody, providing the second signal (see section 1.2.2). In contrast, BCR stimulation with an α-Ig antibody, only, induces weak phosphorylation of CD22 and CD72 and, thus, activates an unrestricted BCR signal. Additionally, α-Ig antibody stimulation of the BCR activates cell proliferation even in absence of CD40 stimulation (Hokazono *et al.*, 2003). During physiological BCR activation the antigen binds to the membrane distal part of the Ig leaving the constant region of the Ig accessible for CD22 and CD72 recruitment and phosphorylation. In contrast, during artificial α-Ig cross-linking the antibody binds to the membrane proximal part of the Ig physically impeding CD22 and CD72 binding. As a consequence, the ITIMs of CD22 and CD72 are not accessible for phosphorylation via Lyn, and the inhibitory BCR signal is missing. For this study, Hokazono *et al*. took advantage of the quasi-monoclonal (QM) mouse established in the lab of Mathias Wabl (Cascalho *et al.*, 1996). In this transgenic mouse, the majority of the B cell population is clonal and expresses an IgM specific for the hapten (4-hydroxy-3-nitrophenyl) acetyl (NP) on B cells. A hapten is a small molecule, which itself does not induce an immune reaction. However, in combination with a protein, e.g. bovine serum albumin (BSA), NP can act as a fully competent antigen. In the QM mouse, the $V_HDJ_H$ segments of the NP-specific murine IgM heavy chain (called 17.2.25) is introduced into the $J_H$ gene segments. After crossing to double knockout mice, the QM mouse is incompetent to express any Ig heavy chain and kappa light chain and has the genotype $V_HDJ_H$ 17.2.25/$H^-$, $\kappa^-/\kappa^-$, $\lambda^-/\lambda^-$ (Cascalho *et al.*, 1996). Almost all B cells show an expression of the 17.2.25 Ig heavy chain and the λ light chain at their plasma membrane capable of binding NP and its derivative (4-hydroxy-5iodo-3-nitrophenyl) NIP, which has higher affinity than NP. Only 20% of peripheral blood B cells have undergone subsequent somatic hypermutations and secondary rearrangements (Cascalho *et al.*, 1997) causing the loss of NP specificity.

B cells from the QM mouse have the advantage that two types of BCR signals can be induced by two different means in B cells with identical genetic background: addition of the antigen complex NP-BSA and cross-linking with an α-murine (m) IgM antibody. In addition, NP antigens with different epitope density (e.g. $NP_2$-BSA vs. $NP_{18}$-BSA) or binding affinity ($NP_x$-BSA vs. $NIP_x$-BSA) can mimic the physical properties of different antigens to study the influence on BCR signal strength (Hokazono *et al.*, 2003).

## 1.3 The Epstein-Barr virus (EBV)

### 1.3.1 General facts

The Epstein-Barr virus (EBV) is one of the most successful human viruses with an infection rate of more than 90% of all humans (Tsurumi *et al.*, 2005). It is transmitted via saliva and can infect epithelial cells and B cells. In infants, infection with EBV usually does not cause any symptoms in the host, but in adolescents and adults infection can cause infectious mononucleosis (IM, also called "kissing disease"), which is characterized by fever, sore throat, and enlarged lymph nodes. IM is self-limiting and cures due to the activation of an immune response. In the absence of a functional immune system, e.g. in immunocompromised patients, EBV can cause post transplant lymphoproliferative disorder (PTLD), a B cell lymphoma. In people with an apparently intact immune system, EBV is associated with different cancers like nasopharyngeal carcinoma, gastric carcinoma, Burkitt's lymphoma, or Hodgkin's lymphoma (Tsurumi *et al.*, 2005).

EBV belongs to the family of γ-herpes viruses. One common feature of herpes viruses is their ability to induce and maintain a lifelong latent infection evading an immune response. EBV latently infects memory B cells *in vivo*, which persist for a lifetime in the host (Babcock *et al.*, 1998). *In vitro,* EBV infects B cells of different stages equally well and drives them into proliferation (Thorley-Lawson, 2001). The ability to transform B cells *in vitro* is of great importance for research in EBV, since infection of any B cell with this virus leads to the establishment of lymphoblastoid cell lines (LCL). LCLs are a model system for viral latency and cellular transformation, which is an important feature of EBV's rich biology.

### 1.3.2 Infection of B cells by EBV – the latency programs

EBV infects tonsillar epithelial cells either directly or via adjacent B cells, which is believed to lead to virus replication and shedding in the throat. Newly synthesized EBV particles infect naive and mature B cells driving them into proliferation by expressing the latency III program (Table 1-1 and Figure 1-6) that comprises six EBV nuclear antigens (EBNA1, 2, 3A, 3B, 3C and LP), three latent membrane proteins (LMP1, 2A and

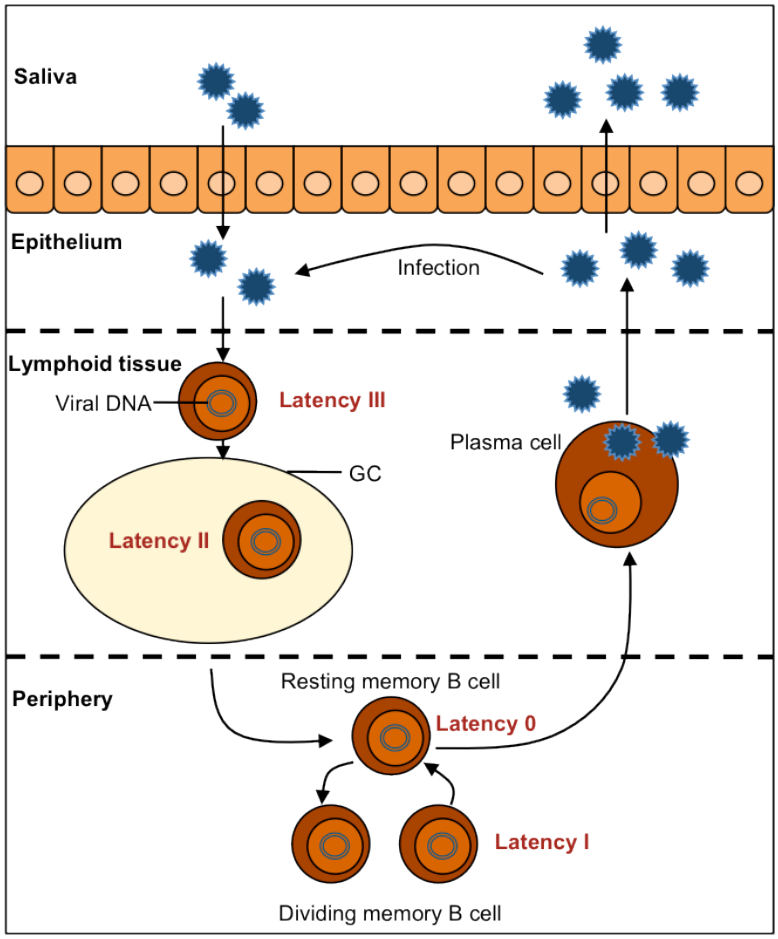


**Figure 1-6: The life cycle of the Epstein-Barr virus (EBV)**
Upon infection of B cells, EBV traverses four latency states, which are characterized by a distinct viral gene expression pattern. EBV induces a life-long latency in its host and evades the attack of the host's immune system. EBV enters the body via saliva and infects epithelial cells. Progeny virus is made, which infects naive B cells in the lymphoid tissues of the nasopharynx. First, the latency III program (Table 1-1) is expressed, which activates infected B cells leading to germinal center (GC)-like reactions, but the expression of nine viral genes during latency III induces a strong response of the immune system, which eliminates most of the infected cells through $CD8^+$ effector T cells. To evade this clearance, the latency II program is activated, in which only four genes are expressed. They ensure that the B cells survive the GC reactions. Infected B cells leaves the GC as resting memory B cells, which do not express any viral genes (latency 0), but during cell divisions, as part of the normal B cell homeostasis, only EBNA1 (EBV nuclear antigen 1) is expressed (latency I), which prevents loss of the EBV genome. If an infected memory B cell is activated by antigen-binding, it further differentiates into plasma cells. At the same time EBV's lytic cycle is induced leading to the production of infectious particles. The figure is adopted from Thorley-Lawson & Allday, 2008.

2B) and a number of non-coding vial RNAs (Thorley-Lawson, 2001; Young & Rickinson, 2004). EBNA1 tethers the EBV genome to the cellular chromosomes ensuring replication of the EBV episome during cell division. EBNA2, together with its co-activator EBNA-LP (Ling *et al.*, 2005), is the major regulator of the viral transcription machinery during latency. It induces the expression of LMP1 and LMP2A providing necessary survival factors. LMP1 is categorized as an oncogene and mimics a constitutively activated CD40 receptor, which transmits the second activation signal (next to the BCR signal) normally provided by T helper cells (see section 1.2.2). LMP2A mimics a constitutively activated BCR, which can provide BCR-negative but EBV-infected B cells the essential survival signals. LMP2B is a truncated version of LMP2A lacking the signaling domain. It is thought to negatively regulate LMP2A's activity (Rovedo & Longnecker, 2007). EBNA3 proteins are transcriptional activators and repressors, which regulate cell cycle progression and epigenetic events in the host cell (Krauer *et al.*, 2004).

Infected B cells and LCLs express high levels of the B cell activation markers CD23, CD30, CD39, CD70, and the cell adhesion molecules LFA-1 (lymphocyte-function-associated antigen 1), LFA3 and intercellular adhesion molecule 1 (ICAM-1, also known as CD54) (Young & Rickinson, 2004).

In the EBV permissive host, most of the infected cells are eliminated by the immune response of mainly cytotoxic T cells a few days post infection. Remaining cells escape and survive due to a downregulation of latent viral gene expression. During the latency II program, only EBNA1 and the LMPs are expressed. EBV infection induces a GC-like reaction (see paragraph 1.2.2). The expression of the LMPs during latency II provides infected cells with BCR- and CD40-like signals ensuring their survival during this process. B cells, which differentiate into memory B cells, shut down viral gene expression entirely (latency 0) and reside as resting memory B cells, which circulate through the periphery. In the peripheral blood, one out of $10^4$ to $10^6$ memory B cells carries EBV. The immune system does not recognize these cells because they do not express any viral gene. Memory B cells that proliferate as part of the normal memory B cell homeostasis expresses EBNA1 only (latency I) (Thorley-Lawson & Allday, 2008). If the latently infected memory B cell binds antigen, the viral lytic cycle can be induced,

which results in progeny virus synthesis (Tovey *et al.*, 1978; Takada, 1984; Hislop *et al.*, 2007).

**Table 1-1: Latency types and transcription program of EBV**

| Latency type | Viral proteins and non-coding RNAs | Function of viral proteins | Associated lymphoma |
|---|---|---|---|
| III | EBNA1, 2, 3A, 3B, 3C, LP<br>LMP1, 2A, 2B<br>viral miRNAs and non-coding RNAs | activate resting B cells to become proliferating B blasts | Post-transplant lymphoma |
| II | EBNA1<br>LMP1, 2A, 2B<br>viral miRNAs and non-coding RNAs | provide B cells with necessary survival signals during germinal center reaction, induces their differentiation to memory B cells | Hodgkin's lymphoma |
| I | EBNA1<br>viral miRNAs and non-coding RNAs | tether the viral genome to the host cell DNA ensuring correct replication during memory B cell proliferation | Burkitt's lymphoma |
| 0 | EBV encoded miRNAs | allow EBV to persist in memory B cells, could regulate viral or cellular genes to ensure immune evasion or cellular survival under stress | |

EBNA: EBV nuclear antigen, LMP: latent membrane protein, miRNA: micro RNA

### 1.3.3 EBV-associated lymphoma

EBV is associated with different lymphomas, which can be characterized by their latency program.

*Post-transplant lymphoproliferative disease (PTLD)*

PTLD mostly occurs in immunocompromised patients. Suppression of the immune system can be caused by drug treatment after organ transplantation to prevent organ rejection or by human immunodeficiency virus (HIV) infection. PTLD can arise from several B cell differentiation stages and shows a latency III phenotype. Due to the suppressed immune system, T cells cannot react properly to EBV antigens, and the proliferating EBV-infected B cells survive.

*Hodgkin's lymphoma (HL)*

40% of HL cases in the developed world are associated with EBV. In Central and South America this fraction increases up to 90% in pediatric HLs (Kuppers, 2009). The mononucleated Hodgkin cells and the multinucleated Reed-Sternberg cells (HRS cells) are the genuine HL cells originating from the B cell lineage. HL is believed to arise from GC B cells, which underwent somatic hypermutation. Interestingly, 100% of crippled HL

B cells that are unable to express a functional BCR are EBV positive. EBV can rescue these cells from apoptosis by providing the BCR mimic LMP2A. HRS cells show a latency II profile and acquire many mutations, which can cause the loss of their B cell phenotype (Kuppers, 2009).

*Burkitt's lymphoma (BL)*

EBV is present in all cases of BL observed in children from Africa and New Guinea but only in 15% of cases observed in children from the developed world (Young & Rickinson, 2004). The major feature of BL is the reciprocal translocation of the *myc* proto-oncogene to one of the various immunoglobulin loci causing its overexpression and constitutive activity. Myc is a transcription factor controlling many cellular pathways especially cell cycle progression, proliferation and apoptosis. Aberrant *myc* expression leads to cell growth, unrestricted proliferation, and genomic instability (Thorley-Lawson & Allday, 2008). EBV might indirectly contribute to *myc* translocation by inducing somatic hypermutation, which causes genetic instability and increases the risk of gene translocations. In normal B cells, an aberrant activation of *myc* induces the expression of the pro-apoptotic Bim protein. During BL pathogenesis, it is assumed that apoptosis is inhibited by EBNA3A and 3C repressing Bim (Anderton *et al.*, 2008). The malignant cells in BL originate from GC cells, which cannot differentiate into a resting memory B cell as they express *myc* constantly. BL cells express the latency I phenotype *in vivo*.

Recently, Vereide and Sudgen induced the loss of the EBV genome in different lymphoma cell lines and determined the survival of the cells. Lymphoma cell lines, which express few viral genes, only, tolerate the induced loss of the EBV genome whereas cells, which express more viral genes, depend on EBV (Vereide & Sugden, 2011). In essence, the dependency on EBV is higher in PTLD-derived cell lines than in BL-derived ones indicating that the different viral protein expression patterns do not reflect different latency stages but show the dependency of the cell on EBV. Cells, which have acquired increasing amounts of suitable mutations during their development, are less dependent on viral gene expression (Hammerschmidt, 2011).

### 1.3.4 The latent membrane protein 2A (LMP2A)

#### *1.3.4.1 Composition of the LMP2A gene locus*

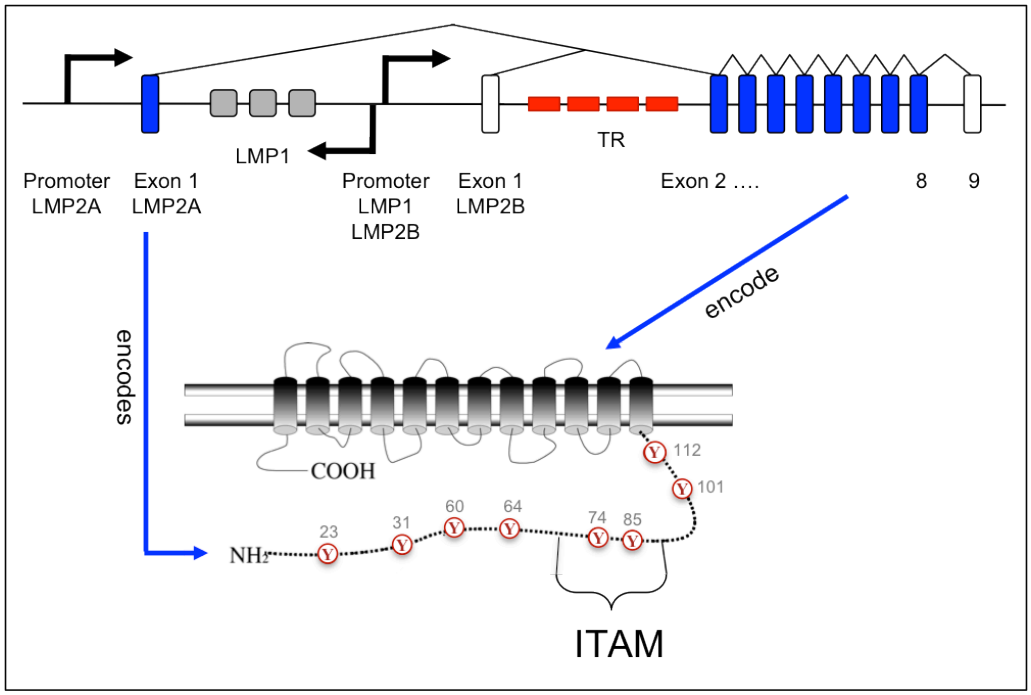


**Figure 1-7: Genomic location and structure of LMP2A**
LMP2A is encoded by nine exons, which flank both sides of EBV's terminal repeats (TR). The first exon encodes the N-terminal signaling domain of LMP2A, which contains eight tyrosines (Y). $Y_{74}$ and $Y_{85}$ form an ITAM (immunoreceptor tyrosine-based activation motif). Exon two to eight encode the C-terminus and 12 transmembrane domains, which are responsible for self-oligomerization of LMP2A. Exon 9 is non-coding. A bidirectional promoter controls the expression of LMP2B and LMP1. LMP2B is independently expressed from another promoter than LMP2A, and its first exon is non-coding. LMP2B shares exons two to nine with LMP2A and is, therefore, an N-terminally truncated form of LMP2A. LMP2B is thought to control LMP2A's activity negatively. The Figure is adapted from Mancao *et al.,* 2006.

The latent membrane protein 2A (LMP2A) is encoded by nine exons, which flank both sides of EBV's terminal repeats (TR) (Figure 1-7). The first exon encodes 119- amino acids of LMP2A's unfolded N-terminus (Park *et al.*, 2005). Exon two to eight encode 12 transmembrane domains and the 27-amino acid long C-terminal tail (Brinkmann & Schulz, 2006). The N- and the C-terminus are both located in the cytoplasm. Exon nine is non-coding. LMP2B's expression is controlled by an own promoter, but the gene is co-terminal with LMP2A and shares exons two to nine with it. The C-terminus and the 12 transmembrane domains of LMP2A are thought to be responsible for LMP2A clustering and lipid raft localization (Matskova *et al.*, 2001; Katzman & Longnecker, 2004). LMP2A's N-terminus is important for signal transduction and contains eight tyrosines of

which two form an ITAM. Lyn and Syk phosphorylate the ITAM of LMP2A as they phosphorylate the ITAMs of Ig-α/β leading to the activation of the PI3K and PLCγ2 pathways by LMP2A. Due to the self-oligomerization of LMP2A, LMP2A-signaling is thought to be constitutive mimicking an antigen-activated BCR.

#### *1.3.4.2 LMP2A signaling*

The N-terminal domain of LMP2A contains eight tyrosines, which are important for the signaling activity (Figure 1-7). The protein-tyrosine kinase (Ptk) Lyn binds to the $Y_{112}$EEA motif of LMP2A and phosphorylates additional tyrosines including $Y_{74}$ and $Y_{85}$ within the ITAM. Their phosphorylation enables the tandem-SH2-containing protein Syk to bind the ITAM (Fruehling & Longnecker, 1997; Fruehling *et al.*, 1998). Syk can activate downstream cascades like PI3K and Akt or Btk and PLCγ2, which are also activated by the BCR (see chapter 1.2.4.). Besides the ITAM, the N-terminus contains two proline rich regions (PPPPY$_{60}$ and PPPPY $_{101}$), which are binding sites for the Nedd4-like ubiquitin protein ligase family (Brinkmann & Schulz, 2006). These proteins ubiquitinate LMP2A as well as its accessory proteins Lyn and Syk leading to their degradation (Ikeda *et al.*, 2000) downregulating LMP2A's signaling capacity. LMP2A is also phosphorylated on serine and threonine residues, but the function of these modifications *in vivo* is not known.

#### *1.3.4.3 Studying LMP2A's function – the LMP2A:mCD69 construct*

The BCR as well as LMP2A contain ITAMs, and both membrane-anchored proteins induce the same signaling cascades. EBV infection can rescue B cells from apoptosis, which are deficient in BCR expression (Mancao *et al.*, 2005), and LMP2A provides the necessary survival signals replacing the functions of the BCR. In this model, LMP2A is a BCR mimic. In contrast, LMP2A was reported to block BCR signaling by two means: LMP2A (i) inhibits the migration of the BCR into lipid-rafts where Lyn is located and (ii) sequesters Lyn and Syk depriving the BCR from its most important signal mediators. These hypotheses were strengthened by the observation that B cells infected with wt EBV do not show calcium influx after BCR activation in contrast to cells infected with LMP2A knock-out EBV (Fruehling & Longnecker, 1997).

To compare BCR and LMP2A signaling in the same cellular background an inducible LMP2A version was designed. It consists of the N-terminal signaling domain of LMP2A and the transmembrane and extracellular part of the murine CD69 (mCD69) protein (Medele, 2010). LMP2A signaling can be induced by adding a cross-linking α-mCD69 antibody. Using this LMP2A:mCD69 chimera, my work group could show that LMP2A does not block but rather supersedes the BCR. LMP2A:mCD69 stimulation induced tyrosine phosphorylation and calcium influx, making it difficult for the BCR to top these signals.

## 1.4 The Kaposi's sarcoma-associated herpes virus (KSHV)

### 1.4.1 General facts

One of the most common cancers in AIDS patients is Kaposi's sarcoma (KS). It is characterized by skin lesions, leaky blood vessels, and extravasated red blood cells. The tumor cells of KS (called KS-cells) are spindle-shaped and show features of lymphatic and vascular endothelium (Mesri *et al.*, 2010). In 1994 a new γ-herpes virus was discovered in KS-cells termed the Kaposi's sarcoma-associated herpes virus (KSHV). KSHV, like EBV, is transmitted via saliva and can infect endothelial as well as B cells. In both cell types, it can induce cancer. *In vitro* KS-cells are dependent on cytokines and growth factors suggesting that KSHV alone is not sufficient to transform these cells (Mesri *et al.*, 2010). KSHV can also cause B cell lymphoma, namely Primary effusion lymphoma (PEL) and Multicentric Castleman's disease (MCD), which are often observed in AIDS patients. Whereas 80% of PEL cells are EBV positive, co-infection of MCD cells with EBV has not been detected (Jenner & Boshoff, 2002). PEL but not MCD cells show hypermutated Ig genes indicating that PEL cells originate from post-GC B cells and MCD cells from naive B cells (Jenner & Boshoff, 2002).

### 1.4.2 KSHV genes expressed during the latent phase

Like other herpes viruses, KSHV shows a latent and a lytic phase in its life cycle. Latency is characterized by a circular, viral episome and the expression of a few latent genes, only. Progeny virus is not produced. It is not clear yet whether KSHV shows different latency programs similar to EBV, but the endothelial cancer KS and the B cell lymphoma PEL show different expression patterns of latent KSHV genes. Commonly, they express

LANA (latency-associated nuclear antigen), v-FLIP (viral FLICE (Fas-associated death-domain like IL-1 β-convertase enzyme) inhibitory protein), v-Cyclin (viral cyclin), kaposins, and viral miRNAs (Wen & Damania, 2010). B but not endothelial cells express v-IRF3 (viral interferon regulatory factor 3) (Rivas *et al.*, 2001).

LANA is a functional homolog of EBV's EBNA1 and important for viral genome maintenance. It also inhibits apoptosis (via binding to the tumor-suppressor protein p53) and transactivates different cellular promoters. v-FLIP inhibits apoptosis, promotes cell survival by inducing NF-κB (Wen & Damania, 2010) and is responsible for the spindle-like morphology of KS cells (Grossmann *et al.*, 2006). v-Cyclin is a homolog of cellular cyclin D, which induces cell cycle progression and thus proliferation (Li *et al.*, 1997). Kaposins are important for signaling and induce cytokine production (Mesri *et al.*, 2010). v-IRF3 inhibits apoptosis by inducing the overexpression of p53 and influences the production of antiviral interferons (Wies *et al.*, 2009). miRNAs encoded by KSHV are involved in the suppression of lytic cycle reactivation and influence endothelial cell differentiation and angiogenesis (Mesri *et al.*, 2010).

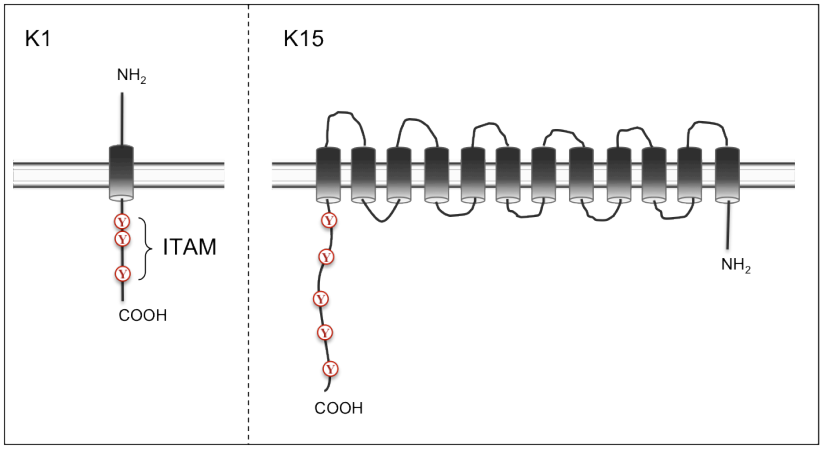


**Figure 1-8: Structure of the KSHV proteins K1 and K15**
Both, K1 and K15, are transmembrane proteins. K1 contains only one transmembrane domain, its C-terminal signaling domain encompasses an ITAM similar to LMP2A and the BCR. K15 contains 12 transmembrane domains and a long C-terminal signaling domain, it harbors five tyrosines but no ITAM.

It is not clear whether K1, K2 (v-IL6), and K15 are latent genes. Recently, low level mRNA transcripts of K1 and v-IL6 have been detected in latently infected cells (Chandriani & Ganem, 2010). v-IL6 is a homolog of the human IL-6 cytokine, which stimulates B cell survival and differentiation (Chandriani & Ganem, 2010). K1, like

LMP2A, contains an ITAM and is thought to be a BCR mimic (Figure 1-8). The viral K15 gene is in a position of the viral genome comparable to LMP2A's gene locus and shows signaling capacities similar to LMP1 and LMP2A. Both, K1 and K15 are upregulated upon lytic cycle induction (Chandriani & Ganem, 2010).

### 1.4.3 K1

K1 is a type I transmembrane protein and consists of an extracellular N-terminus and an intracellular C-terminus (Figure 1-8).

The extracellular domain of K1 shows 50-70% homology to the λ light chain and Ig-α of the BCR (Lee *et al.*, 2003) and it also contains conserved and variable regions (Lee *et al.*, 2005). The extracellular domain is responsible for self-oligomerization making K1 constitutively active (Lagunoff *et al.*, 1999), but clustering of K1 via an α-K1 antibody induces further increase in K1 signaling (Lee *et al.*, 2003). The extracellular domain of K1 might also downregulate BCR's surface expression and might abrogate its signaling by inhibiting the transport of the IgM from the endoplasmic reticulum to the plasma membrane (Lee *et al.*, 2000).

The intracellular C-terminus of K1 contains an ITAM similar to the one of LMP2A and the Ig-α/β chains of the BCR. In a CD8-K1 chimeric protein, the cytoplasmic part of CD8 was replaced by the cytoplasmic part of K1. Clustering of the CD8-K1 chimera by α-CD8 antibody induced tyrosine phosphorylation and calcium influx (Lee *et al.*, 1998). It could be shown, that the ITAM of K1 interacts with phosphorylated Syk and PLCγ2 (Lagunoff *et al.*, 1999). K1 also activates the PI3K/Akt pathway and inhibits the negative regulator of this pathway, the phosphatase and tensin homolog (PTEN) (Tomlinson & Damania, 2004).

As KSHV's K1 membrane protein activates signaling cascades also activated by the BCR or LMP2A, K1 might be a functional homolog of these proteins.

### 1.4.4 K15

The K15 gene is located next to KSHV's terminal repeats but does not span them as LMP2A does. The K15 mRNA is alternatively and multiply spliced. The most prominent transcript contains eight exons, which encode 12 transmembrane domains, a long C-terminus, and a short N-terminus (Choi *et al.*, 2000) (Figure 1-8). Alternative transcripts contain fewer transmembrane domains and do not show signaling activity (Brinkmann *et al.*, 2003). The eight-exon transcript is translated into a protein of app. 45kDa, which is associated with lipid rafts (Choi *et al.*, 2000; Brinkmann *et al.*, 2003). In uninduced PEL cells, a 23kDa K15-isoform could be detected with an antibody directed against the C-terminal domain. In contrast to the 45kDa K15 transcript, expression of the 23kDa isoform decreased upon lytic cycle induction (Sharp *et al.*, 2002). Besides these splice variants, two different K15 open reading frames have been found in different PEL isolates, the predominant (P) type and the minor (M) type. They show similar splicing pattern and protein structure but show a sequence homology of only 30% (Glenn *et al.*, 1999; Poole *et al.*, 1999).

Expression of the 45kDa K15 transcript could be detected in unstimulated PEL cells and increased upon tetradecanoylphorbol acetate (TPA)- mediated induction of KSHV's lytic phase. Since 5% of uninduced PEL cell lines express lytic marker genes, it is not clear whether *K15* is a latent or a lytic gene (Chandriani & Ganem, 2010).

K15 contains three discernable domains: the proline-rich motif, a TRAF binding site, and a pair of potential SH2-domains. The proline-rich motif ($PP_{387}PLPP$) could serve as an SH3-binding site (Brinkmann & Schulz, 2006). Co-transfection of K15 and intersectin 2 in DG75 B cells shows a co-localization of both proteins. Intersectin 2 contains a SH3-domain and regulates endocytosis. Thus, binding of K15 to intersectin 2 may play a role in protein trafficking and might, thereby, lead to the downregulation of BCR signaling (Lim *et al.*, 2007). In biochemical assays, Lyn could also bind to the potential SH3-binding site of K15 (Pietrek *et al.*, 2010).

K15 can also interact with tumor necrosis factor (TNF) receptor-associated factors (TRAFs) similar to LMP1. TRAFs regulate cell death, survival, and cellular stress

responses (Bradley & Pober, 2001). Furthermore, K15 activates the Mitogen-activated protein (MAP) kinase c-jun-N-terminal kinase (JNK) and the transcription factors KF-κB and AP-1 similar to LMP1.

K15 also shares features with LMP2A. In a CD8-K15 chimera, in which the C-terminus of K15 replaces the cytoplasmic part of CD8, the potential SH2-domain (DDLY$_{481}$EEVL) of K15 is constitutively phosphorylated (Choi *et al.*, 2000). Furthermore, CD8-K15 downregulates BCR signaling, a feature, which is dependent on the putative SH3 and SH2 (Y$_{481}$) motifs. The SH2 motif is also a binding site for Lyn (Brinkmann *et al.*, 2003), but, in contrast to LMP2A, K15 does not bind Syk (Cho *et al.*, 2008). The second putative SH2-binding site (VFGY$_{431}$ASIL) is involved in the inhibition of apoptosis via binding to Hax-1, an inhibitor of the pro-apoptotic protein Bax (Sharp *et al.*, 2002). The SH2- and SH3-binding sites of K15 together were shown to inhibit BCR signaling as measured by calcium-influx upon BCR stimulation (Pietrek *et al.*, 2010).

The conclusions are mostly based on studies with overexpressed recombinant K15 protein and cellular lysates to study binding partners of K15 (Sharp *et al.*, 2002). Signaling was mainly studied in transiently transfected epithelial or B cells (Choi *et al.*, 2000; Brinkmann *et al.*, 2003; Cho *et al.*, 2008; Pietrek *et al.*, 2010), but up to now, it has not been addressed whether K15 influences B cell survival and proliferation in primary human B cells.

# 2 Objectives

Hodgkin-Reed Sternberg (HRS) cells are the genuine tumor cells of Hodgkin's lymphoma. They are B cells by many criteria, but not all express the lineage-specific BCR. One of the key criteria is that they passed the steps of somatic hypermutation in GC because their Ig genes are hypermutated. BCR-negative ($BCR^-$) B cells normally undergo apoptosis, but all $BCR^-$ HRS cells are infected with EBV expressing LMP2A. It seems that LMP2A is a constitutively active BCR mimic and provides the necessary survival signals *in vivo*. The group of Richard Longnecker demonstrated in a mouse model that LMP2A expression enabled $BCR^-$ B cells to leave the bone marrow and home to secondary lymphoid organs (Caldwell *et al.*, 1998; Caldwell *et al.*, 2000; Merchant *et al.*, 2000). My work group analyzed mixed populations of $BCR^+$ and $BCR^-$ B cells infected with wt EBV or LMP2A-knock out virus (ΔLMP2A) and studied their phenotypes with respect to cellular transformation and proliferation. Lymphoblastoid cell lines (LCLs), generated from primary B cells infected with wt EBV, contained both $BCR^+$ and $BCR^-$ cells, whereas LCLs generated from ΔLMP2A EBV infection were always $BCR^+$. wt EBV but not ΔLMP2A EBV infection rescued $BCR^-$ sorted GC B cells from apoptosis (Mancao *et al.*, 2005; Mancao & Hammerschmidt, 2007). $BCR^+$ LCLs, which express an inducible LMP2A:mCD69 chimeric protein, were used to compare signaling cascades induced by LMP2A and BCR. Cross-linking of LMP2A:mCD69 or the endogenous BCR demonstrated that both receptors can equally induce phosphorylation of signaling mediators, $Ca^{2+}$-influx, and transcription of similar sets of genes (Medele, 2010). These results indicated that BCR and LMP2A are functional mimics and explained how LMP2A can rescue $BCR^-$ HRS cells from apoptosis.

The aim of my project is to compare the effect of BCR and LMP2A signaling shortly after infection of primary B cells because the previous studies were performed in longtime established LCLs. The cells could have adapted to artificial *in vitro* culture conditions or might have acquired additional somatic mutations overtime (Sugimoto *et al.*, 2004). In addition, latently infected B cells with an expression program similar to LCLs do not prevail in healthy individuals. Therefore, I wished to investigate the functions of LMP2A and the BCR in *ex vivo* isolated primary B cell subpopulations, which could be either

$BCR^+$ or $BCR^-$. The contribution of LMP2A or BCR signaling to the initial survival of EBV-infected B cells is of particular interest.

To this end, I will take advantage of the bacterial artificial chromosome (BAC) encoding the EBV genome (maxi-EBV) established in our lab (Delecluse *et al.*, 1998) and construct two mutant EBVs. In these mutants, the *LMP2A* gene will be replaced by genes encoding either LMP2A:mCD69 (see section 1.3.4.3) or a NP-specific mIgM (see section 1.2.5). The onset and strength of LMP2A:mCD69 and mIgM signaling can be controlled by adding α-mCD69 antibody or NP-antigen. The phenotype of primary B cells infected with the conditional EBV mutants in the presence or absence of the signaling inducers will be informative and reveal the contributions of LMP2A or BCR or both to cellular survival and proliferation control.

KSHV is another human γ-herpes virus classified as a tumor virus like EBV. Similar to EBV, KSHV is associated with rare Primary effusion lymphomas, which are derived from GC B cells (see section 1.4.1). The two KSHV proteins K1 and K15 partially resemble EBV's LMP2A in structure and function. To date, it is unclear whether they can also mimic the function of the BCR. To address this possibility, mutant EBVs with *K1* or *K15* genes replacing the *LMP2A* gene will be generated, and infection experiments will reveal whether they can rescue $BCR^-$ B cells from apoptosis similar to LMP2A. The likely effect of K1 and K15 expression on tyrosine phosphorylation, B cell activation, and cytokine production will be investigated shortly after infection. Finally, I want to assess whether K1 and K15 can block BCR signaling similar to LMP2A.

Infection studies with KSHV and primary B cells are difficult because the rate of KSHV infection is low (5-30% 48h post infection), and the infected B cells do not establish a traceable phenotype (Rappocciolo *et al.*, 2008; Chandran, 2010; Lu *et al.*, 2011; Myoung & Ganem, 2011). Very much in contrast, EBV efficiently infects primary quiescent naive or memory B cells and activated GC B cells. Recombinant EBVs, which carry KSHV genes, are an interesting tool to study heterologous viral genes with respect to survival, differentiation, and proliferation of primary B cells.

# 3 Materials

## 3.1 Plasmids and bacteria strain

### 3.1.1 Maxi-EBV plasmids

The following list contains all maxi-EBV plasmids I used in my thesis.

| Plasmid | Bacteria strain containing the maxi-EBV plasmid | Description of maxi-EBV plasmid |
|---|---|---|
| p2089 | sw105 | codes for wt EBV |
| p2525 | DH5α | promoter and first exon of *LMP2A* is deleted, *LMP2A* is not expressed |
| p3991 | sw105 | *galK* inserted downstream of the first exon of *LMP2A*, derived from p2089 by homologous recombination |
| p3993 | sw105 | *mCD69* fragment inserted downstream of first exon of *LMP2A*, codes for *LMP2A:mCD69*, does not express *LMP2A*, derived from p3991 by homologous recombination |
| p3995 | sw105 | *galK* replacing the first exon of LMP2A, derived from p2089 by homologous recombination |
| p3998 | sw105 | KSHV *K15* replacing the first exon of *LMP2A*, derived from p3995 by homologous recombination |
| p4082 | sw105 | KSHV *K1* replacing the first exon of *LMP2A*, derived from p3995 by homologous recombination |
| p4090 | sw105 | NP-specific murine *IgM* replacing the first exon of *LMP2A*, derived from p3995 by homologous recombination |
| p4251 | sw105 | *galK* replacing the *LMP2A*-promoter, codes for *LMP2A:mCD69*, does not express *LMP2A*, derived from p3993 by homologous recombination |
| p4252 | sw105 | CAG promoter driven *LMP2A:mCD69* replacing the *LMP2A*-promoter and the first exon of *LMP2A*, does not express *LMP2A*, derived from p4251 by homologous recombination |
| p4253 | sw105 | *galK* replacing the *LMP2A*-promoter and the NP-specific murine *IgM* replacing the first exon of *LMP2A*, does not express *LMP2A*, derived from p4090 by homologous recombination |
| p4254 | sw105 | CAG promoter driven NP-specific murine *IgM* replacing the *LMP2A*-promoter and the first exon of *LMP2A*, does not express *LMP2A*, derived from p4253 by homologous recombination |
| p4489 | sw105 | CAG-promoter followed by a loxP-stop-loxP cassette and the *LMP2A:mCD69* gene replacing the *LMP2A*-promoter and the first exon of *LMP2A*, derived from p4251 by homologous recombination |

The sw105 strain is a modified DH10B *Escherichia coli (E. coli)* strain containing the defective lambda prophage and an arabinose-inducible *flpe* gene; DH10B[λ*cI*857(*cro-bio*A)<>*ara*C- P$_{BAD}$*flpe*]. Additionally, it carries a functional *gal* operon, except for a deletion of *galK,* and stems from the strain EL250 (Warming *et al.*, 2005). The DH5α

*E. coli* strain has the following genotype: F-, lacl-, recA1, endA1, hsdR17, Δ(lacZYA- argF), U169, F80d lacZΔM15, supE44, thi-1, gyrA96, relA1.

I established all plasmids and bacteria strains besides p2089/sw105 and p2525/DH5α. The p2089 maxi-EBV was established by Delecluse et al. 1998 and introduced into the sw105 strain by W. Hammerschmidt. The p2525 maxi-EBV was established and introduced into the DH5α strain by C. Mancao (Mancao & Hammerschmidt, 2007).

### 3.1.2 High-copy plasmids

The following list contains all high-copy plasmids that I used in my thesis.

| Plasmid | Bacteria strain containing the plasmid | Description of plasmid |
|---|---|---|
| p509 | DH5α | expression plasmid for BZLF1 |
| p2670 | DH5α | expression plasmid for BALF4 |
| pgalK | DH5α | expression plasmid for galactokinase K (galK) |

## 3.2 Bacteria media and selection plates

The following list contains all bacteria media and selection plates that I used in my thesis.

| Name | Application | Ingredients |
|---|---|---|
| LB medium | medium for liquid bacteria culture | 1% (w/v) tryptone<br>1% (w/v) NaCl<br>0.5% (w/v) yeast extract |
| LB agar plates | plates for cultivation of bacteria | LB medium with 1.5% (w/v) select agar |
| M9 salt medium<br>(1 l, autoclaved) | Transfected sw105 bacteria were washed in M9 salt medium to remove any carbohydrates before plating on galactose or DOG selection plates. | 6g $Na_2HPO_4$<br>3g $KH_2PO_4$<br>1g $NH_4Cl$<br>0.5g NaCl |
| 5x M63 medium<br>(1 l, autoclaved) | used for preparation of galactose and DOG selection plates | 10g $(NH_4)_2SO_4$<br>68g $KH_2PO_4$<br>2.5mg $FeSO_4$ x $7H_2O$<br>adjust to pH 7 with KOH |
| Galactose plates<br>(1 l, autoclaved) | used for positive selection of sw105 bacteria clones that encode the *galactokinase K* (*galK*) gene | 15g agar + 800ml $ddH_2O$<br>→ autoclave, cool down to 50°C<br>add sterile additives:<br>200ml 5XM63 medium<br>1ml 1M $MgSO_4$ x $7H_2O$<br>10ml 20% galactose<br>5ml 0.2mg/ml D-biotin<br>4.5ml 10mg/ml L-leucin<br>500µl 30µg/ml chloramphenicol |
| McConkey plates<br>(1 l, autoclaved) | indicator plate used to verify expression of galK, $galK^+$ bacteria colonies turn pink and $galK^-$ bacteria colonies stay white | 15g agar + 800ml LB medium<br>→ autoclave, cool down to 50°C,<br>add sterile additives:<br>10ml 20% galactose<br>500µl 30µg/ml chloramphenicol |

| | | |
|---|---|---|
| DOG plates<br>(1 l, autoclaved) | used for negative selection of galK$^-$ sw105 colonies | 15g agar + 800ml dd$H_2O$<br>→ autoclave, cool down to 50°C,<br>add sterile additives:<br>200ml 5XM63 medium<br>1ml 1M $MgSO_4$ x $7H_2O$<br>10ml 20% glycerol<br>10ml 20% DOG<br>5ml 0.2mg/ml D-biotin<br>4.5ml 10mg/ml L-leucin<br>500µl 30µg/ml Cm |

## 3.3 Primary eukaryotic cells

Primary human B cells were isolated from adenoids from children younger than six years of age to minimize the risk of wild type EBV infection. Adenoids were received from the children hospital „Kinderklinik Dritter Orden“ in Munich and the university hospital „Universitätsklinikum Großhadern“ from the Ludwig-Maximilians-University Munich.

## 3.4 Eukaryotic cell lines

All cell lines that I used in my thesis are recorded below.

| Cell line | Description | Source |
|---|---|---|
| HEK293 | human embryonic kidney cells, transformed by transfection of sheared fragments of adenovirus type 5 DNA (Graham *et al.*, 1977). | available in the Department of Gene Vectors at the Helmholtz Zentrum München |
| HEK293/p2089 (wt) | HEK293 cell lines stably transfected with the wt (p2089) maxi-EBV plasmid, used to produce wt EBV particles | established by me |
| HEK293/p2525 (ΔLMP2A) | HEK293 cell lines stably transfected with the ΔLMP2A (p2525) maxi-EBV plasmid, used to produce ΔLMP2A EBV particles | established by C. Mancao (Mancao *et al.*, 2005) |
| HEK293/p3991 (LMP2A:mCD69) | HEK293 cell lines stably transfected with the LMP2A:mCD69 (p3991) maxi-EBV plasmid, used to produce LMP2A:mCD69 EBV particles | established by me |
| HEK293/p3998 (K15) | HEK293 cell lines stably transfected with the K15 (p3998) maxi-EBV plasmid, used to produce K15 EBV particles | established by me |
| HEK293/p4082 (K1) | HEK293 cell lines stably transfected with the K1 (p4082) maxi-EBV plasmid, used to produce K1 EBV particles | established by me |
| HEK293/p4254 (NP-mIgM) | HEK293 cell lines stably transfected with the NP-mIgM (p4254) maxi-EBV plasmid, used to produce NP-mIgM EBV particles | established by me |
| Raji | human, EBV$^+$ Burkitt's-lymphoma cell line, used to determine the EBV titer of HEK293/p2089, p2525, p3991, p3998, p4082, p4253 supernatants (Pulvertaft, 1964) | available in the Department of Gene Vectors at the Helmholtz Zentrum München |

| | | |
|---|---|---|
| wt LCLs | lymphoblastoid cell lines, established by infection of human, adenoid, primary B cells with wt EBV particles obtained from HEK293/p2089 cell supernatant | established by me |
| wt LCL (clone A16) | clonal lymphoblastoid cell line, established by infection of human, adenoid, primary B cells with wt EBV particles obtained from HEK293/p2190 cell supernatant. The cell line contains crippled mutations in the Ig genes and does not express a BCR. (Mancao *et al.*, 2005). | established by C. Mancao (Mancao *et al.*, 2005) |
| ΔLMP2A LCLs | lymphoblastoid cell lines, established by infection of human, adenoid, primary B cells with ΔLMP2A EBV particles obtained from HEK293/p2525 cell supernatant | established by me |
| LMP2A:mCD69 LCLs | lymphoblastoid cell lines, established by infection of human, adenoid, primary B cells with LMP2A:mCD69 EBV particles obtained from HEK293/p3991 cell supernatant. | established by me |
| CMV-LMP2A:mCD69 LCL | clonal lymphoblastoid cell line, established by infection of human, adenoid, primary B cells with p3696 EBV particles obtained from the packaging cell line HEK293/TR$^-$ (Medele, 2010) | established by D. Pich (Medele, 2010) |
| NP-mIgM LCLs | lymphoblastoid cell lines, established by infection of human, adenoid, primary B cells with NP-mIgM EBV particles obtained from HEK293/p4254 cell supernatant | established by me |
| K1 LCLs | lymphoblastoid cell lines, established by infection of human, adenoid, primary B cells with K1 EBV particles obtained from HEK293/p4082 cell supernatant | established by me |
| K15 LCLs | lymphoblastoid cell lines, established by infection of human, adenoid, primary B cells with K15 EBV particles obtained from HEK293/p3998 cell supernatant | established by me |
| L929 | L929 is a subclone of the parental L strain, which is derived from normal subcutaneous areolar and adipose tissue of a 100-day-old male C3H/An mouse (Sanford *et al.*, 1948) | available in the Department of Gene Vectors at the Helmholtz Zentrum München |
| hCD32$^+$ L-cells | derived from the murine fibroblast cell line Ltk- (L strain cells deficient for the thymidin kinase (Kit *et al.*, 1963)), which were stably transfected with the hCD32 receptor (Stuart *et al.*, 1987) | available in the Department of Gene Vectors at the Helmholtz Zentrum München |
| TK- | Abelson leukemia virus-transformed murine pre-B cell line (Keyna *et al.*, 1995) | obtained from Prof. Hans-Martin Jäck, University Erlangen |
| TKμ | μ heavy chain-transfected, Abelson leukemia virus-transformed murine pre-B cell line (Keyna *et al.*, 1995) | obtained from Prof. Hans-Martin Jäck, University Erlangen |
| J558L | murine plasmacytoma cell line (Gillies *et al.*, 1983) | obtained from Prof. Hans-Martin Jäck, University Erlangen |

## 3.5 Cell culture media for eukaryotic cells

Cell culture media and additives that I used in my thesis are recorded in the following list.

| Name | Application | Source |
|---|---|---|
| RPMI 1640 | cell culture medium for cultivation of all used cell lines | Invitrogen GmbH |
| Opti-MEM | used during cell transfection | Invitrogen GmbH |
| fetal calf serum (FCS) | nutritive substance (additive for RPMI 1640) | Chromatech |
| penicillin/streptomycin | antibiotics (additive for RPMI 1640) | Invitrogen GmbH |
| cyclosporin A | inhibits T cell and NK cell activity | Sigma-Aldrich |
| sodium pyruvate | antioxidant agent (additive for RPMI 1640) | Invitrogen GmbH |
| α-thioglycerol and bathocuproin disulfonat | antioxidant agent (additive for RPMI 1640) | Sigma-Aldrich |
| sodium selenite | antioxidant agent (additive for RPMI 1640) | Sigma-Aldrich |
| α-tocopherol | antioxidant agent (additive for RPMI 1640) | Sigma-Aldrich |
| β–mercaptoethanol | antioxidant agent (additive for RPMI 1640) | Sigma-Aldrich |
| hygromycin B | antibiotic for the selection of eukaryotic cells | PAA Laboratories GmbH |

## 3.6 Antibodies

### 3.6.1 Antibodies and staining reagents for flow cytometry

The following list records all antibodies and staining reagents that I used for surface molecule analysis and flow cytometry.

| Antibody specificity | Species | Fluorophore | Source | Comment |
|---|---|---|---|---|
| hCD19 | mouse | Biotin | BD Biosciences | clone HIB19 |
| hCD23 | mouse | APC | eBioscience | clone EBVCS2 |
| hCD27 | mouse | APC | BD Biosciences | clone L128 |
| hCD30 | mouse | APC | BioLegend | clone BY88 |
| hCD32 | mouse | Alexa647 | BioLegend | clone FUN-2 |
| hCD38 | mouse | PE | eBioscience | clone HIT2 |
| hCD54 | mouse | APC | Immunotools | clone 1H4 |
| hCD56 | mouse | PE | BD Biosciences | clone NCAM16.2 |
| hCD86 | mouse | APC | BD Biosciences | clone 2331 (FUN-1) |
| mB220 | rat | FITC | BD Biosciences | clone RA3-6B2 |
| mIgM | goat | DyLight | Jackson Research | polyclonal |

h: human, m: mouse

| Staining reagent | Species | Fluorophore | Source | Comment |
|---|---|---|---|---|
| $NP_{18}$-BSA | - | Biotin | Biosearch Technologies | |
| Streptavidin | - | PE-Cy7 | eBioscience | |

### 3.6.2 Antibodies for cell sorting

The following list records all antibodies that I used for cell sorting.

| Antibody specificity | Species | Fluorophore | Source | Comment |
|---|---|---|---|---|
| hκ-light chain | mouse | APC | Invitrogen | clone HP6062 |
| hλ-light chain | mouse | FITC | Invitrogen | clone HP6064 |
| hCD3 | mouse | PE | Immunotools | clone MEM-57 |

h: human

### 3.6.3 Antibodies and NP-antigen for cell stimulation

The following list records all antibodies and the NP-antigen used for cell stimulation.

| Antibody specificity | Species | Molecule | Source | Comment |
|---|---|---|---|---|
| hIgG/M | goat | H+L | Jackson Research | |
| hIgG/A/M | goat | $F(ab')_2$ | Jackson Research | used for calcium flux assay |
| mCD69 | armenian hamster | H+L | Hybridom supernatant from S. Medele, purified by E. Kremmer | |
| armenian hamster | goat | H+L | Jackson Research | |
| mIgM (b7-6) | rat | H+L | Obtained from H.-M. Jäck (University Erlangen) | (Shulman *et al.*, 1982) |

h: human, m: mouse

| NP-antigen | Species | Fluorophore | Source | Comment |
|---|---|---|---|---|
| $NP_{26}$-BSA | - | - | Biosearch Technologies | |

### 3.6.4 Phosphospecific antibodies

The following list records all antibodies that I used for phosphospecific flow cytometry.

| Antibody specificity | Species | Fluorophore | Source | Comment |
|---|---|---|---|---|
| pSyk | mouse | Alexa647 | BD Biosciences | pTyr352 |
| pPLCγ2 | mouse | Alexa647 | BD Biosciences | pTyr759 |

### 3.6.5 Antibodies for Western Blot analysis

The following list records all antibodies that I used for Western Blot analysis.

| Antibody specificity | Species | Conjugate | Source |
|---|---|---|---|
| mμ-heavy chain | goat | HRP | SouthernBiotech |
| mλ-light chain | goat | HRP | SouthernBiotech |
| actin | mouse | - | Sigma-Aldrich |
| mouse | horse | HRP | Cell Signaling |

h: human, m: mouse

## 3.7 Kits

All kits that I used in my thesis are listed below.

| Kit | Application | Source |
|---|---|---|
| NucleoSpin Extract II Kit | PCR-clean up and gel-extraction | Macherey-Nagel |

| | | |
|---|---|---|
| RNeasy Mini Kit | isolation of RNA from cells | Qiagen |
| DNase I Amplification Grade | removal of DNA contaminants from RNA preparations | Invitrogen |
| SuperScript™ III First Strand cDNA Synthesis Kit | reverse transcription of cellular mRNA into cDNA | Invitrogen |
| Human IL-2, IL-6, IL-8, IL-10 FlowCytomix™ Simplex kits, Human FlowCytomix™ Basic kit | IL-2, IL-6, IL-8, IL-10 cytokine analysis of cell supernatant | eBioscience |

## 3.8 Stock solutions and buffers

The following lists record all stock solutions and buffers that I used in my thesis.

### 3.8.1 Plasmid DNA preparation from bacteria

| Name | Ingredients |
|---|---|
| lysis buffer | 1% SDS<br>0.2N NaOH |
| solution I | 50mM glucose<br>25mM Tris-HCl, pH 8<br>10mM EDTA |
| solution II | 0.4% SDS<br>0.2N NaOH |
| solution III<br>(store at 4°C) | 3M $C_2H_3KO_2$<br>2M glacial acetic acid |
| normal TE buffer | 10mM Tris-HCl, pH 8<br>1mM EDTA |
| special TE buffer | 50mM Tris-HCl, pH 8<br>20mM EDTA |

### 3.8.2 Agarose gel electrophoresis

| Name | Ingredients |
|---|---|
| TAE | 40mM Tris-HCl, pH 8<br>20mM glacial acetic acid<br>1mM EDTA |
| agarose loading dye | 1mg/ml bromophenol blue<br>1mg/ml xylene cyanol<br>50% sucrose |

### 3.8.3 Flow cytometry

| Name | Ingredients |
|---|---|
| PBS, pH 7.3 | 10mM $Na_2HPO_4$<br>1.8mM $KH_2PO_4$<br>140mM NaCl<br>2.7mM KCl |
| staining buffer | 2% FCS<br>2mM EDTA<br>in PBS |

| | |
|---|---|
| sorting buffer | 0.5% FCS<br>2mM EDTA<br>in PBS |
| phosflow buffer | 0.5% BSA<br>0.02% sodium azide<br>in PBS |

### 3.8.4 Cell lysis

| Name | Ingredients |
|---|---|
| RIPA buffer | 50mM Tris-HCl, pH 8<br>150mM NaCl<br>0.1% SDS<br>1% NP-40<br>0.5% DOC<br>1 tablet of Complete Mini Protease Inhibitor (Roche) / 10ml RIPA buffer |

### 3.8.5 SDS-polyacrylamide gel electrophoresis (PAGE)

| Name | Ingredients |
|---|---|
| separation gel (12%), 10ml | 4ml 30% acryl amide<br>1.66ml 2M Tris-HCl, pH 8.9<br>66.7µl 0.5M EDTA<br>100µl 10% SDS<br>10µl TEMED<br>70µl 10% APS<br>add $ddH_2O$ to 10ml |
| stacking gel (5%), 50ml | 6.7ml 30% acryl amide<br>7.5ml 2M Tris-HCl, pH 6.8<br>400µl 10% SDS<br>50µl TEMED<br>350µl 10% APS<br>36ml $ddH_2O$ |
| 10 x running buffer, 1l | 30g Tris/Base<br>144g glycine<br>100ml 10% SDS<br>add $ddH_2O$ to 1l |
| 5 x Laemmli buffer, 50ml | 6.25ml 2M Tris-HCl, pH 6.8<br>5g 10% SDS<br>3.9g DTT<br>0.2% bromophenol blue<br>25ml 50% glycerol<br>add $ddH_2O$ to 50ml |

### 3.8.6 Western Blot analysis

| Name | Ingredients |
|---|---|
| 1 x transfer buffer | 3g Tris/Base<br>14g glycine<br>200ml methanol<br>add $ddH_2O$ to 1l |
| blocking buffer | 5g non-fat milk powder<br>100ml PBS-T |
| PBS-T | 0.1% Tween-20 in PBS |

## 3.9 Primer-pairs for quantitative real-time PCR (qRT-PCR)

The following primer pairs were used for qRT-PCR. The numbers behind the primer sequences refer to the lab nomenclature.

| Name | Forward primer (5'→3') | Backward primer (5'→3') |
|---|---|---|
| LMP2A | CGTCACTCGGACTATCAACC (P105) | TACAGGCAGGCATACTGGAT (P104) |
| K1 | GGAGTGATTTCAACGCCTTA (P117) | GCCATGTAATCCAAATGCTC (P114) |
| K15 | GGGCCCTACTGGTATGTTTT (P109) | GGATGAAGGCCATTTAGGAT (P110) |
| Clk2 | CTGACACATACAGACCTCAAGCCTG (IClk2/F7) | ACCAGCCCAACTCAAGGATGAC (IClk2/B12) |

## 3.10 Enzymes and Chemicals

The list below records all enzymes and chemicals that I used in my thesis.

| Source | Enzyme and Chemical |
|---|---|
| Applichem, Darmstadt | RNase A, lysozyme, Tween-20, disodium acetate ($Na_2HPO_4$), potassium acetate ($C_2H_3KO_2$) |
| Bayer AG, Leverkusen | Ciprobay (ciprofloxacin) |
| BD Biosciences, USA | BD Cytofix Fixation Buffer |
| Bio-Rad, Munich | Bradford-Solution |
| Biochrom AG, Berlin | PBS powder |
| Carl Roth GmbH, Karlsruhe | Rothiphorese Gel30 (acryl amide), bovine serum albumin fraction V (BSA) powder, milk powder |
| Fermentas, Leon-Roth | marker for DNA electrophoresis, restriction enzymes |
| Hoechst, Frankfurt | Hoechst-Dye H33342 |
| Invitrogen GmbH, Karlsruhe | agarose, Indo-1 AM, Luria broth base (LB), select agar, trypsin/EDTA |
| Merck-Eurolab GmbH, Darmstadt | cesium chloride (CsCl), acetic acid, ethanol, ethidium bromide, ethylene diamine tetra-acetic acid (EDTA), glucose, glycine, glycerol, isopropanol, potassium chloride (KCl), sodium chloride (NaCl), sodium hydroxide (NaOH), sodium dodecyl sulfate (SDS), sucrose, tetramethylethylenediamine (TEMED), methanol |
| New England Biolabs, Frankfurt | restriction enzymes, Phusion High-Fidelity DNA Polymerase |
| PAN-Biotech GmbH, Aidenbach | Pancoll human (Ficoll) |
| Promega, Mannheim | goTaq-Polymerase, RNasin plus RNase-inhibitor, |
| Roche Diagnostics GmbH, Mannheim | Complete Mini Protease Inhibitor Cocktail tablets, desoxy-nucleotides, LightCycler 480 SYBR Green I Master Mix, Tris-(hydroxymethyl)-aminomethan (Tris) |
| SERVA Electrophoresis GmbH, Heidelberg | sodium azide, ammonium persulfate (APS) |
| Sigma-Aldrich, Munich | Agarose, ampicillin, β-mercaptoethanol, bromophenol blue, chloramphenicol, dimethyl sulfoxide (DMSO), dithiothreitol (DTT), doxycycline, Igepal CA-630 (NP-40), Proteinase K, polyethylene imine (PEI), 5-azacytidine, 2-deoxy-D-galactose (DOG), McConkey agar No1, monopotassium phosphate ($KH_2PO_4$), xylene cyanol, deoxycholic acid (DOC) |

## 3.11 Consumables and Devices

Consumables and devices, which were used in this thesis, are listed below.

| Source | Consumables and Devices |
|---|---|
| AGFA, Cologne | CP1000 developer machine |

| | |
|---|---|
| Beckmann Coulter, Heidelberg | Coulter Counter Z1, ultracentrifuge L8-70M/XL-70, centrifuge Avanti J-25 and Avanti J-26XP, |
| Becton Dickinson GmbH, Heidelberg | FACS-Calibur, FACS-LSR II, FACS-Aria III, well-plates, FASC tubes |
| Bio-Rad, Munich | Gene-Pulser II electroporation device, spectrometer |
| Biozyme Scientific GmbH, Oldendorf | PCR tubes |
| Brand, Wertheim | glass pipettes |
| Carl Roth, Karlsruhe | sterile syringes and needles |
| Eppendorf, Hamburg | reaction tubes, thermomixer comfort |
| GE Healthcare, Munich | Hybond-ECL-Nitrocellulose membrane, ECL-solution |
| Greiner Bio One, Solingen | plastic consumables for cell culture and laboratory work |
| Hartenstein, Würzburg | Whatman paper, Neubauer cell chamber |
| Henry Schein Vet GmbH | Bovivet veterinary needle |
| Hitachi Koki Co., Ltd., Japan | desk centrifuge HIMAC CT15RE |
| Hoefer Scientific Instruments, USA | Semidry Blotting system |
| Nunc GmbH, Wiesbaden | cell culture dishes, cryo tubes |
| Peqlab, Erlangen | agarose gel chamber, NanoDrop ND-1000, electroporation cuvettes |
| Roche Diagnostics GmbH, Mannheim | Light Cycler 480 Real Time PCR system |
| Schleicher & Schüll, Dassel | 0.8 µm and 1.2 µm filter |
| Schott, Mainz | glass ware |
| Stratagene, Heidelberg | Robocycler Gradient 96 |
| Thermo Scientific, USA | Heraeus Multifuge 3L-R |
| Zeiss, Göttingen | fluorescence microscope Axiovert 200M |

## 3.12 Software

All used software is listed below.

| **Software** | **Source** |
|---|---|
| FlowJo | TreeStar Inc., Ashland (USA) |
| FlowCytomix™ Pro | eBioscience, San Diego (USA) |
| OriginPro | OriginLab, Northampton (USA) |
| Endnote | Thomson Reuters, New York (USA) |
| Adobe Illustrator | Adobe Systems Inc., San Jose (USA) |
| MacVector | Accelrys, Cambridge (UK) |

# 4 Methods

## 4.1 Cloning with the Maxi-EBV system

The recombeneering strategy developed by Warming and colleagues enables mutations in BACs without inserting a permanent, e.g. undesired selection marker (Warming *et al.*, 2005). The strategy is based on homologous recombination in *E. coli*, which makes use of three genes, *exo*, *bet,* and *gam,* adopted from the λ phage. A defective λ prophage was stably introduced into the *E. coli* genome, and a temperature sensitive repressor controls the recombination mediating genes. At 32°C, the repressor is active, transgenes are not expressed, and recombination is not supported. If the cells are cultured at 42°C for 15min the repressor is inactivated, the transgenes are expressed mediating homologous recombination of DNA. *Exo* codes for a 5'-3' exonuclease and creates 3'-overhangs to linear, double stranded DNA fragments introduced by transfection. *Bet* binds to the 3'-overhangs and promotes homologous recombination. *Gam* inhibits the *E. coli* exonuclease RecBCD and, thereby, prevents the degradation of the linear DNA cassette. An *E. coli* strain, termed sw105, that (i) expresses the recombination genes *exo*, *bet* and *gam* under control of the temperature sensitive repressor and (ii) contains the maxi-EBV plasmid p2089 was available in the lab. DNA cassettes that contain a sequence homologous to p2089 can be introduced in these cells by electroporation, undergo homologous recombination (mediated by *exo*, *bet,* and *gam*), and become inserted into the p2089 maxi-EBV plasmid DNA.

The *E. coli* strain sw105 does not only contain the genes *exo*, *bet,* and *gam* but the entire galactose operon with the exception of the *galactokinase K* gene (*galK*). *GalK* can be used as a positive and negative marker in this *galk*$^{-}$ sw105 *E. coli* strain. In a first step, positive selection is used. The introduced DNA cassette codes for the *galK* gene, which is flanked by sequences that are homologous to target sites in p2089. Bacteria that have successfully recombined *galK* into p2089 can grow on minimal plates that contain galactose as the only carbon source. Single colonies are picked and struck on a McConkey indicator plate containing galactose as carbon source. When *galK*$^{+}$ bacteria metabolize galactose, they produce acid and lower the pH. The indicator dye in the

McConkey agar changes its color to red. *GalK*$^{-}$ bacteria metabolize the peptone, which raises the pH of the agar leading to yellowish colonies. Accordingly, only bacteria from red colonies are used for further cloning steps. In the next step of recombination, the *galK* cassette is replaced by the gene of interest by negatively selecting *galK*$^{-}$ revertants. A cassette with the gene of interest flanked by homologous arms is introduced into the *galK*$^{+}$ bacteria replacing the *galK* gene. The bacteria are now grown on agar plates that contain glycerol as sole usable carbon source and 2-desoxy-galactose (DOG) as the

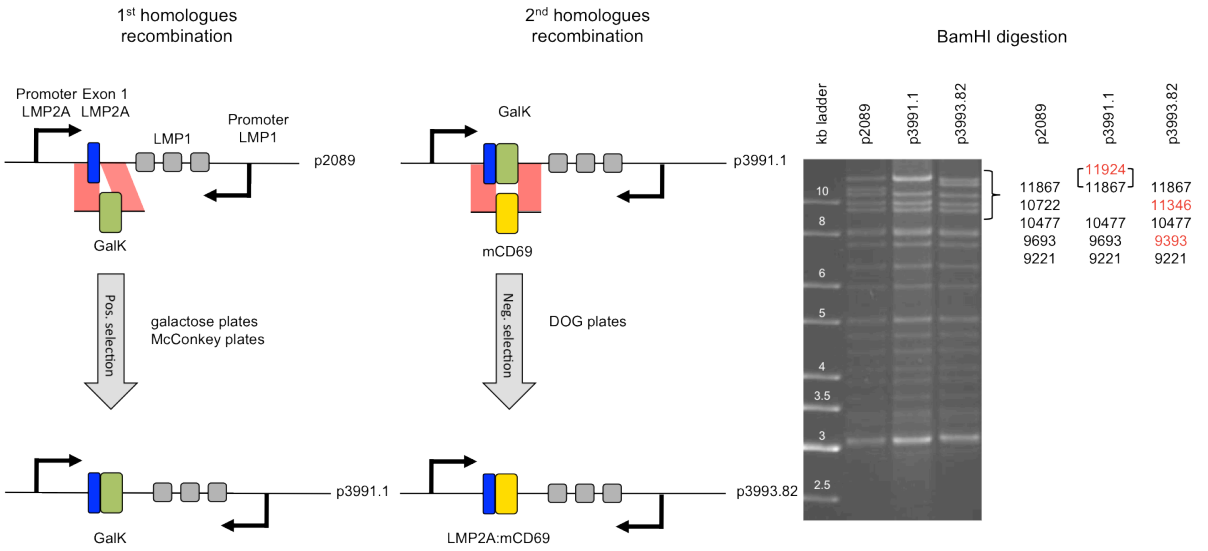


**Figure 4-1: Main steps of the recombineering strategy illustrated by cloning of the LMP2A:mCD69 maxi-EBV p3993.**
The recombineering strategy contains two rounds of homologous recombination and selection. First, a DNA cassette containing the *galactokinase K* gene (*galK*) flanked by sequences that are homologous (red) to the locus of interest in the p2089 maxi-EBV DNA plasmid was introduced into sw105 bacteria containing the p2089 maxi-EBV plasmid. The sw105 *E. coli* strain carries three transgenes (*exo*, *bet,* and *gam*) that promote homologous recombination but is devoid of the *galK* gene. Only bacteria that have successfully recombined *galK* can metabolize galactose and grow on galactose minimal plates. Single colonies were picked and grown on McConkey indicator plates also containing galactose as main carbon source. *GalK*$^{+}$ bacteria metabolize galactose, thereby lower the pH in the McConkey agar turning the colony red, whereas *galK*$^{-}$ colonies stay white. Red *galk*$^{+}$ colonies containing the new maxi-EBV, termed p3991, were used for the second step of homologous recombination whereby the *galK* gene was replaced by the cDNA coding for a truncated *murine CD69* (*mCD69*). Bacteria were grown on selection plates containing glycerol as carbon source and 2-desoxy-galactose (DOG) as selective compound. DOG is harmless unless it is metabolized to a toxic product by galK. Only bacteria that have deleted *galK* survived this negative selection. Correct insertion of the transgene had to be verified by digesting the derived maxi-EBV plasmid with the BamHI restriction enzyme. The fragment pattern was analyzed on an agarose gel (shown right) and compared with the expected fragment sizes. Changes in the fragment size due to correct homologous recombination are marked in red, bands smaller than 9221 kb were identical in DNA of p2089, p3991 and p3993. A correct LMP2A:mCD69 sequence was confirmed by BamHI digestion and sequencing for the maxi-EBV clone p3993.82.

selective compound. DOG itself is harmless but metabolized to a toxic product by the galK protein. During this negative selection, only bacteria that are *galK*$^-$ survive. The *galK* gene can be lost by the spontaneous deletion of the *galK* gene or through the anticipated recombination making it necessary to check the resulting constructs via restriction patterns and DNA sequencing.

Figure 4-1 illustrates the main cloning steps to construct the LMP2A:mCD69 maxi-EBV (p3993). It is used as a representative example to describe the detailed cloning procedure in the following sections.

### 4.1.1 Preparation of the *galK* cassette

The *galK* cassette contains the *galK* gene, which is flanked by DNA stretches that are homologous to sequences in p2089 as shown in Figure 4-1. The cassette was produced via PCR. The PCR primers contained 50 base pairs (bp) homologous to p2089 and bind with their 3' ends to the *galK* gene in the p*galK* plasmid. The primer sequence is shown below:

| Primer | Sequence (5'→3') |
|---|---|
| Forward | 50bp_homology_1st strand-CCTGTTGACAATTAATCATCGGCA-3' |
| Reverse | 50bp_homology_2nd strand -TCAGCACTGTCCTGCTCCTT-3' |

(Warming; Warming *et al.*, 2005)

A proof-reading Taq polymerase (e.g. Phusion from Finnzyme) was used, and the PCR mix was set up according to the manufacturer's protocol. The PCR program was as follows:

| Temperature (°C) | Time (s) | Number of Cycles |
|---|---|---|
| 94 | 30 | 1 |
| 94 | 45 | 15 |
| 54 | 45 | |
| 72 | 150 | |
| 94 | 45 | 20 |
| 62 | 45 | |
| 72 | 150 | |
| 72 | 300 | 1 |

The PCR product was DpnI digested to remove remaining p*galK* DNA. DpnI digests only the *E. coli* methylated plasmid but not the unmethylated PCR product. The PCR product was purified from the DpnI digested p*galk* plasmid fragments using the NucleoSpin

Extract II Kit according to manufacturer's protocol. The DNA was ethanol precipitated and diluted in double-deionized water ($ddH_2O$) for electroporation into sw105 bacteria containing the p2089 maxi-EBV.

### 4.1.2 Production of heat-shocked sw105 electro-competent bacteria

All maxi-EBV plasmids contain a chloramphenicol (Cm) resistance gene. 30ml LB medium, supplied with 15µg/ml Cm, was inoculated with a single p2089/sw105 colony and incubated over night at 32°C in a shaker. Next day, 25ml LB medium (containing 15µg/ml Cm) was inoculated with 1-2ml of the over night culture and incubated at 32°C in a shaker until the optical density measured at 600nm wavelength ($OD_{600}$) was approximately 0.6. 20ml of the sample was transferred to a new Erlenmeyer flask and incubated for 15min at 42°C in a shaking water bath. The heat shock induces the expression of the transgenes *exo*, *bet,* and *gam* necessary for homologous recombination. The culture was shortly cooled on ice, transferred in a round bottom Falcon tube, and spun down (4000rpm, 10min, 0°C). The supernatant was discarded and the bacteria pellet was diluted in 1ml ice-cold sterile $ddH_2O$ by shaking in the ice/water bath slurry. After dilution 9ml ice-cold $ddH_2O$ was added. The bacteria were again spun down (4000rpm, 10min, 0°C), washed in 10ml ice-cold $ddH_2O$, and spun down as described before. After the second washing, the supernatant was removed by inverting the tube on a paper towel. The bacteria pellet was diluted in the remaining solution (approximately 50µl) by shaking in the ice/water bath slurry and kept on ice until electroporation.

### 4.1.3 Electroporation of the *galK* cassette into electro-competent sw105 bacteria and subsequent positive selection

1µg PCR DNA (see section 4.1.1) and 20µl of electro-competent sw105 bacteria (see section 4.1.2) were carefully mixed in an Eppendorf tube on ice and transferred into a pre-cooled 1mm electroporation cuvette. The bacteria were electroporated at 25µF, 200Ω, and 1.75kV and recovered in 1ml LB medium (without any supplements) in a 15ml Falcon tube for 1h at 32°C in a shaker. After recovery, the bacteria were transferred to an Eppendorf tube, pelleted (13200rpm, 15s, 20°C), and washed twice in 1ml M9 salt solution to remove any carbohydrates. After the second wash, the pellet was diluted in 500µl fresh M9 salt solution and 10µl, 50µl, 100µl, and 340µl were plated onto

galactose plates and incubated at 32°C for three to four days until colonies became visible. Single colonies were picked and struck onto McConkey plates to obtain single colonies. McConkey plates were incubated over night at 32°C and red p3991.1 colonies were used for the second recombination step.

### 4.1.4 Electroporation of the DNA cassette into electro-competent sw105 bacteria for reversion of *galK* followed by selection on DOG plates

The DNA cassette, which was introduced into the 3991 plasmid for reversion of *galK,* contained homologous flanks with approximately 200bp in length. Long homologous flanks increase the number of correct recombined clones. Electrocompetent p3991.1/sw105 bacteria were prepared as described in section 4.1.2, and 1µg of the DNA cassette was introduced by electroporation as described in section 4.1.3. After electroporation, bacteria were recovered in 10ml LB medium (without any supplements) for 4h at 32°C in a bacteria shaker. The bacteria were pelleted and washed as described in section 4.1.3 and plated onto DOG plates. DOG plates were incubated for four to five days at 32°C until colonies were visible.

### 4.1.5 Verification of the new maxi-EBV by restriction enzyme digestion and agarose gel electrophoresis

Single colonies were picked from the DOG plate, struck onto one half of an LB agar plate containing 15µg/ml Cm, and incubated over night at 32°C. Next day, the bacteria were scraped off the LB agar plate using a sterile wooden toothpick and transferred into 200µl normal TE buffer. The solution was shortly vortexed, 200µl of freshly made lysis buffer was added, inverted twice, and incubated on ice for 5min. 200µl neutralizing solution III was added. Bacteria solution was mixed by shaking, incubated for 2min on ice, and spun down (full speed, 10min, 4°C). The supernatant was transferred into a fresh Eppendorf tube and 400µl isopropanol was added to precipitate the DNA, which was spun down (full speed, 10min, room temperature (RT)). The DNA pellet was washed in 400µl 80% ethanol and spun down (full speed, 5min, RT). The supernatant was taken off completely and the DNA was diluted in 20µl normal TE buffer. The DNA was digested with BamHI restriction enzyme and loaded onto a 20x25cm, 0.7% agarose gel made with TAE buffer and ethidium bromide. The agarose gel was run with 40V over night and the band pattern was analyzed (Figure 4-1 right).

### 4.1.6 Storage and cultivation of bacteria for DNA preparation

Bacteria that contained the maxi-EBV plasmid were substituted with 20% glycerol and stored at -80°C. Bacteria were plated from the frozen culture on a LB agar plate that contained 15µg/ml Cm and were cultured over night at 32°C. One bacteria colony was picked from the plate, inoculated into 50ml liquid LB medium containing 15µg/ml Cm, and incubated over night at 32°C in bacteria shaker. Finally, six times 400ml LB medium (containing 15µg/ml Cm, 0.3M NaCl) were inoculated with 200µl of the 50ml pre-culture and incubated at 32°C over night until the $OD_{600}$ reached a value of four.

### 4.1.7 Preparation of maxi-EBV DNA using CsCl-gradient centrifugation

The six 400ml over night bacteria cultures were spun down (6000rpm, 15min, RT) and the supernatant was poured off. The six bottles containing the bacteria pellets were frozen at -20°C for 10min. Each of the six bacteria pellets was resuspended in 10ml solution I by vortexing and pipetting, the volume was filled up to 45ml with solution I and kept on ice. 10mg lysozyme was added to each bottle, the bottle was carefully shaken and incubated for 5-10min on ice. 58ml freshly made solution II were added to each bottle, mixed by carefully flipping five times, and incubated on ice for exactly 5min. The pH was neutralized by addition of 70ml pre-cooled solution III and mixed by carefully shaking until a homogenous solution occurred. The bottle was kept on ice for 30min, shook again, and centrifuged (6000rpm, 20min, 4°C). Remaining cell material was filtered out of the supernatant using first gauze and then a fluted filter. The filtered solution was pooled and split into four 500ml bottles. The DNA was precipitated by adding 0.75%/v isopropanol. The solution was mixed by shaking, incubated for 10-30min at RT, and the precipitate was pelleted (9000rpm, 45min, RT). The supernatant was poured off, 200ml 80% ethanol was added to the pellet, which was detached from the bottle wall by gentle shaking. The four bottles containing the DNA/ethanol solution were kept on ice over night. Next day, the DNA was spun down (9000rpm, 20min, RT), the supernatant was poured off, and the pellet was air-dried for 5min to remove remaining ethanol. 10ml of special TE buffer was added to each of the four bottles and the DNA pellet was diluted on a shaker for up to 1h. The DNA solutions of the four bottles were poured in one of the bottles. Contaminating RNA was removed by adding 400µg RNaseA and incubation at 37°C for 15min. Contaminating proteins

were removed by adding 4-6mg Proteinase K and incubation at 50°C for 45min. The maxi-EBV DNA was separated from the bacterial DNA in an ethidium bromide containing CsCl density gradient. Therefore, the DNA solution was equally distributed to two 50ml Falcon tubes. The weight of each solution (without the Falcon weight) was determined. The measured weight of the solution plus 1g was the amount of CsCl that was slowly added to the DNA solution constantly kept at 50°C. After the CsCl was fully dissolved, 1ml ethidium bromide solution (10mg/ml) was added and the solution was transferred into an ultracentrifuge tube (35ml), which was filled to the top with 1.55g/ml CsCl-solution. The DNA solution was centrifuged in a fixed angle rotor (38000rpm, three days, 20°C). After three days of centrifugation, a continuous CsCl density gradient was formed, whose density is higher at the bottom of the tube and lower at the top. The added ethidium bromide intercalates into DNA and makes it visible under UV light. Plasmid DNA is supercoiled and has a high density, whereas linearized bacterial DNA has a low density. The plasmid DNA band is found below the bacterial DNA band in the CsCl gradient and was collected in a syringe by tapping the tube with a 2.1mm veterinary needle. The plasmid DNA of both gradients was pooled in an 11.5 ml ultracentrifuge tube. 500µl ethidium bromide were added, the tube was filled up with 1.55g/ml CsCl-solution and centrifuged again (38000rpm, three days, 20°C). Again, the lower plasmid DNA band was collected and transferred to a glass tube. Ethidium bromide was extracted by adding CsCl-saturated isopropanol, shaking, and removing the upper ethidium bromide/isopropanol organic phase. This step was repeated three times until the DNA solution was clear. The DNA/CsCl-solution (approximately 1ml) was transferred into a 1.5ml QuixSep dialyzer and dialyzed for 1h in 2l normal TE buffer. The normal TE buffer was renewed once and the dialysis was repeated as before. The DNA concentration was determined using the fluorescent dye Hoechst H33342, which intercalates into DNA and can be measured in a fluorimeter. The DNA was digested with BamHI restriction enzyme and the band pattern was analyzed on an agarose gel (0.7% agarose in TAE-buffer).

## 4.2 Cell culture techniques

### 4.2.1 Cultivation of cell lines

Established cell lines were cultivated in a humid atmosphere at 37°C and 5%$CO_2$. HEK293, hCD32$^+$ L-cells, L929, and established human and murine B cell lines were cultured in standard RPMI 1640 medium supplemented with 10% FCS, 100µg/ml streptomycin, 100units/ml penicillin, 1mM sodium pyruvate, 0.433% α-thioglycerol, 20µM bathocuproin disulfonat, and 100nM sodium selenite. The culture medium of HEK293 cells stably transfected with maxi-EBV plasmid was additionally supplemented with 80µg/ml hygromycin to select for the maintenance of the plasmid. Primary B cells that were infected with EBV were cultivated in a humid atmosphere at 37°C, 5% $CO_2$ and 5% $O_2$ to reduce oxidative stress for three weeks. These cells were cultured in RPMI 1640 "infection medium" supplemented with 10% FCS, 100µg/ml streptomycin, 100units/ml penicillin, 1mM sodium pyruvate, 100nM sodium selenite, 50µM β-mercaptoethanol, 250µM α-tocopherol, 10µg/ml ciprofloxacin, and 1µg/ml cyclosporin A. Three weeks post infection, EBV infected primary B cells were cultured without oxygen regulation in standard RPMI 1640 medium as described for established B cell lines.

Adherent HEK293, hCD32$^+$ L-cells and L929 cells were cultivated on cell culture dishes and splitted 1:5 to 1:10 once or twice a week by use of a trypsin/EDTA solution. All other cell lines were cultured as suspension cells in cell culture flasks and diluted 1:5 once or twice a week. The cell density was determined using a cell counter.

### 4.2.2 Storage of cells

1 x $10^7$ cells were diluted in freezing solution containing 90% FCS and 10% DMSO, transferred into a cryo-tube, which was placed in a cryo-box. The cryo-box contained isopropanol, slowing down the freezing process to approximately 1°C/min, and was placed in an -80°C freezer. One week later, the cryo-tube, containing the frozen cells, was transferred into a liquid nitrogen tank for longtime storage.

Frozen cells were quickly thawed by placing the cryo-tube in a 37°C waterbath. Cells were transferred into a 50ml Falcon tube filled with 35ml pre-warmed cell culture medium to remove the DMSO. Cells were pelleted (1200rpm, 10min, RT), diluted in fresh medium, and cultivated as described.

### 4.2.3 Establishment of stable virus producing HEK293 cell lines

The constructed maxi-EBV plasmids were transfected into HEK293 cells to establish stable virus producer cell lines. The cationic polymer polyethylenimine (PEI) was used as transfection agent forming micelles with the maxi-EBV DNA. The complexes bind to the negatively charged cell membrane and are incorporated into the cell by endocytosis (Vancha *et al.*, 2004). 24h prior to transfection 2 x $10^5$ HEK293 cells were seeded in one well of a 6-well-plate. A transfection mix composed of solution A and B was prepared.

Solution A: 500 µl Opti-MEM + 1µg maxi-EBV DNA
Solution B: 500 µl Opti-MEM + 5µl 1mg/ml PEI solution

Solution A and B were prepared separately, mixed, and incubated for 20min at RT enabling PEI/DNA complex formation. During this time cells were washed with 1ml Opti-MEM. After washing, cells were covered with 1ml transfection mix and incubated for 4h in the incubator. Subsequently, the transfection mix was replaced by 2ml RPMI 1640 medium (with supplements, without hygromycin). After 24h, the cells were trypsinized, diluted in 25ml RPMI 1640 medium (supplemented with all additives including 80µg/ml hygromycin), and plated onto a cell culture dish (15cm diameter). Routinely, a transfection efficiency of approximately 10% was achieved. Stably transfected cells proliferated under hygromycin selection and formed visible colonies after three weeks. Because the maxi-EBV encodes the *green fluorescent protein* gene (*GFP*), green $GFP^+$ colonies were picked and further expanded.

### 4.2.4 Induction of virus production in stably transfected HEK293 cell lines

Clonal HEK293 cell lines, stably transfected with a maxi-EBV plasmid, were transfected with expression plasmids, encoding the viral genes BZLF1 (p509) and BALF4 (p2670), which induce EBV particle production. 48h prior transfection, approximately 3 x $10^6$

cells were seeded in a cell culture dish (15cm diameter). The transfection mix was prepared:

Solution A: 2 ml Opti-MEM + 18µg p509 DNA + 18µg p2670 DNA
Solution B: 2 ml Opti-MEM + 90µl 1mg/ml PEI solution

Solution A and B were prepared separately, mixed, and incubated for 20min at RT. During this time, cells were washed once with PBS and covered with 20ml Opti-MEM. 4ml transfection mix was added to the cells. After 4h of incubation, the transfection medium was replaced by 20ml RPMI (with all supplements, without hygromycin), and the cells were incubated for three days. The cell supernatant containing the EBV particles was transferred to a Falcon tube, and remaining cells were pelleted (1200rpm, 10min, RT). The supernatant was transferred to a new Falcon tube and cleared from cell debris by centrifugation (5000rpm, 10min, RT).

### 4.2.5 Determination of virus titer

5 x $10^4$ Raji cells were seeded in a single well of a 24-well-plate and infected with different amounts of HEK293/maxi-EBV cell supernatant containing EBV particles (see section 4.2.4) in a total volume of 1ml. Infected Raji cells express GFP. The percentage of $GFP^+$, infected Raji cells was determined via flow cytometry. The number of $GFP^+$ Raji cells correlates with the number of infectious EBV particles, and the amount of green Raji units per milliliter (GRU/ml) was calculated.

### 4.2.6 Concentration of virus supernatant by ultra centrifugation

If the virus concentration in the HEK293/maxi-EBV supernatant was below 1 x $10^4$GRU/ml, EBV particles were concentrated by ultra centrifugation (25000rpm, 2h, 4°C). After centrifugation, the supernatant was reduced in volume to 1:10, and the pellet was diluted in the remaining supernatant by pipetting up and down with a glass pipette. The concentration of infectious EBV particles was determined as described in section 4.2.5.

### 4.2.7 Preparation of primary human B cells from adenoids

Adenoids, which are lymphoid tissues found in the nasopharynx, are a source of human lymphocytes. Adenoids are often enlarged in children and block breathing through the nose, which makes their surgical removal necessary. Adenoids of children younger than six years were used for preparation of primary B cells to reduce the likelihood of an EBV-infection of the donor. Few hours post surgery, adenoids were chopped into small pieces with a scalpel, pressed through a 100µm mesh, and the cell suspension was filled up to 35ml with PBS. T cells were depleted by rosetting. Therefore, 500µl sheep blood was added to the cell suspension and incubated for 5min. The cell suspension was carefully loaded onto 15ml of a 30% Ficoll solution (density 1.077g/ml). After density centrifugation (1900rpm, 30min, 10°C, without centrifuge brake), B cells were taken off the interphase with a pipette. The remaining Ficoll was removed by washing three times with cold PBS (centrifugation steps 1600rpm/ 1400rpm/ 1200rpm, each 10min, 4°C). After washing, the cells were diluted in staining buffer, sorting buffer or in cell culture medium. The cell number was determined with a Neubauer chamber.

### 4.2.8 Infection and outgrowth of adenoid B cells

Adenoid B cells were diluted in infection medium (see section 4.2.1), and EBV containing supernatant (see section 4.2.4) was added at a multiplicity of infection (MOI) of 0.05 or 0.1. Cell density during infection was kept as high as possible to obtain a high infection rate. After approximately 16h of incubation in a humid incubator at 37°C, 5% $CO_2$, and 5% $O_2$, the cells were pelleted (1200rpm, 10min, RT) and diluted in fresh infection medium with a cell density of 1.5-10 x $10^5$ cells/ml depending on the experimental setup. Infected cells were incubated in a humid incubator at 37°C, 5% $CO_2$, and 5% $O_2$ in infection medium for three weeks. Subsequently, the cells were transferred to normal medium and cultured without oxygen adjustment.

### 4.2.9 Determination of cell doubling time

A proliferation assay of EBV-infected B cells was set up as described in Figure 5-12 to determine the number of EBV transformed cells at different days p.i.. The number of transformed cells (y-axis, log 2-scale) was plotted over time (x-axis) in a diagram. The linear fit function was calculated using the software OriginPro. The doubling time is the slope of the linear fit function.

## 4.3 Flow cytometric methods

### 4.3.1 Detection of surface molecules

2 x $10^5$ cells were transferred to a 1.3ml small FACS tube, washed in cold staining buffer, and pelleted (300xg, 7min, 4°C). The cell pellet was recovered in 50µl staining buffer, antibodies were added as shown in Table 4-1 and incubated for 20min on ice in the dark. Stained cells were washed in staining buffer, diluted in 50µl fresh staining buffer and, if needed, secondary antibody was added. After 20min staining on ice in the dark, cells were again washed once with staining buffer and analyzed on a FACS Calibur flow cytometer.

**Table 4-1: Antibody and staining reagent dilutions used for flow cytometry**

| **Antibody specificity** | **Dilution** | **Source** |
|---|---|---|
| hCD19-Biotin (primary staining) | 1:5 | BD Biosciences |
| hCD23-APC | 1:100 | eBioscience |
| hCD27-APC | 1:50 | BD Biosciences |
| hCD30-APC | 1:50 | BioLegend |
| hCD32-Alexa647 | 1:20 | BioLegend |
| hCD38-PE | 1:50 | eBioscience |
| hCD54-APC | 1:50 | Immunotools |
| hCD56-PE | 1:50 | BD Biosciences |
| hCD86-APC | 1:50 | BD Biosciences |
| mB220-FITC | 1:20 | BD Biosciences |
| mIgM-DyLight649 | 1:3000 | Jackson Research |
| **Staining reagent** | **Dilution** | **Source** |
| $NP_{18}$-BSA-Biotin (primary staining) | 1:100 | Biosearch Technologies |
| Steptavidin-PE-Cy7 (secondary staining) | 1:400 | eBioscience |

h: human, m: mouse

### 4.3.2 Cell sorting of BCR-negative B cells

B cells were prepared from adenoids as described in section 4.2.7. 3 x $10^8$ cells were washed once in cold sterile filtered sorting buffer and diluted in 2ml sorting buffer. 30µl α-κ-APC, 150µl α-λ-FITC, and 150µl α-CD3-PE antibodies were added, and the cells were incubated on a roller machine at 4°C for 30min in the dark. The cells were washed once in 15ml sorting buffer, the supernatant was aspirated, and the cells were diluted in 8ml fresh sorting buffer. Cell clumps were removed using a 35µm nylon mesh incorporated into the cap of a FACS tube. $BCR^-$ ($CD3^-$, $\lambda^-/\kappa^-$) and $BCR^+$ ($CD3^-$, $\lambda^+/\kappa^+$) cells

were sorted through a 70µm nozzle using the four-way purity mask on a FACS Aria III cell sorter.

### 4.3.3 Phosphospecific flow cytometry

The staining protocol for phosphorylated intracellular signaling molecules was established by Stephanie Medele in the laboratory (Medele, 2010). Accordingly, 5 x $10^5$ cells were transferred to a 1.3ml small FACS tube, washed in PBS (RT), and pelleted (300xg, 7min, RT). The cell pellet was recovered in PBS, stimulation antibodies or antigen were added as shown in Table 4-2 and incubated for 15min on ice to allow binding to the target. Subsequently, cell signaling was activated by incubating the cells at 37°C in a water bath for 10min. Equal volume of prewarmed BD Cytofix Fixation Buffer was added to the cell solution, which was again incubated for 10min at 37°C to fix phosphorylated proteins. Cells were pelleted (300xg, 7min, RT), diluted in 50µl of left over supernatant, and permeabilized in 1ml ice-cold methanol for 30min on ice. Cells were washed twice in phosflow buffer to remove methanol, and the supernatant was aspirated to 50µl. Cells were mixed by vortexing, 10µl of phosphospecific-antibodies, directed against phosphorylated Syk or phosphorylated PLCγ2, were added, and the cells were incubated for 30min at RT in the dark. Finally, cells were washed once in phosflow buffer and analyzed on a FACS Calibur flow cytometer.

**Table 4-2: Antibodies used for cell stimulation**

| Stimulated surface molecule | Antibody used for stimulation | Concentration during stimulation | Source |
|---|---|---|---|
| human BCR | goat-α-hIgG/M | 25µg/ml | Jackson Research |
| LMP2A:mCD69 | armenian hamster-α-mCD69 | 1µg/ml, 15µg/ml | Hybridom supernatant |
| | goat-α-armenian hamster | 5µg/ml, 15µg/ml | Jackson Research |
| NP-specific murine IgM | rat-α-mIgM (b7-6) | 60µg/ml | Obtained from H.-M. Jäck |
| | $NP_{26}$-BSA | 10µg/ml, 100µg/ml | Biosearch Technologies |

### 4.3.4 Cytokine release assay

1 x $10^6$ B cells from adenoids were infected with recombinant EBV strains with MOIs of 0.1 and 0.05 and cultured in 1ml infection medium. One day p.i. cells were supplied with fresh medium at a cell density of 1 x $10^6$ cells/ml. Eight days p.i. the number of transformed cells was determined as described in Figure 5-12. Cell cultures, which contained equal numbers of transformed cells, were chosen for cytokine analysis to exclude variations in cytokine production due to different cell densities. IL-2, IL-6, IL-8, and IL-10 concentrations in cell supernatants of EBV-infected B cells were determined

using the FlowCytomix™ Multiplex Technology, which allows analyzing multiple cytokines simultaneously on a FACS Calibur. In brief, beads are coated with antibodies directed against a single analyte in the cell supernatant (IL-2, IL-6, IL-8, or IL-10). The cell supernatant was added to the beads, and the analytes bound to the coupled antibodies. A mixture of biotin-coupled secondary antibodies was added. The secondary antibodies bind to the same analyte, which has already bound to the beads via the first antibody. Streptavidin-PE was added and bound to the biotin conjugated secondary antibodies emitting a fluorescent signal, which could be detected by flow cytometry. Two features are important to discriminate the signals for the different analytes: (i) Two sets of beads with 4µm and 5µm diameter, which can be discriminated in the FSC/SSC diagram, were used. (ii) The beads are dyed with different intensities of a fluorescent dye, which can be detected in the fluorescence channel 3 (FL-3). Accordingly, analytes were discriminated by their bead size (FSC/SSC signal) and their fluorescence intensity in the FL-3 channel. The PE signal intensity in the FL-2 channel correlates to the amount of analyte that has been bound to the beads, and the analyte concentration in the cell culture medium could be calculated from standard curves.

### 4.3.5 Calcium flux analysis

Cells were loaded with Indo-1, which is a fluorescent dye that changes its emission wavelength from 475nm (blue) to 400nm (violet) upon calcium binding. An increase in cytosolic $Ca^{2+}$-concentrations can be measured by an increase in the violet/blue wavelength ratio. Accordingly, 1 x $10^7$ cells were washed in PBS and resuspended in 1ml RPMI 1640 containing 3µM Indo-1 AM. Cells were incubated at 37°C for 30min in the dark, washed once in 10ml RPMI 1640, diluted in 2ml fresh RPMI 1640, and kept on ice. 200µl of the cell suspension (1 x $10^6$ cells) were pre-warmed at 37°C for 20min, and the baseline violet/blue ratio of Indo-1 loaded cells was measured for 1min on a FACS LSR II flow cytometer. Subsequently, the BCR was cross-linked with 25µg/ml goat-α-hIgG/A/M $F(ab')_2$ fragment, cells were quickly mixed, and the $Ca^{2+}$-influx was measured by the change in the violet/blue ratio for 5min.

## 4.4 Protein analytic techniques

### 4.4.1 Cell lysis and determination of protein concentration

Cells were washed once in PBS, pelleted (300xg, 7min, 4°C), and lysed in RIPA buffer for 30min on ice. Cell debris was pelleted (21000xg, 10min, 4°C), and the supernatant containing the proteins was transferred to a new tube. Protein concentration was determined using the Bradford Assay. 700µl of a 20% Bradford reagent solution (Bio-Rad) was mixed with 2µl of protein solution, and the light absorbance at a wavelength of 595nm was measured with a spectrophotometer (Bio-Rad). The protein concentration correlates to the increase in absorbance at 595nm.

### 4.4.2 SDS-PAGE

The SDS-PAGE was performed on a Protean Mini device from Bio-Rad. Polyacrylamide gels were prepared as described in section 3.8.5. Proteins were diluted to equal concentration with RIPA buffer and mixed with 5x Laemmli buffer in a ratio 4:1 (7µg protein, 7 µl 5x Laemmli in a total volume of 35µl). Proteins were heat denatured at 100°C for 5min in a sand bath, shortly centrifuged, and loaded onto a polyacrylamide gel. Proteins were separated at 125V for approximately 2h.

### 4.4.3 Western Blot analysis

The SDS-PAGE gel, a sheet of nitrocellulose membrane, and Whatman paper were soaked in transfer buffer. A semidry Western Blot device was used at 23V for 1h to transfer the proteins from the gel to the membrane. The membrane was incubated for 30min in blocking buffer at RT and, subsequently, incubated with the primary antibody (diluted in blocking buffer, Table 4-3) at 4°C over night. The membrane was washed five times in PBS-T for 5min to remove unbound antibodies. Binding of the secondary antibody (HRP-conjugated, diluted in blocking buffer, Table 4-3) was performed for 45min at RT. The membrane was washed five times for 5min with PBS-T. The membrane was treated with ECL-solution. ECL is the substrate of HRP, which catalyzes a luminescence reaction. Accordingly, antibody bound proteins can be detected on an x-ray film. Used antibodies and dilutions are shown in Table 4-3.

**Table 4-3: Antibody dilutions used for Western Blot analysis**

| Antibody specificity | Dilution | Conjugate | Source |
|---|---|---|---|
| goat-α-mμ-heavy chain | 1:3000 | HRP | SouthernBiotech |
| goat-α-mλ-light chain | 1:3000 | HRP | SouthernBiotech |
| mouse-α-actin (1st antibody) | 1:5000 | - | Sigma-Aldrich |
| horse-α-mouse (2nd antibody) | 1:3000 | HRP | Cell Signaling |

## 4.5 DNA/RNA analytic techniques

### 4.5.1 Extraction of cellular RNA

RNA was isolated using the RNeasy Mini Kit (Qiagen) according to the instruction of the manufacturer. 7 x $10^6$ cells were used for each sample, and the lysate was homogenized with QiaShredder columns (Qiagen). RNA was eluted in 40µl RNase-free water and stored at -80°C. The RNA concentration was determined using the NanoDrop spectrophotometer.

### 4.5.2 Reverse transcription of RNA into cDNA

Before reverse transcription of RNA into cDNA, contaminating DNA was removed from the RNA eluate. Therefore, 2µg of isolated RNA were digested with 2 Units DNase I (Invitrogen) in 1x DNase buffer (Invitrogen), 1µl RNasin RNase inhibitor (Promega), and a total volume of 20µl at 37°C for 90min. The DNase I was heat inactivated at 65°C for 10min. Complete digestion was approved by a PCR reaction. The RNA concentration was determined using the NanoDrop spectrophotometer.

The cDNA synthesis was performed with the SuperScript III First-Strand Synthesis System (Invitrogen) according to the manufacturer's protocol using oligo dT as primers for reverse transcription.

### 4.5.3 qRT-PCR

Transcripts of interest were quantified with a Roche LightCycler 480 device. The method bases of on the incorporation of the fluorescent dye SYBR-Green I into newly synthesized, double stranded DNA detected after each elongation cycle (Higuchi *et al.*, 1993).

The RNA expression levels were evaluated by relative quantification. The crossing point (Cp) for the target gene was compared to the Cp of the reference or housekeeping gene. The Cp is the cycle number at which the amplified DNA is detectable for the first time. The *CDC-like kinase 2* gene (*Clk2*) was used as housekeeping gene being constantly expressed in all cells. The analysis was performed with the LightCycler 480 software in the advanced modus. The Cp(target)/Cp(reference) ratio was calculated. The primer efficiencies of the different primer pairs were determined by serial dilutions of the DNA sample and calculated by the LightCycler 480 software. The Cp values of targets and reference were corrected for the different primer efficiencies. The PCR mix and the PCR program for qRT-PCR are listed below.

| **Component** | **Amount** |
|---|---|
| template | 3µl of 1:3 diluted cDNA |
| primer | 5pmol each |
| 2x SYBR Green I Master | 5µl |
| $H_2O$ | 1.5µl |

| **Program** | **Target temperature (°C)** | **Hold (s)** | **Acquisition mode** | **Ramp Rate (°C/s)** | **Cycles** | **Analysis mode** |
|---|---|---|---|---|---|---|
| pre-incubation | 95 | 600 | none | 4.4 | 1 | none |
| amplification | 95 | 1 | none | 4.4 | 45 | quantification |
| | 62 | 10 | none | 2.2 | | |
| | 72 | 10 | none | 4.4 | | |
| | 75 | 3 | single | 4.4 | | |
| melting curve | 97 | 1 | none | 4.4 | 1 | melting curve |
| | 67 | 10 | none | 2.2 | | |
| | 97 | / | continuous | 0.11 | | |
| cooling | 37 | 15 | none | 2.2 | 1 | none |

# 5 Results

## 5.1 Establishment of a sorting protocol of BCR-negative primary human B cells

### 5.1.1 Sorting protocol

EBV infects mature, naive, and memory B cells equally well *in vitro* and drives them into proliferation (Thorley-Lawson, 2001). The ability to transform B cells *in vitro* is of considerable importance for research in EBV, since infection of any B cell leads to the establishment of lymphoblastoid cell lines (LCL). LCLs are an important model for viral transformation and latency in EBV research. The viral proteins EBNA1, EBNA2, and LMP1 are essential for B cell transformation (Hammerschmidt & Sugden, 2004). Recently, our group could document that infection of $BCR^-$ B cells with wt EBV but not LMP2A-knock out (ΔLMP2A) EBV can rescue $BCR^-$ B cells from apoptosis (Mancao *et al.*, 2005; Mancao & Hammerschmidt, 2007). LMP2A is a constitutively active BCR mimic and provides the necessary survival signals usually received from the BCR. LCLs that express an inducible LMP2A:mCD69 molecule instead of LMP2A were used to compare LMP2A:mCD69 and BCR signaling. Both receptors can induce protein phosphorylation, $Ca^{2+}$-influx, and transcription of similar sets of cellular genes upon antibody-mediated receptor cross-linking (Medele, 2010). These signaling studies were performed in established LCLs in our group. The aim of my project is to investigate the contribution of LMP2A signaling to the transformation of $BCR^-$ B cells shortly after infection. To this end, pure human $BCR^-$ B cell were required. Adenoids, which are lymphoid tissues found in the nasopharynx, are one source of human lymphocytes including $BCR^-$ B cells. Adenoids are often enlarged in children and block breathing through the nose, which makes their surgical removal necessary.

Adenoids were obtained from different Munich hospitals and used to isolate B cells. To this end, adenoids were sheared, pressed through a 100µm mesh, depleted from T cells, and purified by Ficoll density centrifugation. For infection studies, $BCR^-$ B cells as well as control $BCR^+$ B cells were needed. Fluorescence-activated cell sorting (FACS) was used

to separate BCR$^+$ and BCR$^-$ B cells with high purity. Untouched, non-activated B cells were required to study the activation and proliferation of BCR$^-$ B cells upon EBV infection. Because staining of B cells with antibodies can already activate the cell, depletion of BCR$^+$ B cells from the prepared B cell population was used to obtain non-activated BCR$^-$ B cells. The Ig-λ or Ig-κ light chains of BCR$^+$ B cells were stained, and BCR$^-$ cells were defined as λ and κ double negative (λ$^-$/κ$^-$). T cells, which are also Ig light chain-negative, were identified with α-CD3 antibodies and depleted from the B cell populations.

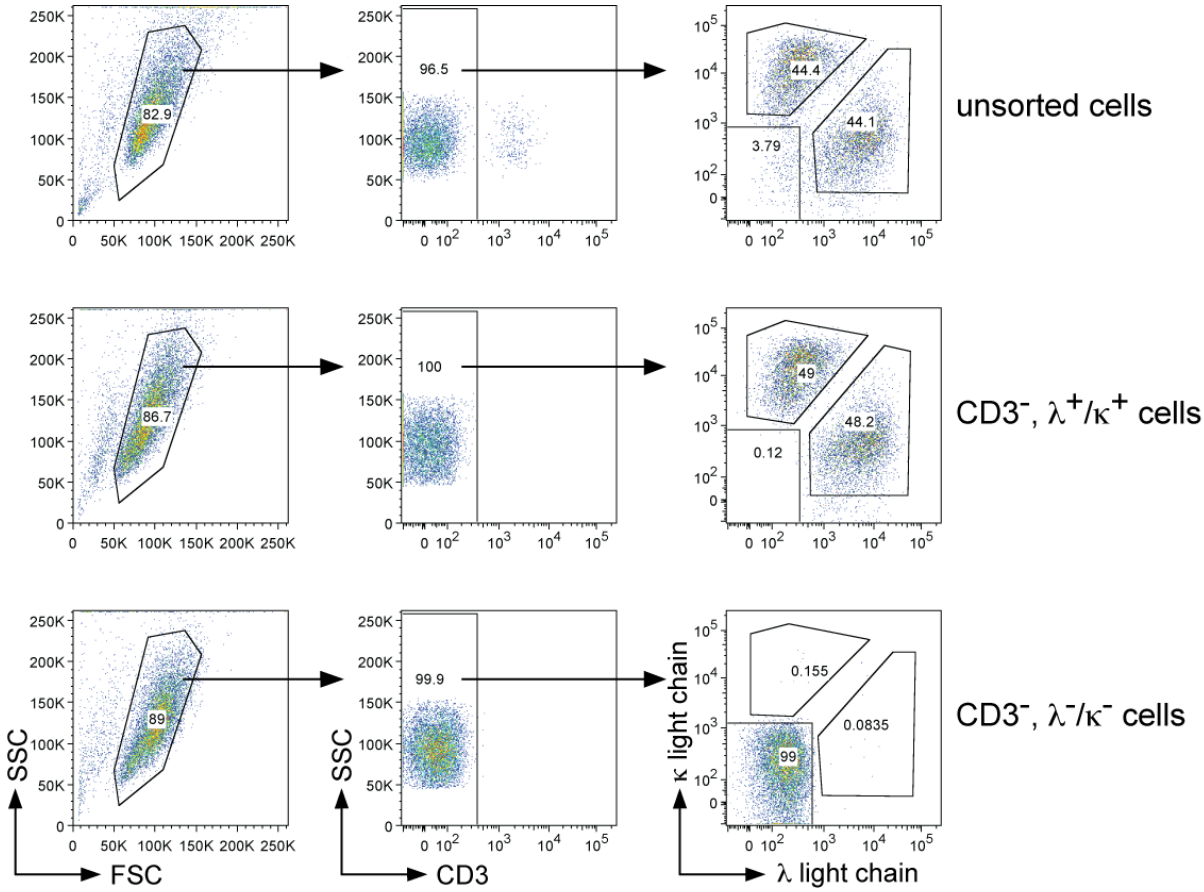


**Figure 5-1: Cell sorting protocol for CD3$^-$, λ$^+$/κ$^+$ and CD3$^-$, λ$^-$/κ$^-$ B cells from adenoids.**
Single cell suspensions were stained with α-CD3-PE, α-λ-FITC, and α-κ-APC antibodies and analyzed with the aid of a FACS Aria III cell sorter. As depicted in the first column, lymphocytes were gated in the forward scatter (FSC) vs. sideward scatter (SSC) diagram. Only CD3$^-$ cells were chosen for further analysis (second column) to exclude remaining T cells from the lymphocyte population. λ or κ positive (λ$^+$/κ$^+$) cells and λ and κ negative (λ$^-$/κ$^-$) cells were sorted from the CD3$^-$ population (third column). The first row shows the phenotype of cells before sorting. After sorting, BCR$^+$ (CD3$^-$, λ$^+$/κ$^+$) or BCR$^-$ (CD3$^-$, λ$^-$/κ$^-$) cells were reanalyzed for their purity (row two and row three). Both sorted populations had a purity of 97-99%.

As shown in Figure 5-1, 82.9% of unsorted cells located to the lymphocyte gate of the FSC/SSC diagram (first column). Of these cells only, 3.5% were $CD3^+$ T cells (second column, top row). Of the $CD3^-$ fraction, 88.5% of all cells were either $\kappa^+$ or $\lambda^+$ $BCR^+$ B cells (third column, top row). Only 3.79% of cells of the $CD3^-$ fraction were $\lambda^-$ and $\kappa^-$ $BCR^-$ cells. $BCR^+$ ($CD3^-$, $\lambda^+/\kappa^+$) and $BCR^-$ ($CD3^-$, $\lambda^-/\kappa^-$) cells were sorted and analyzed for their purity (second and third row). Both sorted populations had a purity of 97-99%.

### 5.1.2 Analysis of BCR-negative sorted cells

$BCR^-$ cells were sorted from adenoid lymphocytes by depleting T cells and $BCR^+$ B cells from the unsorted cell population. The number of B cells and their differentiation state in the $CD3^-$, $\lambda^-/\kappa^-$ sorted fraction were determined. Unsorted cells and $BCR^-$ ($CD3^-$, $\lambda^-/\kappa^-$) sorted B cells were stained with antibodies specific for the B cell marker CD19, the memory B cell marker CD27, or the germinal center marker CD38 and analyzed by flow cytometry.

As depicted in Figure 5-2, most of the unsorted cells were B cells (96%, $CD19^+$), which could be separated into naive B cells (53%, $CD38^-$, $CD27^-$), resting memory B cells (16%, $CD38^-$, $CD27^+$), and activated memory B cells (17%, $CD38^+$, $CD27^+$) (Jackson *et al.*, 2009). In $CD3^-$, $\lambda^-/\kappa^-$ lymphocytes, the fraction of $CD19^+$ B cell was 47%, which consisted of mainly B cells with surface markers reminiscent of activated germinal center B cells on their route to memory B cells (81%, $CD38^+$, $CD27^+$).

Natural killer (NK) cells are also $BCR^-$ lymphocytes. They have the ability to kill virus-infected cells and limit cells, which can be transformed by EBV long term. NK cells can be distinguished from other lymphocytes by their surface expression of CD56. $CD19^-$, $CD56^+$ NK cells constituted only 0.4% in the population of unsorted cells but increased to 12.4% in the population of $CD3^-$, $\lambda^-/\kappa^-$ cells after sorting. The calcineurin inhibitor Cyclosporin A (CsA), which inhibits an EBV-specific T cell response, was added to all infection studies. CsA also blocks NK cell proliferation and induces apoptosis in NK cells (Wang *et al.*, 2007) but does not impair the transformation of B cells by EBV (Mancao *et al.*, 2005). Accordingly, treatment of EBV infected cells with CsA diminishes the EBV-

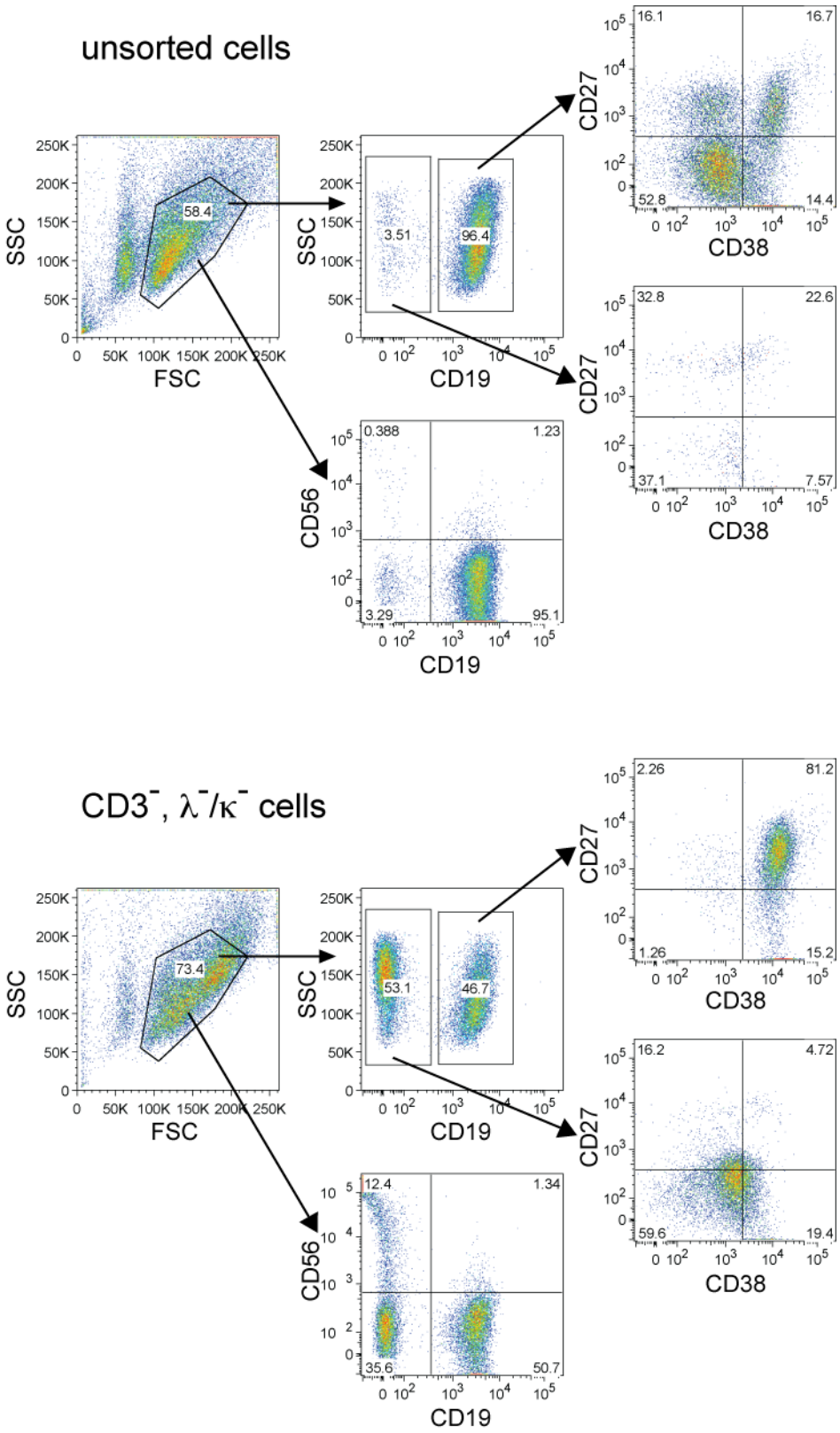


**Figure 5-2: Phenotypic analysis of BCR$^-$ (CD3$^-$, λ$^-$/κ$^-$) sorted cells from adenoids.**
Non-activated BCR$^-$ B cells were needed to study EBV induced B cell activation and proliferation. BCR$^-$ sorted lymphocytes were obtained by depletion of CD3$^+$ T cells and BCR$^+$ (λ$^+$/κ$^+$) B cells from the unsorted population. The B cells marker CD19, the memory B cell marker CD27, the germinal center marker CD38, as well as the natural killer (NK) cell marker CD56 of unsorted cells and BCR$^-$ (CD3$^-$, λ$^-$/κ$^-$) sorted cells were stained with fluorophore-coupled antibodies and analyzed by flow cytometry.

Unsorted cells (top) were B cells (96%, $CD19^+$), which could be separated into naive B cells (53%, $CD38^-$, $CD27^-$), resting memory B cells (16%, $CD38^-$, $CD27^+$), and activated memory B cells (17%, $CD38^+$, $CD27^+$). Only 0.4% of unsorted lymphocytes were $CD56^+$ NK cells. Only half of the $CD3^-$, $\lambda^-/\kappa^-$ sorted lymphocytes (bottom) were B cells (47%, $CD19^+$), 81% of which were $CD38^+$, $CD27^+$. The fraction of $CD56^+$ NK cells was up to 12%. 36% of $CD3^-$, $\lambda^-/\kappa^-$ sorted lymphocytes were neither B cells nor NK cells ($CD19^-$, $CD56^-$) but probably monocytes.

specific response of NK cells (Bird *et al.*, 1981; Britton & Palacios, 1982). 36% of $CD3^-$, $\lambda/\kappa^-$ sorted cells were $CD19^-$, $CD56^-$ and, thus, neither T, B, nor NK cells. The reddish color of the $CD3^-$, $\lambda/\kappa^-$ sorted cell pellet suggested that $CD19^-$, $CD56^-$ cells could be monocytes, which might have taken up sheep erythrocytes by phagocytosis. Sheep erythrocytes were used to deplete T cells from the lymphocyte preparation (see section 4.2.7).

### 5.1.3 Analysis of infected cells

About half of $BCR^-$ ($CD3^-$, $\lambda/\kappa^-$) sorted cells were shown to be $CD19^+$ B cells (Figure 5-2) and, thus, are targets of EBV. Unsorted and $CD3^-$, $\lambda^-/\kappa^-$ sorted cells were infected with wt EBV at a multiplicity of infection (MOI) of 0.1 to show that EBV only infects B cells in both populations. One day post infection, infected cells were stained with $\alpha$-CD19 antibodies and analyzed by flow cytometry, uninfected cells were included as negative control. Infected cells can be discriminated from uninfected cells by their expression of GFP, which the maxi-EBV plasmid encodes. Uninfected cells were defined as $GFP^-$. All $GFP^+$ cells, either unsorted or $CD3^-$, $\lambda^-/\kappa^-$ sorted, were also $CD19^+$ corroborating that EBV infects B cells exclusively (Figure 5-3).

In contrast to infected and unsorted cells (Figure 5-3, middle row), hardly any uninfected $CD19^+$ B cell survived in the $CD3^-$, $\lambda^-/\kappa^-$ B cell population one day post infection (Figure 5-3, bottom row). Unsorted cells are mainly $BCR^+$ (see section 5.1.2), but $CD3^-$, $\lambda^-/\kappa^-$, $CD19^+$ cells are GC B cells that lack the BCR and thus have very limited life span *in vivo* and *in vitro*.

In summary, I could sort $BCR^-$ B cells from adenoid lymphocytes, which contained only a very small fraction of $BCR^+$ B cells. However, the population contained also about 50% non-B cells, some of which were NK cells. They were enriched during $BCR^-$ cell sorting, but CsA in the culture medium can block their activation. Contaminating non-B cells did

not pose a problem because EBV only infects CD19⁺ B cells in the unsorted and BCR⁻ sorted cell fractions.

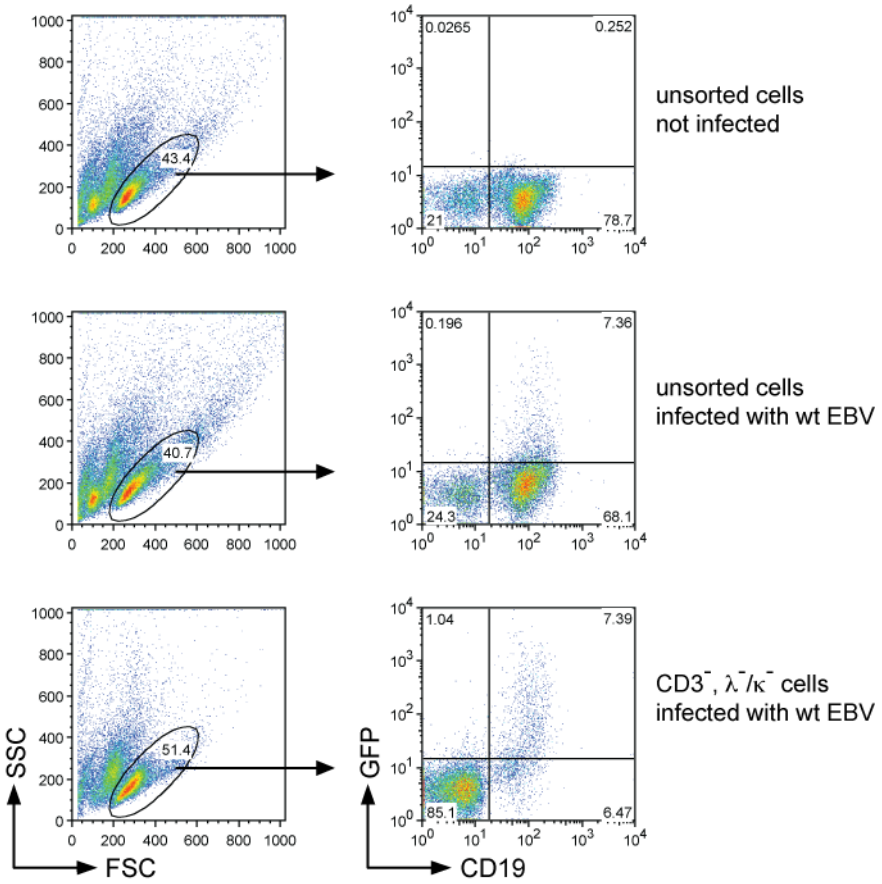


**Figure 5-3: EBV infects CD3⁻, λ⁻/κ⁻ B cells.**
BCR⁻ (CD3⁻, λ⁻/κ⁻) lymphocytes from adenoids were sorted. Unsorted and CD3⁻, λ⁻/κ⁻ sorted cells were infected with wt EBV (MOI 0.1) and stained for the B cell marker CD19 one day post infection. Infected cells can be separated from uninfected cells by their expression of GFP encoded in the maxi-EBV plasmid. Uninfected cells were GFP⁻ (first row), whereas only CD19⁺ B cells showed an increase in GFP expression after wt EBV infection (second and third rows) confirming that EBV exclusively infected B cells in the unsorted and CD3⁻, λ⁻/κ⁻ lymphocyte fractions. In contrast to infected and unsorted cells (middle row), hardly any CD19⁺ B cells survived in the CD3⁻, λ⁻/κ⁻ B cell population one day post infection (bottom row). This phenomenon is anticipated because λ⁻/κ⁻ B cells are GC B cells that lack the BCR and thus have a very limited life span *in vivo* and *in vitro*.

## 5.2 Comparison of BCR and LMP2A signaling shortly after infection

### 5.2.1 Replacement of LMP2A by an inducible LMP2A:mCD69 chimera or NP-specific murine IgM (NP-mIgM)

Miller et al. established the B95.8 cell line by infecting marmoset B cells with EBV from an infectious mononucleosis (IM) patient (see section 1.3.1) (Miller *et al.*, 1972). Twelve years later, the B95.8 EBV genome was sequenced (Baer *et al.*, 1984), and in 1998

Delecluse and colleagues cloned the B95.8 EBV genome into a bacterial F factor plasmid, which allowed the generation of viral mutants in *E. coli* (Delecluse et al., 1998). To achieve this goal, they introduced the linearized F factor plasmid into the B95.8 marmoset cell line. The linearized F factor plasmid contained two flanking regions, which were homologous to sequences in EBV, to target its locus-specific integration. The linearized plasmid contained two marker genes, *GFP* and the hygromycin phosphotransferase gene *hyg,* as phenotypic and selectable markers, respectively. It also included the mini-F-origin of DNA replication and the chloramphenicol resistance gene

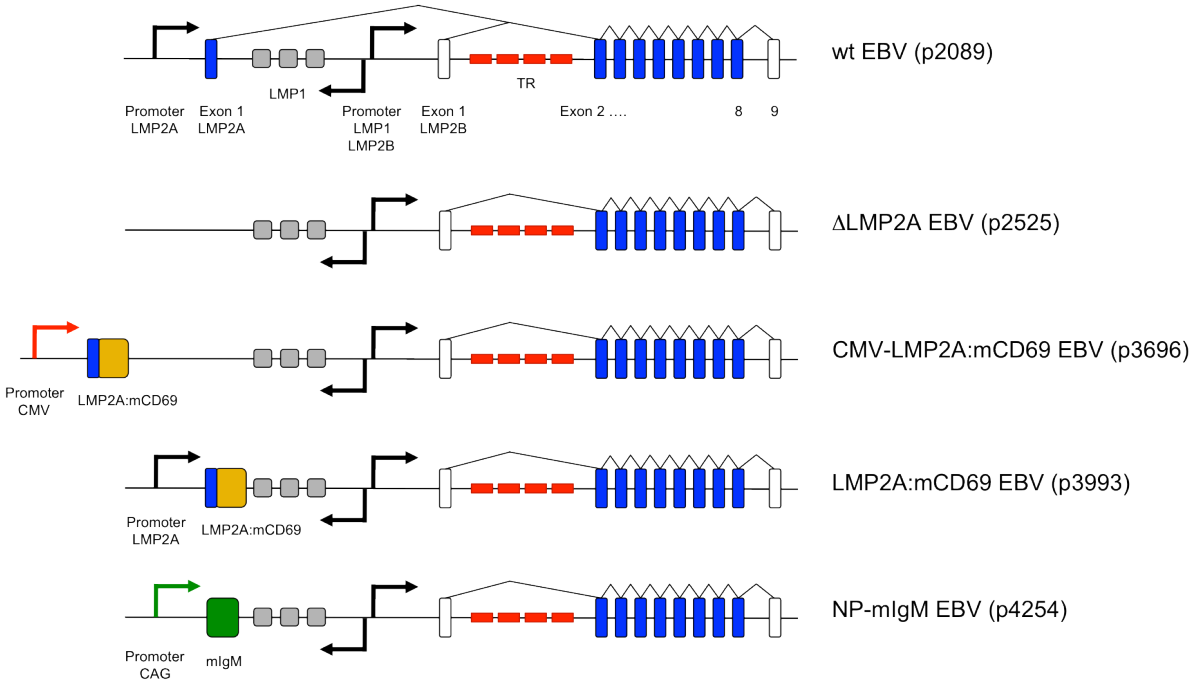


**Figure 5-4: Genomic structure of the LMP2A locus in wt EBV (p2089) as well as in ΔLMP2A, CMV-LMP2A:mCD69, LMP2A:mCD69, and NP-mIgM mutant EBVs.**
LMP2A is encoded by nine exons, which flank both sides of EBV's terminal repeats (TR). The first exon of LMP2A encodes its signaling domain. Exon two to nine are shared by LMP2A and LMP2B. The first exon of LMP2B and exon nine of LMP2A and LMP2B are noncoding. Two different promoters drive LMP2A and LMP2B expression. Four mutant maxi-EBVs were employed to compare LMP2A and BCR signaling shortly after infection. 1) In the ΔLMP2A maxi-EBV p2525, the promoter and the first exon of LMP2A were deleted. LMP2B but not LMP2A can be expressed. 2) In the CMV-LMP2A:mCD69 maxi-EBV p3696, the CMV promoter, the first exon of LMP2A, and the cDNA, coding for the transmembrane and extracellular part of murine CD69 (mCD69), were introduced into the *BALF1* locus of the ΔLMP2A construct. LMP2A:mCD69 expression is driven by the CMV promoter. The ΔLMP2A and CMV-LMP2A:mCD69 mutant maxi-EBVs were already available in the lab. 3) A new LMP2A:mCD69 maxi-EBV (p3993) was designed because stable virus producing HEK293 cells could not be generated from the maxi-EBV p3696 (CMV-LMP2A:mCD69). The mCD69 fragment was directly cloned downstream of the first exon of LMP2A, and the fusion gene is under control of the LMP2A promoter. In the LMP2A:mCD69 maxi-EBV construct p3993, wt LMP2A is not expressed because the splice site downstream of the first exon of LMP2A is deleted. 4) The promoter of the LMP2A gene and its first exon were replaced by the CAG composite promoter and the cDNA coding for a 4-hydroxy-3-nitrophenyl (NP)-specific murine IgM (mIgM) in the maxi-EBV p4254.

for propagation and selection in *E. coli*. The F factor plasmid was introduced into the B95.8 EBV genome by homologous DNA recombination. The plasmid that contained the recombinant EBV genome was termed p2089 maxi-EBV. Viral particles could be reconstituted in HEK293 cells, which carried the p2089 maxi-EBV plasmid stably. LCLs generated with p2089 EBV have the same wild-type (wt) phenotype as infected with B95.8 EBV but express GFP.

The first exon of LMP2A codes for the N-terminal part of LMP2A (see section 1.3.4.1) and is important for LMP2A signaling. LMP2A is constitutively active, but an inducible LMP2A version was planed to study LMP2A signaling. A chimeric LMP2A:mCD69 protein, which consists of the extracellular and transmembrane domain of murine CD69 (mCD69) as well as the N-terminal domain of LMP2A, was designed. CD69 is a type II transmembrane protein expressed on activated lymphocytes. A ligand for CD69 is not known, but mCD69 can be cross-linked with an α-mCD69 antibody. The cytomegalovirus (CMV) promoter together with the open reading frame coding for LMP2A:mCD69 were cloned into the BALF1 locus of the ΔLMP2A maxi-EBV (p2525) via homologous recombination. BALF1 is one of the two known viral homologs of the anti-apoptotic protein Bcl-2 (B cell lymphoma 2). Deletion of BALF1 from the EBV genome does not influence EBV's transformation capacity (Altmann & Hammerschmidt, 2005). The maxi-EBV plasmid was transfected into HEK293 cells, which were hygromycin selected to obtain stable virus producing cell lines. Unexpectedly, stable virus producer cell lines could not be established with this mutant virus in several attempts. Limited numbers of viral particles, sufficient to establish LCLs with the CMV-LMP2A:mCD69 maxi-EBV, could be generated with the aid of a packaging cell line (Hettich *et al.*, 2006). A detailed analysis of the genetic DNA of this mutant EBV revealed a partial deletion of family repeats (FRs). The FRs together with EBNA1 are important for vial genome maintenance (Ali *et al.*, 2009). Therefore, I cloned a new LMP2A:mCD69 maxi-EBV (p3993) in an attempt to obtain high titers of EBV supernatants for infection studies. In this approach, the cDNA coding for the transmembrane and extracellular part of mCD69 was directly cloned downstream of the first exon of LMP2A in the wt maxi-EBV (p2089) to bring LMP2A:mCD69 expression under control of the viral LMP2A promoter. wt LMP2A is not expressed because the introduction of the mCD69 fragment deletes the

splice donor signal sequence downstream of the first exon of LMP2A. I could establish high titer virus producer cell lines from the LMP2A:mCD69 maxi-EBV.

An additional mutant EBV with an antigen-inducible immunoglobulin (Ig) gene replacing LMP2A was designed to compare LMP2A and BCR signaling. A murine IgM (mIgM) that binds the hapten 4-hydroxy-3-nitrophenyl (NP) was chosen because its functionality has already been shown in the quasi-monoclonal mouse (see section 1.2.5). mIgM signaling can be induced by adding $NP_x$-BSA antigen or cross-linking with an α-mIgM specific antibody. The cDNA coding for the murine μ heavy and murine λ light chains of the NP-mIgM was introduced into LMP2A's first exon thereby deleting it. In initial experiments, expression of the mIgM in LCLs infected with the NP-mIgM mutant EBV could not be detected by Western blot or flow cytometry. Therefore, the weak LMP2A promoter was replaced by the much stronger CAG composite promoter (Miyazaki *et al.*, 1989; Niwa *et al.*, 1991; Xu *et al.*, 2001). This promoter consists of the CMV immediate early enhancer, the chicken β actin promoter, followed by the first chicken β actin intron, and a splice acceptor sequence derived from the second rabbit β globin intron. Addition of introns to the promoter increased gene expression (Niwa *et al.*, 1990; Choi *et al.*, 1991). In the NP-mIgM maxi-EBV p4254, which is $LMP2A^-$ but expresses the genes encoding LMP2B and LMP1, the CAG promoter controls the NP-mIgM expression. The molecular structure of the mIgM cDNA is explained below (see section 5.2.1.2)

### *5.2.1.1 Expression and functionality of LMP2A:mCD69 in LCLs*

Wild type LMP2A is constitutively active, which does not allow studying LMP2A signaling easily. Therefore, a maxi-EBV, which encodes the inducible LMP2A:mCD69 protein instead of LMP2A, was established (p3993, Figure 5-4). Infection of adenoid B cells with this mutant EBV generated LCLs, which were stained with α-mCD69 antibodies and analyzed by flow cytometry to investigate whether the LMP2A:mCD69 protein can be detected on the cell surface. LCLs established from wt EBV infection were used as negative control. Established CMV-LMP2A:mCD69 LCLs (p3696), which express the LMP2A:mCD69 protein under control of the CMV promoter and were available in the laboratory, served as positive control. Figure 5-5 shows the distribution of the

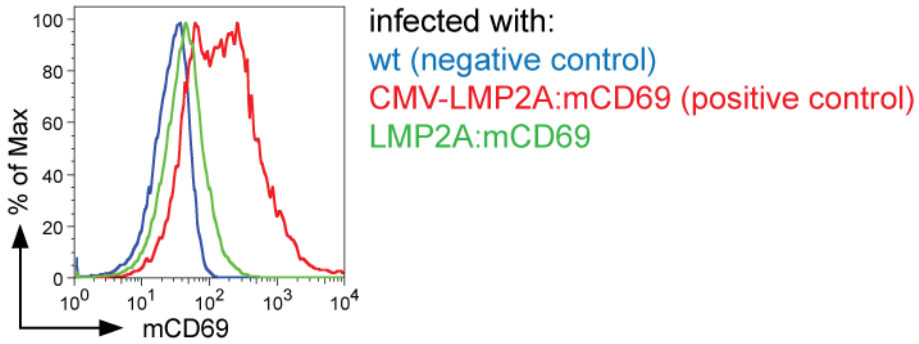


**Figure 5-5: Comparison of LMP2A promoter-driven and CMV promoter-driven LMP2A:mCD69 protein expression in established LCLs.**
Established LMP2A promoter-driven and CMV promoter-driven LMP2A:mCD69 LCLs were stained with α-mCD69-APC antibody and analyzed by flow cytometry. LCLs generated from wt EBV infection (blue) served as negative control. CMV-LMP2A:mCD69 and LMP2A:mCD69 LCLs show an increase in mCD69 signal compared to the negative control. The expression level of CMV promoter-driven (red) was 6-fold higher than that of LMP2A promoter driven LMP2A:mCD69 (green) according to the mean fluorescent intensities of the mCD69 specific signals.

LMP2A:mCD69 expression for the three different cell lines. CMV-LMP2A:mCD69 LCLs (red) showed a high expression of the LMP2A:mCD69 protein compared to wt LCLs (blue). LCLs, which express LMP2A:mCD69 under control of the viral LMP2A promoter (green), expressed the chimeric protein at lower levels as compared to CMV-LMP2A:mCD69 LCLs.

A hallmark of LMP2A signaling is the induced protein phosphorylation of Syk and PLCγ2 (see section 1.3.4.2). I analyzed the induced Syk and PLCγ2 phosphorylation upon mCD69 cross-linking in LMP2A:mCD69 LCLs. The endogenous human BCR was cross-linked with an α-hIgG/M antibody (25µg/ml) in LCLs established with wt EBV, CMV-LMP2A:mCD69 EBV, and LMP2A:mCD69 EBV to document Syk and PLCγ2 phosphorylation. LMP2A:mCD69 was cross-linked with a hamster-α-mCD69 (1µg/ml or 15µg/ml) followed by α-hamster secondary antibody (5µg/ml or 15µg/ml). All cross-links were performed at 37°C for 10min. Cells were fixed, permeabilized, and stained with phosphospecific antibodies binding to phosphorylated Syk (pSyk) or phosphorylated PLCγ2 (pPLCγ2). Uninduced cells were stained equally but in the absence of the cross-linking antibody. Stained cells were analyzed by flow cytometry.

Cross-linking of the BCR with α-hIgG/M antibody induced Syk and PLCγ2 phosphorylation in all three cell lines (Figure 5-6, A and B, first row) indicating that the

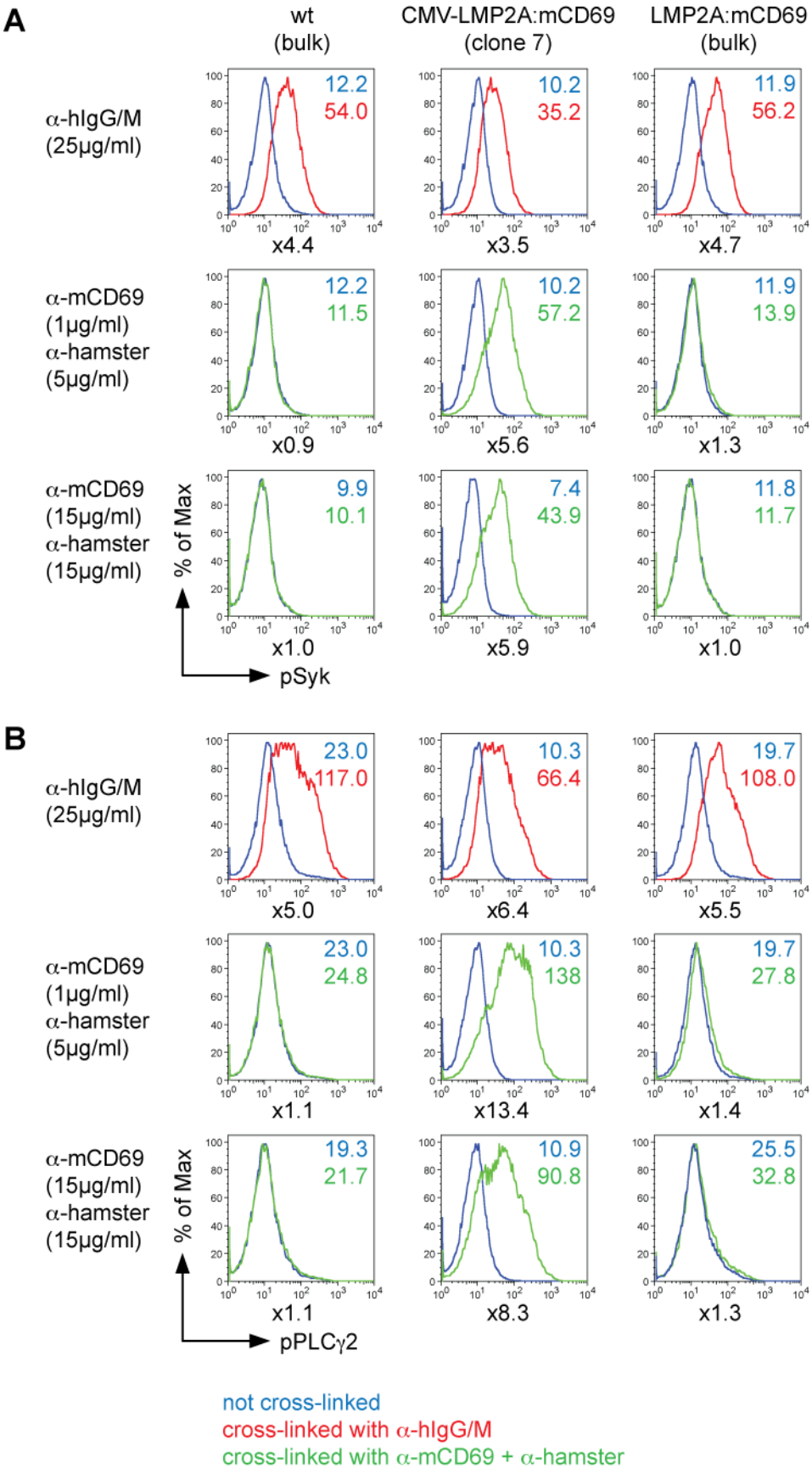
A
wt (bulk)
CMV-LMP2A:mCD69 (clone 7)
LMP2A:mCD69 (bulk)
α-hIgG/M (25µg/ml)
α-mCD69 (1µg/ml) α-hamster (5µg/ml)
α-mCD69 (15µg/ml) α-hamster (15µg/ml)
12.2
54.0
x4.4
10.2
35.2
x3.5
11.9
56.2
x4.7
12.2
11.5
x0.9
10.2
57.2
x5.6
11.9
13.9
x1.3
9.9
10.1
x1.0
7.4
43.9
x5.9
11.8
11.7
x1.0
% of Max
pSyk
B
α-hIgG/M (25µg/ml)
α-mCD69 (1µg/ml) α-hamster (5µg/ml)
α-mCD69 (15µg/ml) α-hamster (15µg/ml)
23.0
117.0
x5.0
10.3
66.4
x6.4
19.7
108.0
x5.5
23.0
24.8
x1.1
10.3
138
x13.4
19.7
27.8
x1.4
19.3
21.7
x1.1
10.9
90.8
x8.3
25.5
32.8
x1.3
% of Max
pPLCγ2
not cross-linked
cross-linked with α-hIgG/M
cross-linked with α-mCD69 + α-hamster

**Figure 5-6: Induction of BCR and LMP2A:mCD69 signaling in BCR$^+$ established LCLs.**
BCR and LMP2A:mCD69 signaling was investigated in three different LCLs with antibodies directed against phosphorylated Syk (pSyk, panel A) and phosphorylated PLCγ2 (pPLCγ2, panel B). The two different LCLs were generated from either wt EBV- (left column) or LMP2A:mCD69 mutant EBV-infection of primary B cells (right column). The two bulk populations were compared to a positive control, which is a clonal LCL infected with the CMV-LMP2A:mCD69 mutant EBV (middle column). The BCR of wt, CMV-LMP2A:mCD69, and LMP2A:mCD69 BCR$^+$ established LCLs was cross-linked with an α-hIgG/M antibody. LMP2A:mCD69 was cross-linked with hamster-α-mCD69 and α-hamster antibodies. The cross-link was accomplished for 10min at 37°C. Cells were fixed, permeabilized and stained with α-pSyk-Alexa647 or α-pPLCγ2-Alexa647.

cells were able to induce protein phosphorylation upon BCR stimulation. wt EBV infected LCLs did not show an increase in pSyk and pPLCγ2 upon cross-linking with hamster-α-mCD69 and α-hamster antibodies, as expected (Figure 5-6, A and B, first column). mCD69 cross-linking increased pSyk and pPLCγ2 levels in LCLs expressing the LMP2A:mCD69 protein under control of the CMV promoter (Figure 5-6, A and B, second column) but not the LMP2A promoter (Figure 5-6, A and B, third column). An increase of hamster-α-mCD69 and α-hamster cross-linking antibody concentrations did not increase pSyk and pPLCγ2 levels in LMP2A promoter driven LMP2A:mCD69 LCLs suggesting that the LMP2A:mCD69 protein expression level in these cells might not be high enough to allow LMP2A:mCD69 signaling.

The LMP2A promoter was replaced by the CAG promoter in another maxi-EBV (p4252 maxi-EBV) to increase the expression of LMP2A:mCD69. Unexpectedly, it was not possible to generate stable HEK293 virus producer cell lines because transfected, GFP$^+$ HEK293 cells died shortly after p4252 maxi-EBV transfection followed by hygromycin selection. Because overexpression of the *LM2A:mCD69* gene from the CAG promoter might have caused reduced HEK293 survival, a "loxP - neomycin resistance gene - stop - loxP" cassette was introduced downstream of the CAG promoter in the p4252 maxi-EBV construct. In the resulting p4489 maxi-EBV, LMP2A:mCD69 expression is blocked, but, again, stable HEK293 virus producer cell lines could not be established. The reason for this unexpected and uncommon characteristics could not be identified although parts of the maxi-EBV plasmid were confirmed by DNA sequencing. It cannot be excluded that unrecognized additional mutations in the maxi-EBV were the cause of this failure.

### *5.2.1.2 Strategy of NP-mIgM expression in EBV-infected B cells*

As described in section 5.2.1, I established a mutant maxi-EBV p4254, which is LMP2A$^-$ but encodes a CAG promoter driven NP-hapten specific murine IgM surface molecule (NP-mIgM).

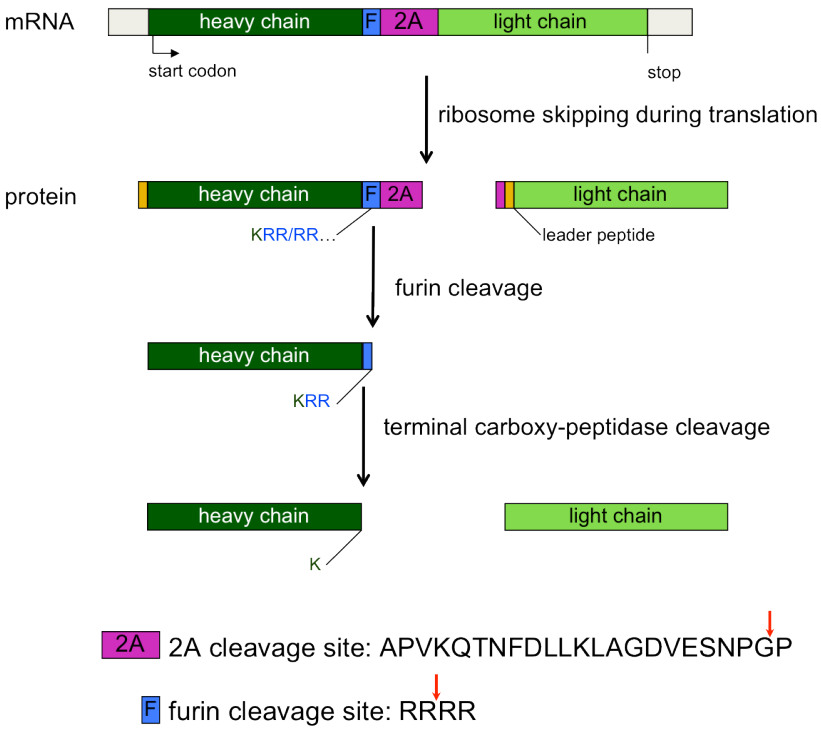


**Figure 5-7: Schematic strategy of NP-specific mIgM (NP-mIgM) protein expression and processing.** The NP-mIgM is encoded by a single open reading frame, which encompasses the cDNAs of a murine Ig μ heavy and an Ig λ light chain separated by furin and 2A cleavage sites. The 2A cleavage site is adopted from the foot-and-mouth disease virus and induces ribosome skipping during mRNA translation. Thereby, the Ig heavy and light chains are expressed as single polypeptides. This process leaves 22 amino acids of the 2A sequence at the C-terminus of the heavy chain. A furin cleavage site was introduced upstream of the 2A site. Furin is a cellular endoprotease, which cuts the consensus sequence R-X-K/R-R. The terminal carboxy-peptidase removes basic amino acids (K and R) from the C-terminus of proteins. The additional P at the N-terminus of the light chain is removed together with the leader peptide during light chain maturation.

In this mutant, the heavy and light chain cDNAs were expressed from the CAG promoter as a single open reading frame (ORF) to ensure equimolar expression of both Ig chains. The cDNAs were separated by a furin and a 2A cleavage site (Figure 5-7). The 2A cleavage site was adopted from the food-and-mouth disease virus (Ryan *et al.*, 1991; Fang *et al.*, 2005) and consists of 24 amino acids. The DxExNPG amino acid sequence of the 2A motif pauses the ribosome during translation and impairs the formation of a peptide bond between the glycine and the following proline by sterical hindering (called

ribosome skipping) (de Felipe *et al.*, 2006). The already translated peptide, which is the heavy chain (Figure 5-7), is extended by 22 amino acids of the 2A site at its C-terminus. A furin cleavage site was therefore introduced between the heavy chain cDNA and the 2A site to remove this overhang. Furin is a cellular endoprotease that is widely expressed in the ER and cuts in the middle of its R-X-K/R-R recognition site (Nakayama, 1997). A R-R-R-R sequence was finally chosen because it is a substrate for both, furin and the terminal carboxypeptidase (CP), to ensure full trimming of the carboxy terminus of the Ig heavy chain. The CP is expressed in the trans Golgi network and removes the basic amino acids lysine (K) and arginine (R) from C-termini (Reznik & Fricker, 2001; Fang *et al.*, 2007). Fang *et al.* expressed an antibody from a single ORF, which was separated by a R-R-R-R sequence and a 2A site. They could show a full cleavage of the R-R-R-R sequence by furin and an elimination of the RR-overhang by the CP obtaining a native heavy chain C-terminus (Fang *et al.*, 2007). Their intention was to produce soluble antibodies, which are transported through the Golgi network. It is not clear whether the CP is also active during the processing of membrane bound Igs like the NP-mIgM. It also has to be taken into account, that the last amino acid of the heavy chain is a K, which could also be removed by the CP. After ribosome skipping, translation of the light chain protein is expected to occur, which contains an additional P at its N-terminus. During translocation of the heavy and the light chains into the ER, the leader sequence is clipped of eliminating the additional P (Figure 5-7) (Janeway *et al.*, 2001).

#### *5.2.1.3 Expression of the NP-mIgM in LCLs*

SDS-Page and Western Blot analysis of LCLs, established with the p4254 mutant EBV expressing NP-mIgM, was performed to check whether the murine μ heavy (mμ) and λ (mλ) light chains were expressed and processed as anticipated. Cleared cell lysates were loaded onto SDS-gels and blotted on nitrocellulose membranes, which were stained with α-mμ, α-mλ, and α-actin (loading control) antibodies. The following control cell lines were used to approve the specificity of the α-mμ and α-mλ antibodies: (i) the murine Ableson transformed murine pre-B cell line $TK^-$ that does not express Ig heavy and light chains served as negative control for both antibodies, (ii) the mμ-transformed $TK^-$ cell line (TKμ) served as positive control for the α-mμ antibody, and (iii) the J558L murine

plasmacytoma cell line, which expresses high levels of mλ light chain, served as positive control for the α-mλ antibody.

Established LCLs, which were generated from infecting adenoid B cells with ΔLMP2A EBV and wt EBV, did not show expression of mμ and mλ, as expected (Figure 5-8). In contrast, mμ and mλ were detectable in NP-mIgM LCLs at two weeks post infection indicating that the heavy and the light chains were expressed and processed as single polypeptides. The mμ band of NP-mIgM LCLs ran slightly higher than of TKμ cells, which might be either due to an incomplete removal of the 2A sequence by furin and CP cleavage (see section 5.2.1.2) or additional protein glycosylation.

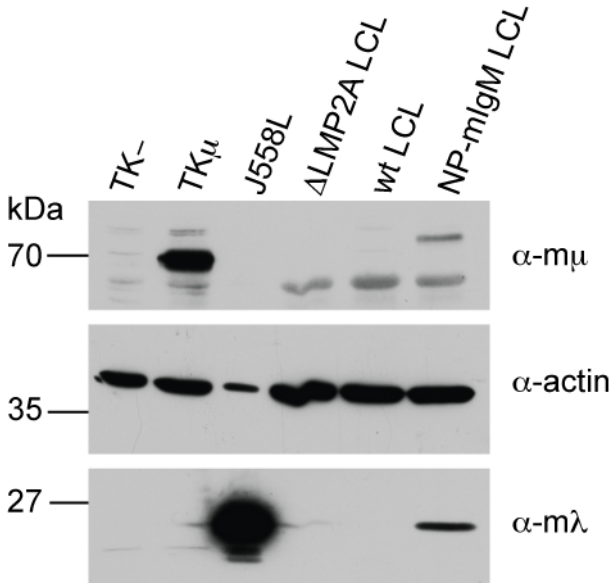


**Figure 5-8: Protein expression of the murine heavy and light chains in established NP-mIgM LCLs determined by Western Blot analysis.**
LCLs were established by infecting adenoid B cells with wt, ΔLMP2A, and NP-mIgM EBVs. SDS-page and Western blot analysis were performed to determine whether the NP-mIgM was expressed in NP-mIgM LCLs. Cleared cell lysates were loaded onto a SDS-gel and blotted to a nitrocellulose membrane. The membrane was stained with α-murine IgM heavy chain (α-mμ) and α-murine λ light chain (α-mλ) antibodies. α-actin antibody staining was used as loading control. The following control cell lines were used to verify the specificity of the α-mμ and α-mλ antibodies. The Ableson transformed murine pre-B cell line TK-, which does not express Ig heavy and light chains, served as a negative control for the α-mμ and α-mλ antibodies. The mμ-transformed TK- cell line (TKμ) served as a positive control for the α-mμ antibody. The J558L murine plasmacytoma cell line, which expresses high levels of mλ, served as a positive control for the α-mλ antibody. LCLs generated from wt EBV and ΔLMP2A EBV infection did not show expression of mμ and mλ chains, as expected. Expression of mμ heavy chain and mλ light chain in NP-mIgM LCLs was detectable. The mμ band of the NP-mIgM LCLs ran slightly higher than of the TKμ cell line, which might be either due to an incomplete cleavage of the heavy chain-2A fragment by furin or due to protein glycosylation.

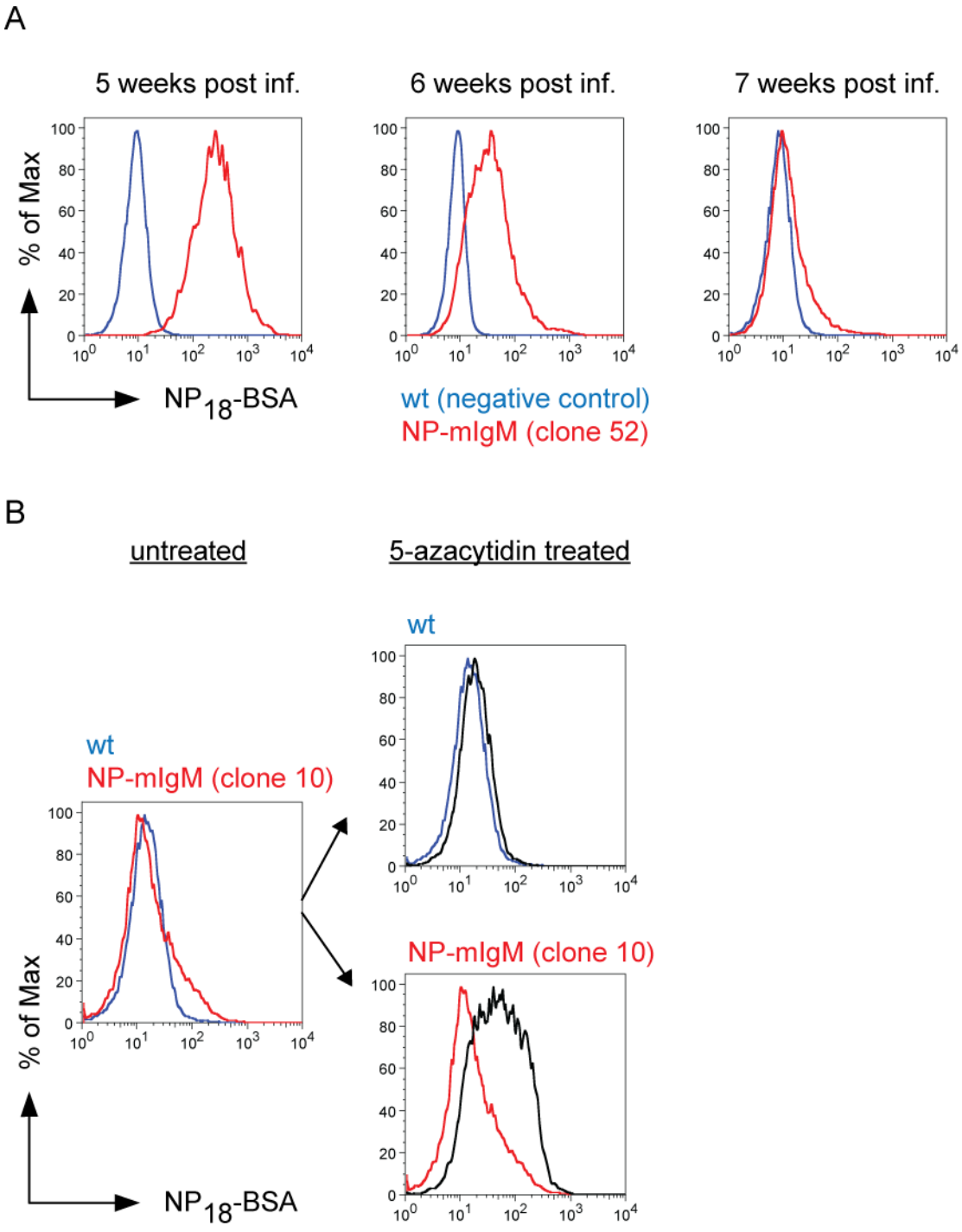


**Figure 5-9: Methylation-dependent down regulation of NP-mIgM expression in established LCLs.** NP-mIgM LCL clones were established by limited dilution infection of adenoid B cells with NP-mIgM EBV. Ectopic expression of the mIgM in the LCL clones was determined by their ability to bind the antigen $NP_{18}$-BSA. The cells were stained with $NP_{18}$-BSA-biotin and streptavidin-PE-Cy7 and analyzed by flow cytometry. A) LCLs generated from wt EBV infection were used as negative control (blue line). Clone 52 showed a strong NP binding capacity five weeks post EBV infection. However, one and two weeks later the $NP_{18}$-BSA-binding dramatically decreased. B) NP-mIgM LCL clone 10 and wt LCLs were treated with 5µM 5-azacytidine for 72h to revert CpG methylation of DNA. LCLs were stained with $NP_{18}$-BSA-biotin and streptavidin-PE-Cy7 and analyzed by flow cytometry. NP-mIgM LCL clone 10 but not wt LCLs showed an increase in NP-binding capacity after treatment with 5-azacytidine. (post inf.: post infection)

Flow cytometry analysis was performed to test whether NP-mIgM immunoglobulin was also transported to the cell surface and could bind its antigen NP-BSA. Single cell clones were established by infecting limited numbers of adenoid B cells with NP-mIgM EBV (p4254). Binding of the antigen NP and ectopic expression of the NP-mIgM was tested by staining with $NP_{18}$-BSA-biotin in combination with streptavidin-PE-Cy7 followed by flow cytometry analysis. Two LCL clones (10 and 52) were obtained, which expressed high levels of the NP-mIgM five weeks post infection compared to wt EBV-infected LCLs. However, when the staining was repeated six and seven weeks post infection, the NP-binding capacity was dramatically decreased (Figure 5-9, A). This was most probably due to a decrease in NP-mIgM expression induced by methylation-dependent promoter silencing, which, in general, can be reversed by 5-azacytidin treatment. Accordingly, wt and NP-mIgM LCLs were treated with 5µM 5-azacytidin for 72h. 5-azacytidin is converted into 5-azacytosin in the cell and incorporated into the DNA. 5-azacytosin irreversibly tethers DNA methyltransferase 1 (Dnmt1) to the DNA, which leads to a loss of DNA methylation and promoter reactivation in dividing cells (Christman, 2002). Prior to 5-azacytidin treatment, only a minor fraction of NP-mIgM LCLs was able to bind $NP_{18}$-BSA as compared to wt LCLs. After 5-azacytidin treatment, $NP_{18}$-BSA binding increased (Figure 5-9, B) indicating that the reduced NP-binding capacity in established NP-mIgM LCLs was due to methylation-dependent promoter silencing and epigenetic repression of this gene.

B cells of the quasi-monoclonal (QM) mouse express the NP-mIgM immunoglobulin (see section 1.2.5) and bind $NP_{15}$-BSA *ex vivo* leading to an activation of BCR signaling cascades (Hokazono *et al.*, 2003). Accordingly, the QM B cells can serve as a positive control for NP-mIgM expression level and functionality.

I analyzed the expression levels of NP-mIgM on the surface of LCLs and QM B cells. Splenic cells from the QM mouse were purified and stained for the murine B cell marker B220. These murine B cells were compared to established NP-mIgM LCLs (clone 10) and ΔLMP2A LCLs. The results of the flow cytometry analysis with $NP_{18}$-BSA and α-mIgM antibodies are shown in Figure 5-10. All $B220^+$ QM B cells were mIgM and $NP_{18}$-BSA double positive indicating high expression level of mIgM molecules, which bind the

antigen $NP_{18}$-BSA. NP-mIgM LCLs showed a distribution of the α-mIgM signal ranging from low to high expressing cells. Only 40% of NP-mIgM LCLs, which showed a high mIgM expression similar to QM B cells, bound $NP_{18}$-BSA suggesting that $NP_{18}$-BSA could only be bound if the surface density of the mIgM was high enough.

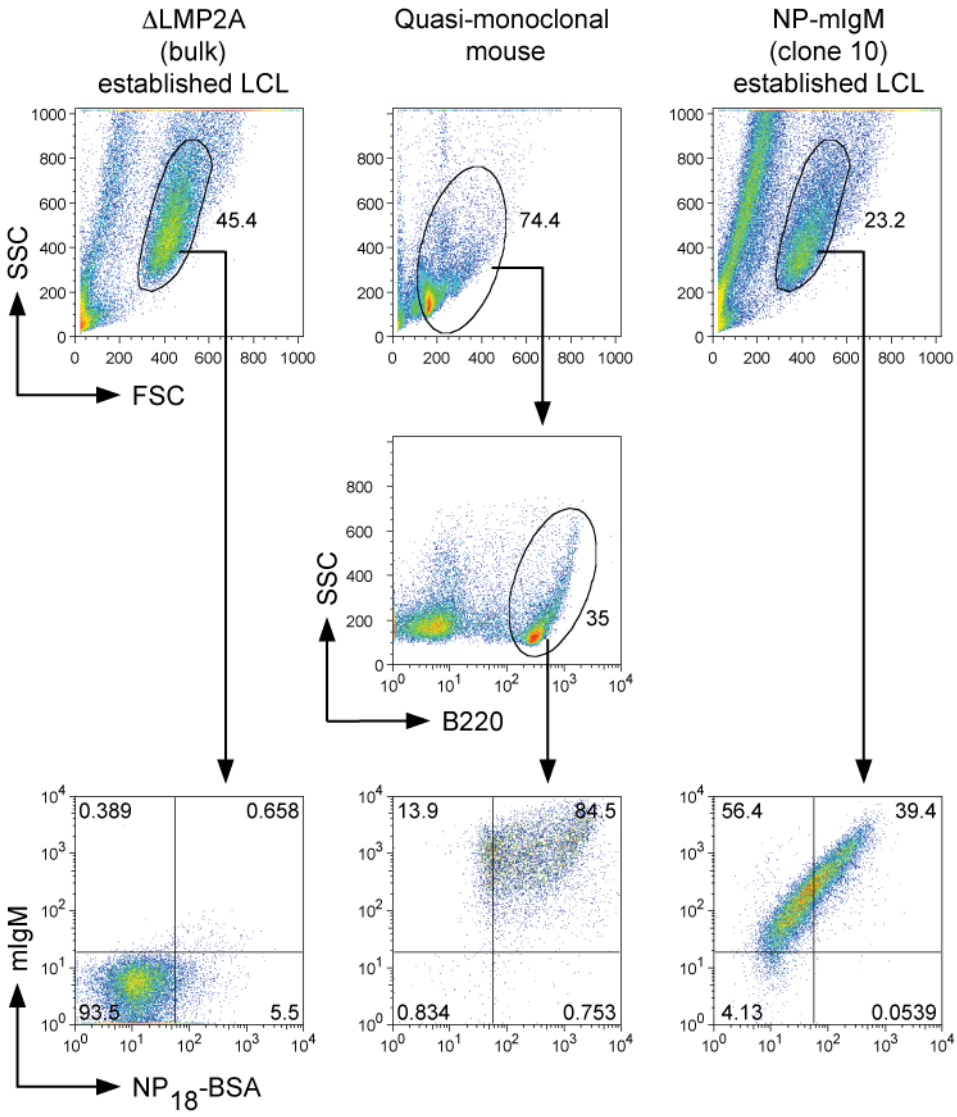


**Figure 5-10: Ectopic expression and NP-binding of the NP-mIgM in established LCLs and splenic B cells of the quasi-monoclonal mouse (QM mouse).**
NP-mIgM LCL (clone 10) was compared to ΔLMP2A EBV-infected LCLs and splenic B cells from the QM mouse for surface expression of mIgM immunoglobulin and binding of $NP_{18}$-BSA. Cells were stained with α-mIgM-Dylight647, $NP_{18}$-BSA-biotin, and streptavidin-PE-Cy7, the murine B cell marker of splenic QM mouse cells was stained with α-B220-FITC antibody. All QM $B220^+$ B cells showed a high and uniform mIgM surface expression and were able to bind the antigen $NP_{18}$-BSA. The expression level of the mIgM in established NP-mIgM LCLs ranged from low to high expressing cells. Only NP-mIgM LCLs, which showed a high mIgM surface density, were able to bind $NP_{18}$-BSA.

To sum up, Western blot and flow cytometry analysis verified the expression of NP-mIgM heavy and light chains in newly established LCLs, but the NP-mIgM expression level diminished over time due to methylation-dependent promoter silencing. As a consequence, only 40% of established NP-mIgM LCLs of clone 10 were able to bind $NP_{18}$-BSA.

#### *5.2.1.4 Signaling capacity of the NP-mIgM in LCLs compared to splenic B cells from the quasi-monoclonal mouse*

My experiments showed that about 40% of NP-mIgM established LCLs (clone 10) expressed high levels of the NP-specific mIgM immunoglobulin sufficient to bind the NP-antigen. I wanted to know whether the expression level supported antigen-dependent BCR signaling. Antigen- or antibody-mediated BCR cross-linking induces BCR clustering and intracellular protein phosphorylation, such as Syk (see section 1.2.3). The endogenous human BCR was cross-linked via an α-hIgG/M antibody in ΔLMP2A and NP-mIgM LCLs. The mIgM surface molecule of NP-mIgM LCLs and spleen cells from the QM mouse was triggered with the $NP_{26}$-BSA antigen or cross-linked with an α-mIgM antibody (b7-6). ΔLMP2A LCLs served as negative control, whereas QM spleen cells were the benchmark for NP-mIgM activation. The cross-link was accomplished for 10min at 37°C. Cells were fixed, permeabilized, and stained with a phosphospecific α-pSyk antibody. The pSyk levels of cross-linked and untreated cells were compared in Figure 5-11.

Upon stimulation of the endogenous human BCR, ΔLMP2A LCLs and NP-mIgM LCLs displayed a three and five fold increase in pSyk levels indicating that these cells were capable of Syk phosphorylation. Cross-linking antibodies directed against mIgM surface molecule promoted pSyk levels in both, NP-mIgM LCLs and QM spleen cells. Because spleen cells from the QM mouse were not enriched for B cells in this assay, they showed only a small peak of pSyk enrichment after α-mIgM treatment, which could be assigned to the B cell fraction. The successful induction of Syk phosphorylation in NP-mIgM LCLs upon antibody-mediated cross-linking pointed out that a murine IgM immunoglobulin is able to transmit signals into a human B cell. It was shown previously that a human IgM is

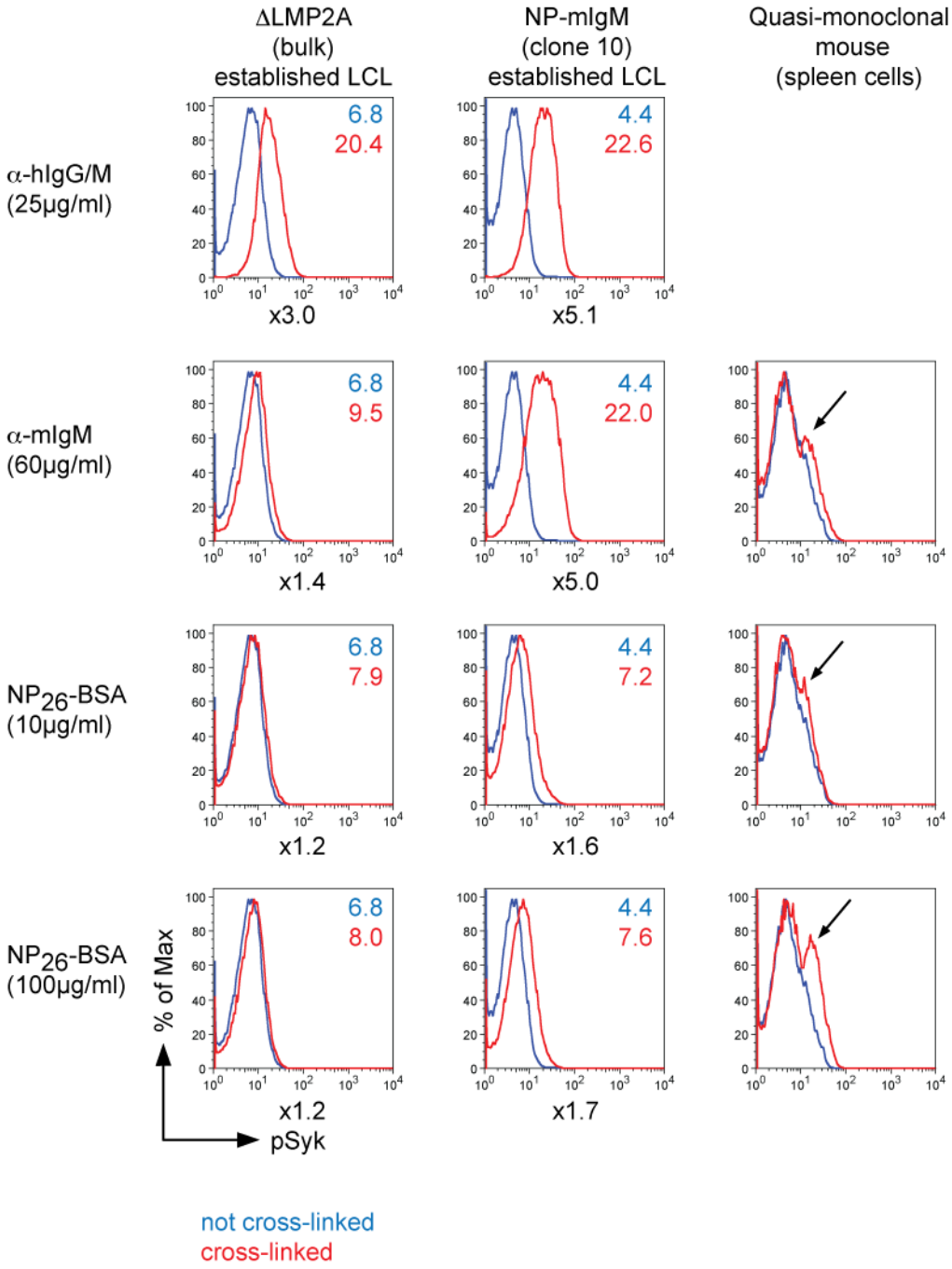


**Figure 5-11: Signaling of human (h) BCR and NP-specific murine (m) IgM surface immunoglobulin in BCR⁺ established LCLs.**

Stimulation of the surface BCR by antigen or via antibody-mediated cross-linking activates signaling cascades that induce phosphorylation of Syk (pSyk). Signaling of the endogenous hBCR and the transgenic mIgM in NP-mIgM LCLs were measured by pSyk phosphospecific antibodies and flow cytometry. The hBCR of ΔLMP2A and NP-mIgM BCR⁺ established LCLs was cross-linked with an α-hIgG/M antibody for 10min at 37°C. The mIgM of NP-mIgM BCR⁺ established LCLs as well as splenic QM B cells was cross-linked with an α-mIgM antibody (b7-6) or stimulated with $NP_{26}$-BSA antigen for 10 min at 37°C, ΔLMP2A LCLs served as negative control. Cells were fixed, permeabilized, and stained with α-pSyk-Alexa647. Histograms of the pSyk-Alexa647 fluorescence intensities are shown. Numbers next to the graphs display the mean fluorescent intensities of unstimulated (blue) and stimulated (red) cells. Numbers below the graphs show the fold increases in mean fluorescent intensity of the pSyk-signal after BCR stimulation. Splenic cells of the QM mouse contain only about 20% of B cells, which led to the split of a minor subpopulation (arrows) of pSyk-positive cells, only. (Row 1) hBCR cross-linking via α-hIgG/M antibody

induced a three- and five-fold increase in pSyk levels in ΔLMP2A and NP-mIgM LCLs indicating Syk phosphorylation. (Row 2) Antibody-mediated mIgM stimulation with α-mIgM induced a five-fold increase in pSyk levels in NP-mIgM LCLs compared to unstimulated cells demonstrating that the murine IgM was able to transmit signals in human B cells. Splenic QM mouse cells showed only a small peak of pSyk after α-mIgM treatment (arrow), because only the small fraction of B cells in the mixed population reacted on BCR stimulation. (Row 3) Antigen-mediated mIgM stimulation with $NP_{26}$-BSA caused a small increase in pSyk levels in NP-mIgM LCLs compared to unstimulated cells. In splenic QM mouse cells, again, a small fraction of cells reacted on antigen stimulation. (Row 4) A 10-fold increase in antigen-concentration did not enhance Syk phosphorylation in NP-mIgM LCLs but in splenic QM mouse cells.

functional in murine B cells, but the reversed situation was not documented (Shaw *et al.*, 1990; Pleiman *et al.*, 1994; Grupp *et al.*, 1995; Zidovetzki *et al.*, 1998).

Stimulation with the $NP_{26}$-BSA antigen led to elevated pSyk levels in QM mouse spleen cells but hardly in NP-mIgM LCLs, and a 10-fold increase in antigen concentration did not elevate Syk phosphorylation in NP-mIgM LCLs, in contrast to QM mouse spleen cells. It can be concluded that the low surface expression of the NP-mIgM on LCLs is sufficient for antibody-mediated induction of the BCR but hardly to signal antigen binding.

### 5.2.2 LMP2A:mCD69 but not NP-mIgM rescued BCR-negative B cells from apoptosis

Previous experiments demonstrated that NP-mIgM expression and NP-antigen binding was heterogeneous and generally low. mIgM signaling was only measurable after antibody crosslink ,but $NP_{26}$-BSA antigen barely induced pSyk levels (Figure 5-11). The NP-mIgM LCLs (clone 10), which were used for the signaling study, expressed an endogenous human IgM providing all necessary survival signals, and the B cells did not depend on mIgM expression. $BCR^-$ B cells, which are unable to express a human BCR, undergo apoptosis because they lack tonic BCR signaling. If the virally expressed mIgM molecule were functional, it would rescue $BCR^-$ B cells from apoptosis and select those B cells, which express high levels of the mIgM. I tested whether infection of $BCR^-$ adenoid B cells with NP-mIgM mutant EBV prevents apoptosis and induces proliferation indicating that the NP-mIgM can functionally replace a human immunoglobulin.

Towards this end, a proliferation assay was established. EBV infects primary B cells *in vitro*, which start to proliferate and increase in size and granularity. Both characteristics can be monitored by flow cytometry. The FSC (forward scatter) represents the size and

the SSC (sideward scatter) the granularity of a cell. Established LCLs show a population with high FSC/SSC signals defining the "LCL gate". In the example in Figure 5-12, 6 x $10^5$ adenoid cells were infected with wt EBV at a MOI of 0.1. One day post infection (p.i.), cells were supplied with fresh medium and divided into four samples, one for each analysis time point, with a cell density of 1.5 x $10^5$ cells/ml each. When the cell density increased to approximately 1 x $10^6$ cells/ml, fresh medium was added. One, five, nine, and 21 days p.i., one quarter of the cell suspension was analyzed by flow cytometry. Cells in the LCL gate were counted and multiplied by the factor four to obtain the total number of transformed cells per sample.

One day p.i., there was no clear increase in cellular size and granularity (Figure 5-12). Cells, which appeared in the LCL gate, were outliers of the primary lymphocyte population that located to the LCL gate. Five days p.i., the uninfected primary lymphocytes population below the LCL gate nearly disappeared, but EBV transformed cells entered the LCL gate. The numbers of cells in this gate constantly increased between day nine and 21 p.i., which reflected the EBV-induced proliferation of newly established LCL cultures.

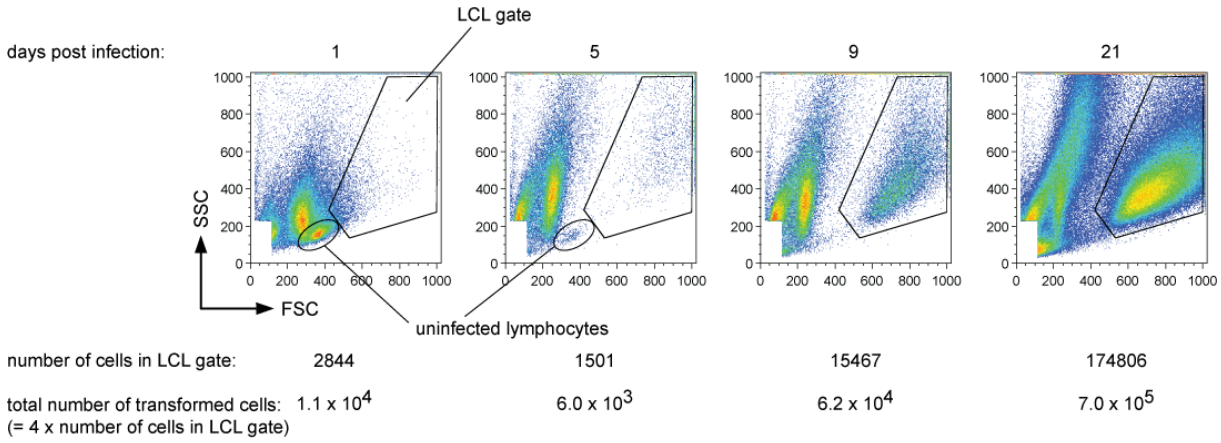


**Figure 5-12: Determination of the number of transformed cells after EBV infection.**
EBV-infected primary B cells start to proliferate and increase in size and granularity, which can be detected in flow cytometry. The forward scatter (FSC) signal reflects the size and the sideward scatter (SSC) signal the granularity of the analyzed cell. EBV-infected cells fall into the "LCL gate", as indicated, as early as five days post infection (p.i.). 6 x $10^5$ adenoid B cells were infected with wt EBV (MOI 0.1). One day p.i., infected cells were supplied with fresh medium, divided into four samples with a cell concentration of 1.5 x $10^5$ cells/ml each. One, five, nine and 21 days p.i., one quarter of the cell suspension was analyzed by flow cytometry. The number of cells in the LCL gate was determined and used to calculate the total number of transformed cells. The figure shows an example of a typical experiment.

A

| infected with \ $NP_{26}$-BSA addition | 0 µg/ml | 0.2 µg/ml | 2 µg/ml | 20 µg/ml |
|---|---|---|---|---|
| wt EBV | X | | | |
| ΔLMP2A EBV | X | X | X | X |
| NP-mIgM EBV | X | X | X | X |

B

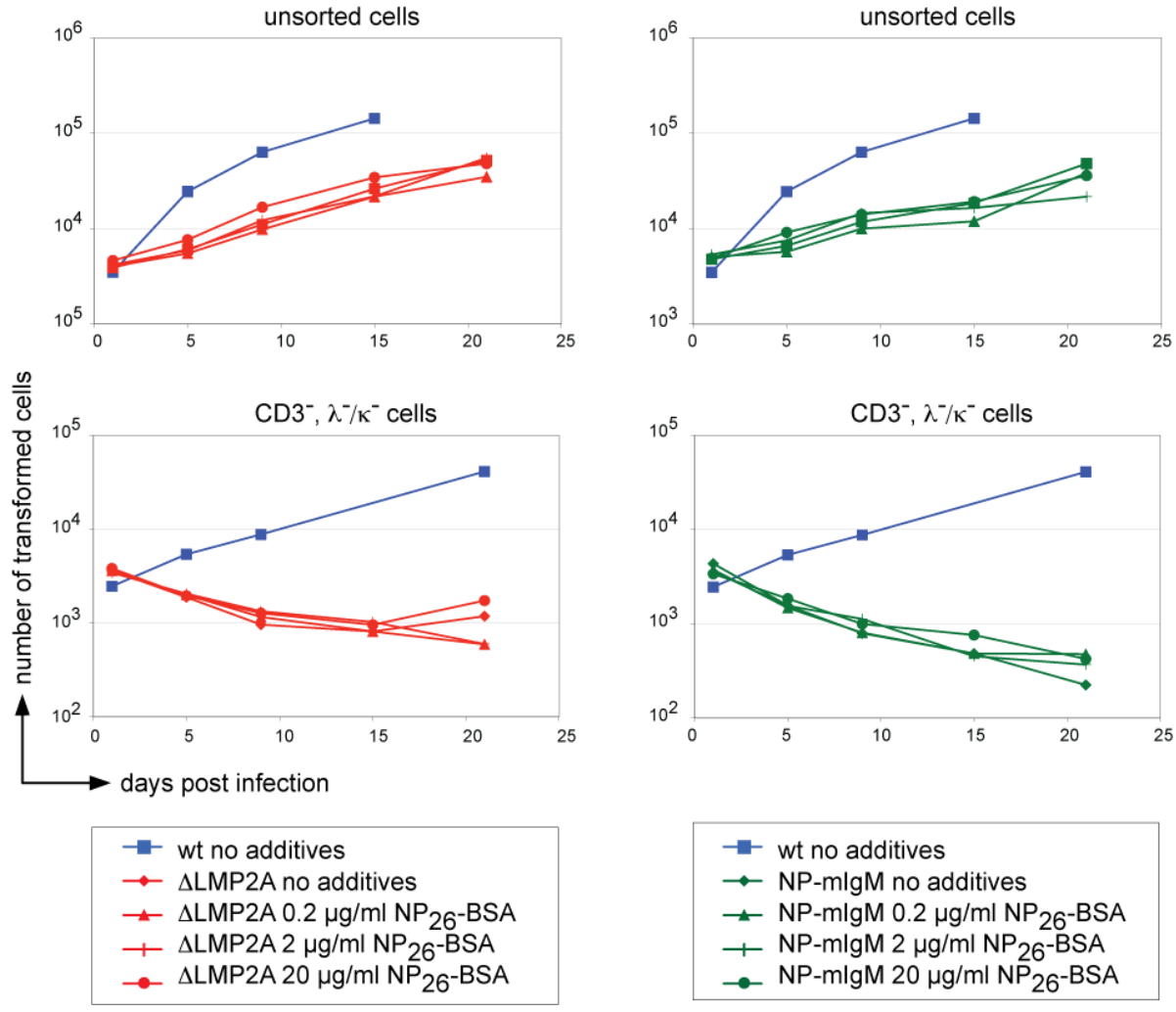

**Figure 5-13: NP-mIgM EBV does not rescue BCR$^-$ B cells from apoptosis.**
2.4 to 3.0 x $10^5$ unsorted and BCR$^-$ sorted cells were infected with wt EBV, ΔLMP2A EBV, or NP-mIgM EBV with an MOI of 0.1 and an initial cell density of 1x$10^5$ cells/ml. ΔLMP2A EBV or NP-mIgM EBV-infected cells were treated with 0.2, 2, and 20µg/ml $NP_{26}$-BSA to stimulate mIgM mediated signals or left untreated. The numbers of cells in the LCL gate were determined as described in Figure 5-12. A) Schematic overview of the experimental design. B) (Upper diagrams) Unsorted B cells were mainly BCR$^+$ and did not dependent on LMP2A or mIgM expression. Proliferation of ΔLMP2A and NP-mIgM EBV infected cells was slightly reduced compared to wt EBV infected cells. Addition of $NP_{26}$-BSA to ΔLMP2A EBV infected unsorted cells did not enhance proliferation, as expected. (Lower diagrams) BCR$^-$ (CD3$^-$, λ$^-$/κ$^-$ sorted) B cells were rescued from apoptosis by infection with wt EBV, which encodes for LMP2A. BCR$^-$ B cells, infected with NP-mIgM EBV, did not proliferate even in the presence of antigen indicating that the NP-specific mIgM did not substitute for the endogenous human BCR or EBV's LMP2A.

With this assay at hand, I asked whether mIgM expression could rescue BCR$^-$ B cells from apoptosis and support cell proliferation. BCR$^-$ lymphocytes were sorted from adenoid cells (see section 5.1.1) and infected with NP-mIgM EBV. BCR$^-$ sorted cells were expected to proliferate upon NP-mIgM EBV infection if the mIgM replaced the missing human BCR. 0.2, 2, or 20µg/ml $NP_{26}$-BSA antigen was added to increase the survival signals. Unsorted cells, which are mainly human BCR$^+$ and thus proliferate independently of mIgM expression, were used as a positive control. BCR$^-$ cells were also infected with ΔLMP2A EBV to document their dependence on either BCR or LMP2A. A summary of the different infections and their results are shown in Figure 5-13. Infection of unsorted cells with wt EBV, ΔLMP2A EBV, or NP-mIgM EBV induced their proliferation (Figure 5-13 B, upper diagrams). ΔLMP2A and NP-mIgM EBV infected unsorted cells proliferated similarly but slower than wt EBV-infected cells. In accordance with established LCLs infected with NP-mIgM EBV, which expressed only low levels of NP-mIgM on the cell surface (see section 5.2.1.3), the experiment suggested that the NP-mIgM expression levels were too low to drive proliferation of BCR$^+$ B cells. As expected, addition of $NP_{26}$-BSA to ΔLMP2A EBV-infected and unsorted cells did not increase proliferation excluding an unspecific effect of $NP_{26}$-BSA on B cell proliferation. Infection of BCR$^-$ (CD3$^-$, λ$^-$/κ$^-$) B cells with NP-mIgM EBV and addition of $NP_{26}$-BSA did not rescue them from apoptosis (Figure 5-13 B, lower diagrams).

In summary, infection of B cells with ΔLMP2A EBV or NP-mIgM EBV did not reveal any phenotypic differences: BCR$^-$ B cells went into apoptosis and BCR$^+$ B cells proliferated slower than wt EBV infected cells, documenting that the mIgM molecule did not affect B cell proliferation in this assay. Also, $NP_{26}$-BSA did not influence proliferation of NP-mIgM

EBV infected B cells, which is in line with the observation that antigen-mediated mIgM stimulation in established NP-mIgM LCLs barely increased Syk phosphorylation (see section 5.2.1.4). In the same experiment, antibody-mediated mIgM cross-linking strongly increased pSyk levels in established LCLs. To follow up on this finding, I wanted to investigate whether antibody-mediated mIgM stimulation rescues $BCR^-$ B cells from apoptosis if they were infected with NP-mIgM EBV.

I took advantage of $hCD32^+$ L-cells, which are established murine fibroblasts stably transfected with the hCD32 receptor also termed FcγRII (Peltz *et al.*, 1988). CD32 molecules bind the Fc part of IgG antibodies coupling IgG antibodies to adherent hCD32 expressing L-cells. Additionally, untransfected and hCD32 transfected L-cells provide an extracellular matrix and act as feeder cells, which secrete growth factors and support the survival of fastidious cells (Banchereau *et al.*, 1991). With this system, I investigated both, the effect of antibody-mediated mIgM and mCD69 cross-linking of NP-mIgM and LMP2A:mCD69 EBV-infected $BCR^-$ B cells, respectively.

$hCD32^+$ L-cells were stained with an α-hCD32 antibody and analyzed by flow cytometry. L929 cells, which are a sub-clone of the untransfected parental L-cell line and, thus, do not express hCD32, were used as a negative control (Sanford *et al.*, 1948). As shown in Figure 5-14 (A), almost all L-cells expressed hCD32 but L929 cells did not.

Next, I tested if the rat-α-mIgM (b7-6) and hamster-α-mCD69 antibodies, which are both IgG subtype, bound to $hCD32^+$ L-cells. 5 x $10^5$ $hCD32^+$ L-cells and L929 cells, which were used as negative control, were incubated with 60µg/ml rat-α-mIgM (b7-6) or 90µg/ml hamster-α-mCD69 antibodies for 30min at 37°C in PBS. Cells were washed and the antibodies bound to hCD32 were stained with two different secondary antibodies for 20min on ice: α-rat $F(ab')_2$-Cy5 or α-mouse $F(ab')_2$-Cy5, which cross-reacts with hamster antibodies. $F(ab')_2$ fragments lacking the Fc part were used as secondary antibodies to prevent their unspecific binding to hCD32. Staining of $CD32^+$ L-cells and L929 cells with secondary antibody alone were used as negative control. Stained cells were analyzed by flow cytometry.

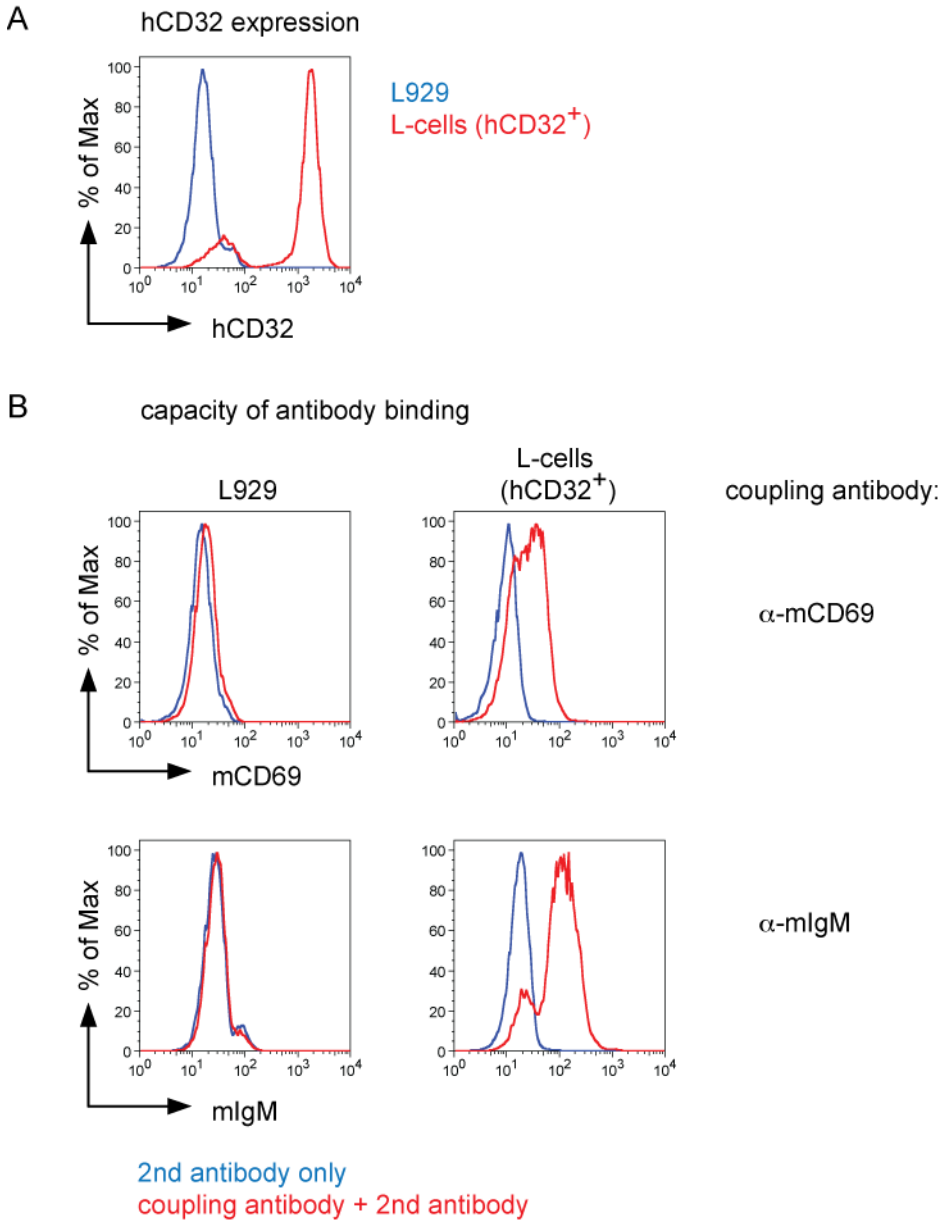


**Figure 5-14: Binding of stimulatory antibodies to hCD32⁺ L-cells.**
L–cells are established murine fibroblasts. They were stably transfected with the hCD32 receptor and designated hCD32⁺ L-cells (Stuart *et al.*, 1987). The L929 cell line is a sub-clone of the parental, untransfected L-cell line and does not express hCD32 (Sanford *et al.*, 1948). (A) hCD32⁺ L-cells were stained with an α-hCD32-Alexa647 antibody and analyzed by flow cytometry. L929 cells were used as negative control. Almost all L-cells (red) but no L929 cells (blue) showed a strong expression of hCD32. (B) 5 x $10^5$ hCD32⁺ L-cells and L929 cells, which were used as negative control, were coupled with 60µg/ml rat-α-mIgM (b7-6) or 90µg/ml hamster-α-mCD69 antibodies for 30min at 37°C in PBS. Cells were washed and stained with secondary antibodies: α-rat F(ab')$_2$-Cy5 or α-mouse F(ab')$_2$-Cy5, which cross-reacts with hamster antibodies, and analyzed by flow cytometry. The hCD32 receptor on hCD32⁺ L-cells bound the Fc-part of the two monoclonal IgG antibodies rat-α-mIgM antibody (b7-6) and the hamster-α-mCD69.

L929 cells did not stain with rat-α-mIgM or hamster-α-mCD69 antibodies (red) (Figure 5-14 B). In contrast, hCD32$^+$ L-cells showed a clear increase in fluorescent intensity upon adding the coupling-antibodies rat-α-mIgM (b7-6) or hamster-α-mCD69.

Finally, I analyzed if antibody-coupled hCD32$^+$ L-cells might rescue BCR$^-$ B cells infected with NP-mIgM or LMP2A:mCD69 EBV from apoptosis. To this end, 5x10$^5$ BCR$^-$ (CD3$^-$, λ$^-$/κ$^-$) sorted cells were infected with NP-mIgM and LMP2A:mCD69 EBV (Figure 5-15 A). Unsorted B cells, which are mainly BCR$^+$, and infection of BCR$^-$ sorted B cells with wt EBV were used as positive controls for EBV induced cell proliferation. BCR$^-$ sorted cells were expected to be rescued from apoptosis by wt EBV, which encodes the viral BCR mimic LMP2A. BCR$^-$ sorted cells were also infected with ΔLMP2A EBV, which is incapable of rescuing BCR$^-$ B cells from apoptotic death. One day p.i., cells were supplied with fresh medium and split into five samples. Each sample was plated on either uncoupled or antibody coupled (15µg/ml), irradiated hCD32$^+$ L-cells. wt EBV infected cells were plated on antibody-coupled feeder cells to assess their possible contribution to cellular proliferation. Cell density of infected cells was 1x10$^6$ cell/ml after plating on feeder-cells. Six and 13 days p.i. infected cells were plated on fresh, irradiated, and antibody-coupled hCD32$^+$ L-cells. Once a week, half of the medium was changed and fresh medium was added. Several time points p.i., the number of transformed cells in the LCL gate was determined as described before (Figure 5-12).

Unsorted B cells with a functional BCR do not dependent on survival signals from LMP2A, LMP2A:mCD69, or NP-mIgM and proliferated independently of the EBV strain used (Figure 5-15 B). wt EBV-infected unsorted B cells showed the highest proliferation rate, and α-mIgM and α-mCD69 antibodies-coupled feeder cells did not contribute to cellular proliferation. LMP2A:mCD69 and NP-mIgM infected unsorted B cells proliferated slower than wt EBV-infected cells but faster than ΔLMP2A EBV-infected cells. Stimulation with α-mIgM and α-mCD69 antibody-coupled feeder cells slightly increased the proliferation rate of the infected B cells.

A

| infected with \ coupling antibody | none | α-mIgM (b7-6) | α-mCD69 |
|---|---|---|---|
| wt EBV | X | X | X |
| ΔLMP2A EBV | X | | |
| NP-mIgM EBV | X | X | |
| LMP2A:mCD69 EBV | X | | X |

B

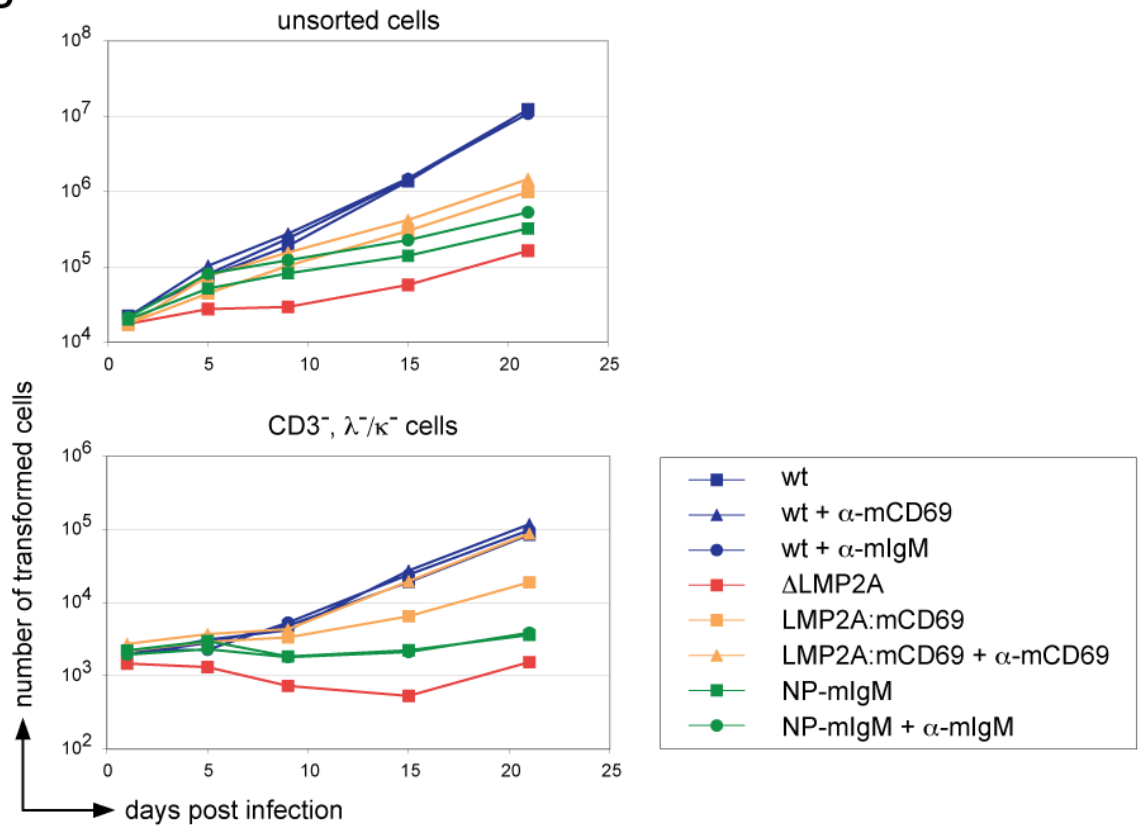


**Figure 5-15: LMP2A:mCD69 EBV but not NP-mIgM EBV rescued BCR⁻ B cells from apoptosis upon antibody-stimulation on hCD32⁺ L-cells.**
Unsorted and BCR⁻ B cells were infected with wt EBV, ΔLMP2A EBV, LMP2A:mCD69 EBV, and NP-IgM EBV strains and cellular proliferation was determined by flow cytometry, as described in Figure 5-12. A) $5x10^5$ unsorted and CD3⁻, λ⁻/κ⁻ sorted (BCR⁻) cells were infected with wt EBV, ΔLMP2A EBV, LMP2A:mCD69 EBV,

or NP-mIgM EBV (MOI 0.1) and incubated on hCD32$^+$ L-cells or hCD32$^+$ L-cells precoupled with 15µg/ml α-mCD69 or α-mIgM (b7-6) antibodies, as shown in this matrix. B) (Upper diagram) Infection with all tested EBV strains induced proliferation of unsorted B cells. Unsorted cells infected with wt EBV showed the fastest and ΔLMP2A EBV infected cells the slowest proliferation rate. Stimulation of wt EBV infected unsorted B cells with α-mCD69 or α-mIgM antibodies did not enhance proliferation. Antibody stimulation of LMP2A:mCD69 and NP-mIgM EBV infected unsorted B cells enhanced proliferation slightly. (Lower diagram) BCR$^-$ (CD3$^-$, λ$^-$/κ$^-$) sorted cells showed profound proliferation when infected with wt EBV, which encodes the BCR mimic LMP2A. Also, LMP2A:mCD69 EBV infected BCR$^-$ B cells proliferated on α-mCD69 antibody-coupled hCD32$^+$ L-cells. Unstimulated and antibody-stimulated NP-mIgM EBV infected BCR$^-$ B cells did not proliferate indicating that the NP-specific mIgM could not rescue BCR$^-$ B cells from apoptosis. CD3$^-$, λ$^-$/κ$^-$ sorted cells infected with ΔLMP2A EBV proliferated slowly probably due to contaminating λ$^+$/κ$^+$ cells, which were phenotypically λ$^-$/κ$^-$ at the time of sorting.

LMP2A$^+$ wt EBV rescued BCR$^-$ sorted B cells from apoptosis, as expected, and α-mIgM and α-mCD69 antibody-coupled feeder cells had no effect on their proliferation rate. BCR$^-$ sorted B cells infected with LMP2A:mCD69 EBV proliferated slowly, and α-mCD69 antibody-coupled feeder cells increased their rate of proliferation to wt EBV levels (Figure 5-15 B). This result was unexpected since cross-linking of LMP2A:mCD69 EBV infected cells with α-mCD69 antibody did not induce Syk and PLCγ2 phosphorylation (see section 5.2.1.1). This signaling study was accomplished in established BCR$^+$ LCLs, which expressed only low level of LMP2A:mCD69. Primary BCR$^-$ B cells, which are pro-apoptotic, depend on LMP2A:mCD69-induced signals for their survival, which might have led to a selection of cells with high levels of LMP2A:mCD69. In this experiment, cross-linked and presumably signaling LMP2A:mCD69 receptors, replaced LMP2A's function in rescuing BCR$^-$ B cells from apoptosis whereas NP-mIgM infected BCR$^-$ cells did not even when stimulated with α-mIgM antibody. Together with the experiment shown in Figure 5-13, my results suggested that BCR$^-$ infected B cells expressed insufficient levels of NP-mIgM to support their survival. Cultivation on feeder cells as well as antigen- and antibody-mediated mIgM stimulation, did not improve this situation markedly.

The objective of my project was to compare the effect of BCR and LMP2A signaling shortly after infection, which provide the necessary survival signals for BCR$^-$ B cells. To this end, the two LMP2A:mCD69 and NP-mIgM mutant EBVs were established. In principle, they should provide the opportunity to vary the timing and strength of LMP2A- and BCR-mediated signaling in infected human BCR$^-$ B cells. Infection of these cells with LMP2A:mCD69 EBV rescued them from apoptosis when cultivated on

α-mCD69 antibody-coupled feeder cells, but NP-mIgM EBV failed in this assay. Under these circumstances, a functional comparison of LMP2A and BCR-mediated signals was not possible and the planed experiments could not be accomplished.

## 5.3 Comparison of EBV's LMP2A to K1 and K15 from KSHV

### 5.3.1 Construction of K1 and K15 mutant EBVs

The two KSHV proteins K1 and K15 partially resemble LMP2A in structure and function (Damania, 2004; Brinkmann & Schulz, 2006), but it was not known if they can rescue BCR$^-$ B cells from apoptosis like LMP2A does. To address this question, I constructed two

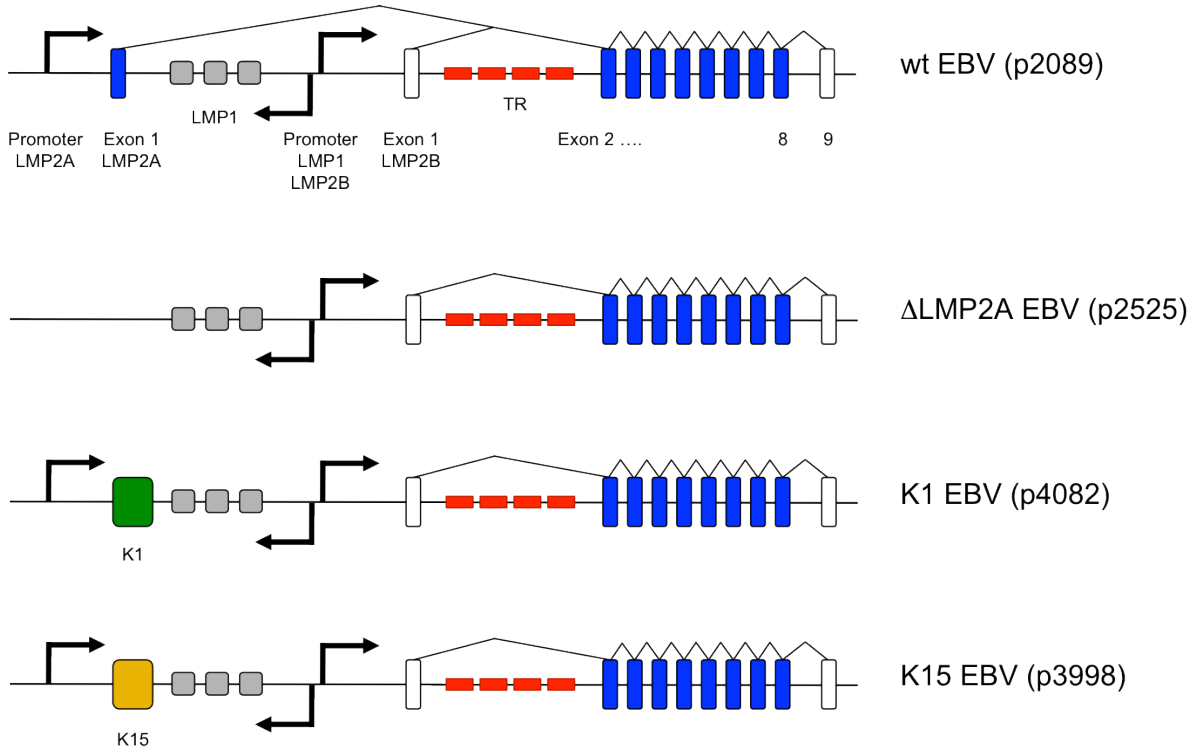


**Figure 5-16: Genomic structure of the LMP2A locus of wt EBV as well as of ΔLMP2A EBV, K1 EBV, and K15 mutant EBV.**
Nine exons encode the LMP2A gene. They flank both sides of EBV's terminal repeats (TR). The first exon encodes the signaling domain of LMP2A. Exon two to nine are shared by LMP2A and LMP2B. The first exon of LMP2B and exon nine of LMP2A and LMP2B are noncoding. Separate promoters drive LMP2A and LMP2B expression. The wt EBV p2089 generic locus reflects this situation (top). Three mutants were used to analyze the function of LMP2A, K1, and K15. In the ΔLMP2A mutant (p2525), the promoter and the first exon of LMP2A were deleted. LMP2A is deleted leaving LMP2B intact. In the K1 and K15 EBV mutants, the first exon of LMP2A was replaced by the cDNA coding for *K1* (p4082) or *K15* (p3998). The LMP2A promoter controls the expression of *K1* and *K15* genes.

mutant EBV strains (Figure 5-16). In both, the first exon of LMP2A was replaced by the cDNA coding for *K1* or *K15* P-type (45kDa isoform) in the wt maxi-EBV. The K1 maxi-EBV (p4082) and the K15 maxi-EBV (p3998) were obtained, which express K1 or K15 instead of LMP2A under control of the endogenous LMP2A promoter. The wt EBV and the ΔLMP2A EBV strains were already described in section 5.2.1.

### 5.3.2 Expression of K1 and K15 in LCLs

The expression levels of K1, K15, and LMP2A were determined in LCLs, which were established by infecting primary B cells with wt EBV, K1 EBV, or K15 EBV. To this end, mRNA was extracted from two independently generated LCL lines and transcribed into cDNA. Equal cDNA fractions, obtained from each LCL, were used to assess the transcript levels of LMP2A, K1, and K15 mRNA. The cDNA levels of LMP2A, K1, and K15 were normalized to the housekeeper gene *CDC-like kinase 2 (CLK2)*. LMP2A cDNA levels were set to one and corresponding mean and standard deviations of the three analyzed cDNAs are depicted in Figure 5-17. The expression levels of LMP2A and K1 in established LCLs were about equal whereas the expression level of K15 was reduced by a factor of 2.6.

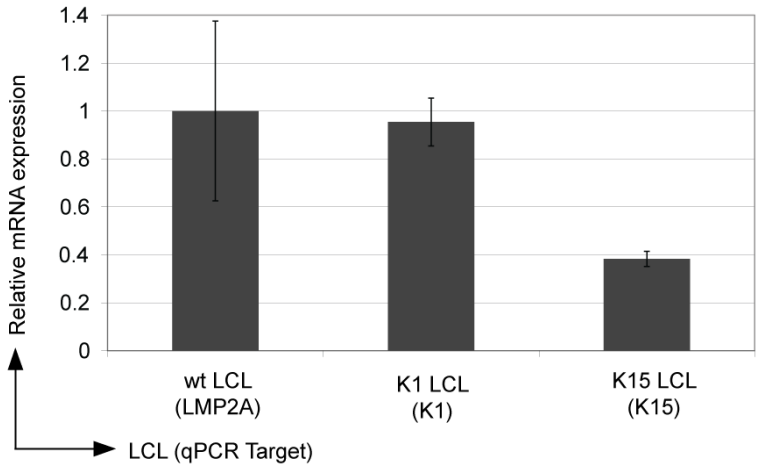


**Figure 5-17: K1 and K15 transcript levels were compared to LMP2A transcript levels in established LCLs.**
The *LMP2A* gene was replaced by the KSHV genes *K1* or *K15* in two EBV mutants, which were used to generate LCLs. mRNA expression levels were determined by cDNA synthesis and subsequent qPCR analysis. The levels of LMP2A, K1, and K15 cDNAs were normalized to the housekeeper *CLK2*. LMP2A cDNA levels were set to one. The mean and the standard deviation of two independent experiments are shown. The steady state levels of LMP2A and K1 mRNAs in bulk LCLs were about equal whereas the level of K15 mRNA was reduced by a factor of 2.6 as compared to LMP2A transcripts, which is a minor difference.

The PCR analysis also documented that K1 and K15 mRNAs are transcribed and likely translated into protein. A Western Blot assay was set up to confirm K1 and K15 protein expression. Mouse-α-K1 and rat-α-K15 antibodies produced in the laboratories of Jae U. Jung and Thomas Schulz, respectively, were used (Brinkmann *et al.*, 2003; Lee *et al.*, 2003). BCBL-1 cells, which are infected with KSHV, were used as positive control for the K1 and K15 antibodies. K1 and K15 expression in BCBL-1 cells was supposed to be increased by lytic cycle induction with 200ng/ml 12-O-tetradodecanoyl-phorbol-13-acetate (TPA) and 1 mM sodium-butyrate for 72h. Cells lysates were analyzed after Western blotting with mouse-α-K1 and rat-α-K15 as well as α-mouse-HRP and α-rat-HRP antibodies. Untreated BCBL-1 cells as well as wt EBV infected established LCL, negative for K1 and K15, were used as additional controls for mouse-α-K1 and rat-α-K15 antibodies. Staining with the α-K1 antibody did not show any bands, and staining with the α-K15 antibody did not display any bands that were present in induced BCBL-1 cells but absent in LCLs. The failure to detect K1 and K15 could have several reasons: (i) the proteins did not dissolve in Ripa buffer, (ii) the mouse-α-K1 and rat-α-K15 antibodies did not work as expected, or (iii) the lytic cycle was not induced.

Infection of $BCR^-$ B cells with K1, and K15 EBV as compared to ΔLMP2A EBV (see next section) showed a clear phenotype suggesting that K1 and K15 proteins are functional when expressed from the two mutant EBVs.

### 5.3.3 Comparison of LMP2A, K1, and K15 shortly after infection

*In vitro* infection studies of primary B cells with KSHV focusing on the functions of K1 and K15 are not practical because KSHV infects the cells inefficiently *in vitro.* Inefficient infection might be due to the low expression of heparan sulfate on non-activated B cells indispensable for KSHV adherence (Chandran, 2010). In contrast to KSHV, EBV infects all subpopulations of B cells *in vitro,* which encouraged me to use EBV as a vector for the expression of the K1 and K15 genes in primary human B cells. In these experiments, the functions of LMP2A, K1, and K15 could be compared shortly after infection of primary B cells.

#### *5.3.3.1 Rescue of BCR-negative B cells from apoptosis*

$BCR^-$ B cells are pro-apoptotic because they lack the survival signals normally provided by the BCR. They can be rescued from apoptosis by infection with EBV encoding LMP2A, which can take over the function of the BCR. In a proliferation assay, I investigated whether the KSHV proteins K1 and K15 can replace the functions of LMP2A and rescue $BCR^-$ B cells from apoptosis. To this end, 7.5 x $10^5$ unsorted, $BCR^+$ sorted ($CD3^-$, $\lambda^+/\kappa^+$) and sorted $BCR^-$ ($CD3^-$, $\lambda^-/\kappa^-$) B cells (see section 5.1.1) were infected with wt EBV, ΔLMP2A EBV, K1 EBV, and K15 EBV at an MOI of 0.1. One day p.i., the cells were supplied with fresh medium and split into five samples, which had an initial cell density of 3x$10^5$ cells/ml each. Infected cells were cultured in a humid incubator at 37°C, 5% $CO_2$, and 5% $O_2$, only, to reduce oxygen related stress. Once per week, half of the medium was replaced by fresh medium. When the cell density exceeded approximately 1 x $10^6$ cells/ml, the cell culture volume was raised. One, five, nine, 15, and 21 days p.i., the number of transformed cells in the LCL gate was determined, as described before (Figure 5-12). Proliferation of unsorted or $BCR^+$ sorted B cells does not depend on LMP2A, K1, or K15 expression because the endogenous BCR provides the necessary survival signals (Figure 5-18 A). ΔLMP2A EBV-infected $BCR^-$ sorted B cells did not proliferate because they lack necessary survival signals supplied by BCR or LMP2A and went into apoptosis reflected by a negative doubling time (Figure 5-18 B). $BCR^-$ B cells were rescued from apoptosis, if infected with wt EBV, K1 EBV, or K15 EBV strains. The doubling times of K1 and K15 EBV-infected $BCR^-$ B cells were 4.65 and 5.2 days, respectively, and lower than wt EBV-infected $BCR^-$ B cells (3.25 days). It can be concluded that K1 and K15 can partially replace LMP2A's function rescuing $BCR^-$ B cells from apoptosis.

With a similar experimental set up, I tested in a single experiment whether $BCR^-$ B cells co-infected with K1 EBV and K15 EBV strains benefit from possible cooperative functions of the two KSHV gene products. As shown in Figure 5-19, the proliferation rate of single or co-infected $BCR^+$ or $BCR^-$ B cells did not differ suggesting that K1 and K15 have similar functions in B cells, which do not act additively or synergistically.

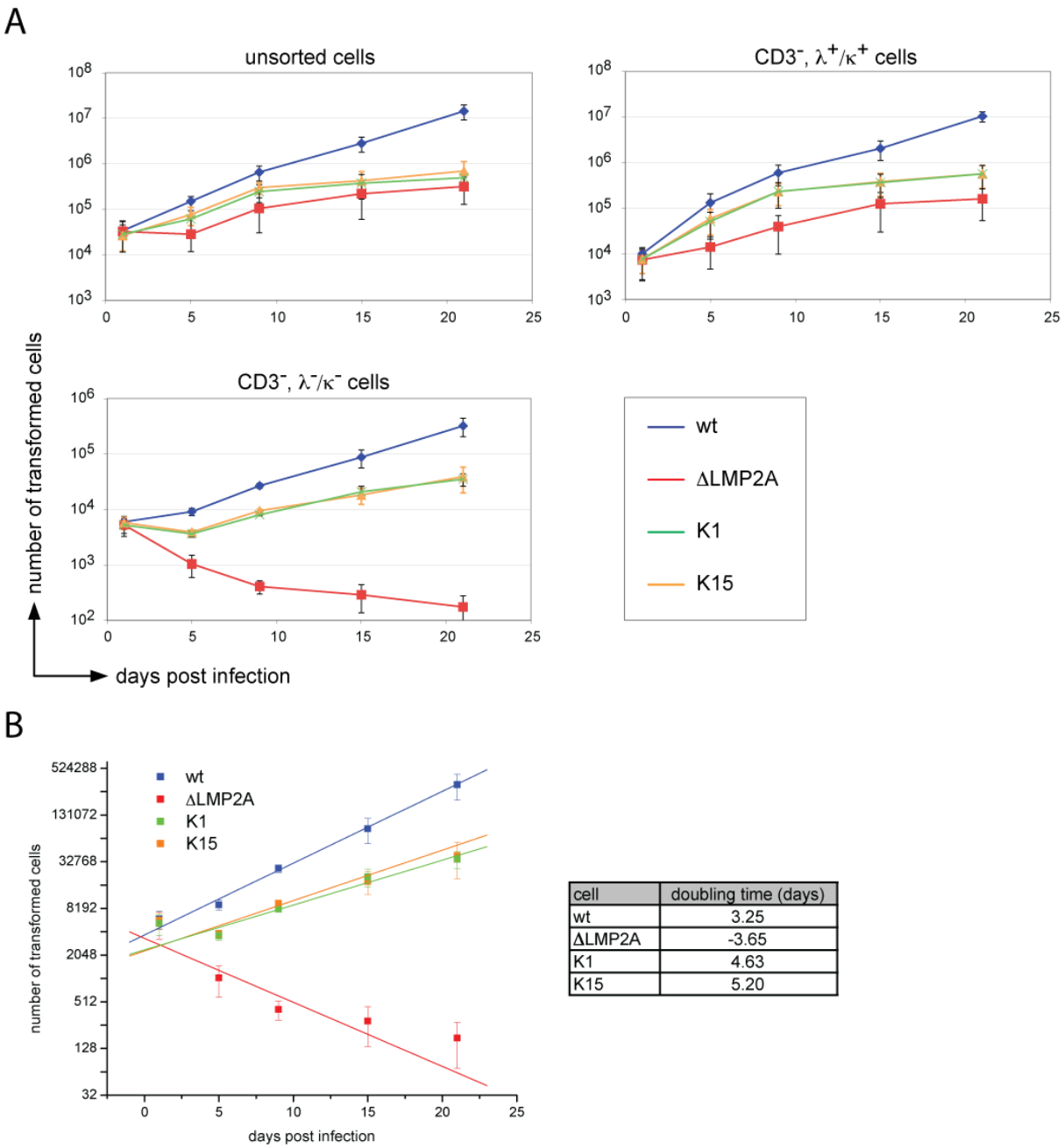


| cell | doubling time (days) |
|---|---|
| wt | 3.25 |
| ΔLMP2A | -3.65 |
| K1 | 4.63 |
| K15 | 5.20 |

**Figure 5-18: The KSHV genes *K1* and *K15* can partially rescue BCR-negative B cells from apoptosis.** 7.5 x $10^5$ unsorted, BCR$^+$ (CD3$^-$, λ$^+$/κ$^+$), and sorted BCR$^-$ (CD3$^-$, λ$^-$/κ$^-$) B cells were infected with wt EBV, ΔLMP2A EBV, K1 EBV, and K15 EBV. At the given time point p.i., the absolute numbers of cells in the LCL gate (Figure 5-12) was determined by flow cytometry. The mean and the standard deviation of three independent experiments are shown. A) Proliferation of unsorted and sorted BCR$^+$ (CD3$^-$, λ$^+$/κ$^+$) B cells does not depend on LMP2A, K1, or K15 expression as the endogenous BCR provides the necessary survival signals. The efficiency of cell proliferation was reduced in cell populations infected with ΔLMP2A EBV, K1 EBV, and K15 EBV as compared to cells infected with wt EBV. In contrast, ΔLMP2A EBV-infected BCR$^-$ (CD3$^-$, λ/κ$^-$) B cells did not proliferate. B) The numbers of BCR$^-$ (CD3$^-$, λ$^-$/κ$^-$) cells (y-axis, log 2-scale) transformed by infection with four different EBV strains was plotted over time (x-axis). The doubling time is the slope of the linear fit function. The graph of ΔLMP2A EBV-infected cells had a negative slope consistent with dying cells. Cells infected with wt EBV, K1 EBV, and K15 EBV proliferated as indicated by the positive slope of the linear fit. The doubling time of K1 and K15 EBV-infected cells was prolonged compared to wt EBV-infected cells suggesting that K1 and K15 can only partially replace LMP2A's functions.

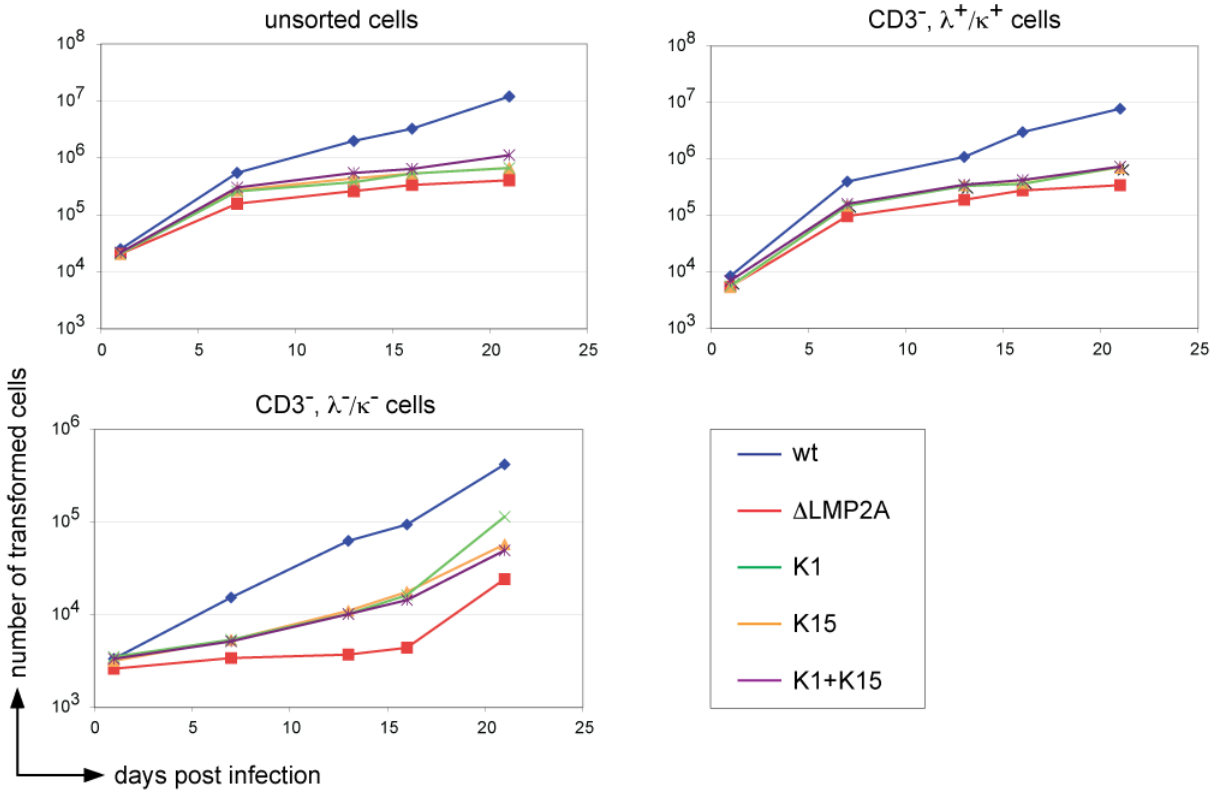


**Figure 5-19: Double infection with K1 EBV and K15 EBV strains shows no cooperativity of the two KSHV genes.**
7.5 x $10^5$ unsorted or sorted BCR$^+$ (CD3$^-$, λ$^+$/κ$^+$) and BCR$^-$ (CD3$^-$, λ$^-$/κ$^-$) B cells were infected with wt EBV, ΔLMP2A EBV, K1, and K15 mutant EBV strains. At the indicated time points p.i., the absolute numbers of cells in the LCL gate (Figure 5-12) was determined by flow cytometry. The experiment was performed once. Proliferation of unsorted and BCR$^+$ B cells does not depend on LMP2A, K1, or K15 expression because the endogenous BCR provides the necessary survival signals, but the infected B cells proliferate slower than wt EBV-infected BCR$^+$ B cells. wt EBV, K1 EBV, and K15 EBV infected BCR$^-$ B cells proliferated better than ΔLMP2A infected cells, but the proliferation rates of K1 EBV and K15 EBV-infected cells were reduced compared to wt EBV-infected cells. Co-infection of all investigated B cell subpopulations (unsorted; CD3$^-$, λ$^+$/κ$^+$ and CD3$^-$, λ$^-$/κ$^-$) with K1 and K15 EBV strains did not show any apparent differences suggesting that K1 and K15 genes have no complementing but similar functions in B cells.

### *5.3.3.2 Basal Syk phosphorylation levels*

LMP2A contains an ITAM, which is phosphorylated by the protein kinase Lyn (see section 1.3.4.2). Syk can bind with its tandem SH2-domains to the phosphorylated ITAM, which induces a conformal change and activates its kinase domain. Syk auto-phosphorylates and recruits additional signaling mediators (Mocsai *et al.*, 2010). I investigated whether K1 and K15 can also induce and increase the phosphorylation of Syk shortly after B cell infection.

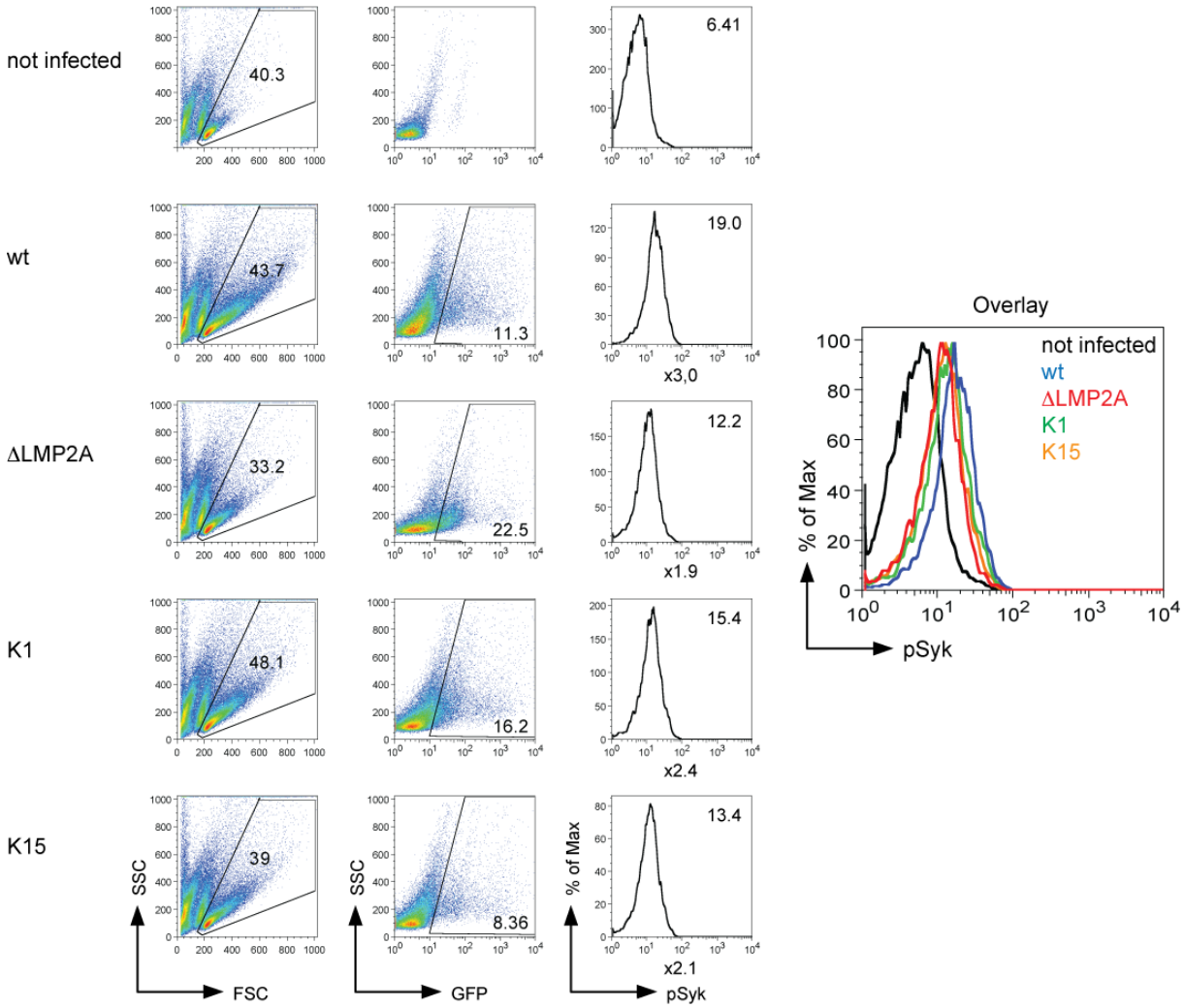


**Figure 5-20: Basal Syk phosphorylation levels in B cells infected with wt EBV, ΔLMP2A EBV, K1 EBV, or K15 EBV strains two days post infection.**
Expression of LMP2A in B cells induces an increase in Syk phosphorylation (pSyk), which was compared to K1 and K15 expression. 6 x $10^5$ B cells from adenoids were either uninfected or infected with the indicated EBV strains. Two days post infection, cells were fixed, permeabilized and the amount of pSyk was determined using phosphospecific antibodies (α-pSyk-Alexa647) and flow cytometry in the infected ($GFP^+$) and uninfected ($GFP^-$) B cell population. Numbers next to the graphs (third column) display the mean fluorescent intensities of the pSyk signal. Numbers below the graphs show the fold increase in mean fluorescent intensities compared to uninfected cells. Right, an overlay of the histograms is shown. The experiment was repeated twice, and one representative experiment is shown. All infected cells showed an increase in pSyk levels compared to uninfected cells. There were only minor differences in pSyk levels between the different infected cells, but wt EBV infected cells showed the highest and ΔLMP2A EBV infected cells the lowest pSyk level. K1 and K15 expressing cells had intermediate pSyk levels.

To this end, 6x$10^5$ unsorted B cells were infected with wt EBV, ΔLMP2A EBV, K1 EBV, or K15 EBV strains. Two days post infection, the cells were fixed, permeabilized, and stained with a phosphospecific pSyk antibody. In Figure 5-20, flow cytometry analysis of uninfected and infected B cells is shown. Lymphocytes were gated in the FSC/SSC diagram and analyzed for their GFP expression. $GFP^+$ cells infected with the recombinant

EBV strains were analyzed further along with uninfected cells. Uninfected lymphocytes (Figure 5-20, top row) were used for basal pSyk levels of resting B cells. $GFP^+$ lymphocytes (Figure 5-20, middle row) were analyzed for pSyk levels in infected B cells.

All infected cells show an increase in pSyk levels compared to uninfected cells. There was no major difference between the different EBV strains, but wt EBV-infected cells showed the highest and ΔLMP2A EBV infected cells the lowest pSyk levels. K1 and K15 EBV infected cells had intermediate pSyk levels.

#### *5.3.3.3 Activation of B cell markers*

EBV infection of B cells induces the expression of B cell activation markers CD23, CD30, CD39, CD70, and the cell adhesion molecules LFA-1 (lymphocyte-function-associated antigen 1), LFA3, and intercellular adhesion molecule 1 (ICAM-1, also known as CD54) (Young & Rickinson, 2004). Unsorted B cells were infected with wt EBV, K1 EBV, K15 EBV, and ΔLMP2A EBV and stained with fluorophore-coupled antibodies directed against CD23, CD30, CD54, and CD86. B cells were identified via their CD19 surface marker. Stained cells were analyzed by flow cytometry, and the expression levels of $CD19^+$ B cells at day zero, and $GFP^+$ infected B cells at day three and nine post infection were compared.

All infected cells showed a very similar increase in CD23 expression three and nine days p.i.. CD23 expression is activated mainly by EBNA2 (Calender *et al.*, 1987; Wang *et al.*, 1987), which all four used EBV stains encode explaining the similar expression level. CD30 expression increased later than CD23 expression in all infected cells on day nine p.i.. wt EBV-infected cells showed the highest CD30 expression level compared to ΔLMP2A EBV-, K1 EBV-, and K15 EBV-infected cells, which were similarly low in this surface molecule. There are reports indicating that LMP1 and CD30 expression correlate (Niedobitek, 1996), which might explain the increase in CD30 expression in all infected cells. The high CD30 level in wt EBV-infected cells also suggests an influence of LMP2A. CD30 is a marker of Hodgkin-Reed-Sternberg cells, and its expression activates CD54 expression (Uchihara *et al.*, 2006), which is in line with the increase in CD54 expression upon B cells infection with all four EBV strains. Again, wt EBV-infected cells showed the

highest CD54 expression and ΔLMP2A EBV, K1 EBV, and K15 EBV-infected cells slightly slower expression levels, which were similar.

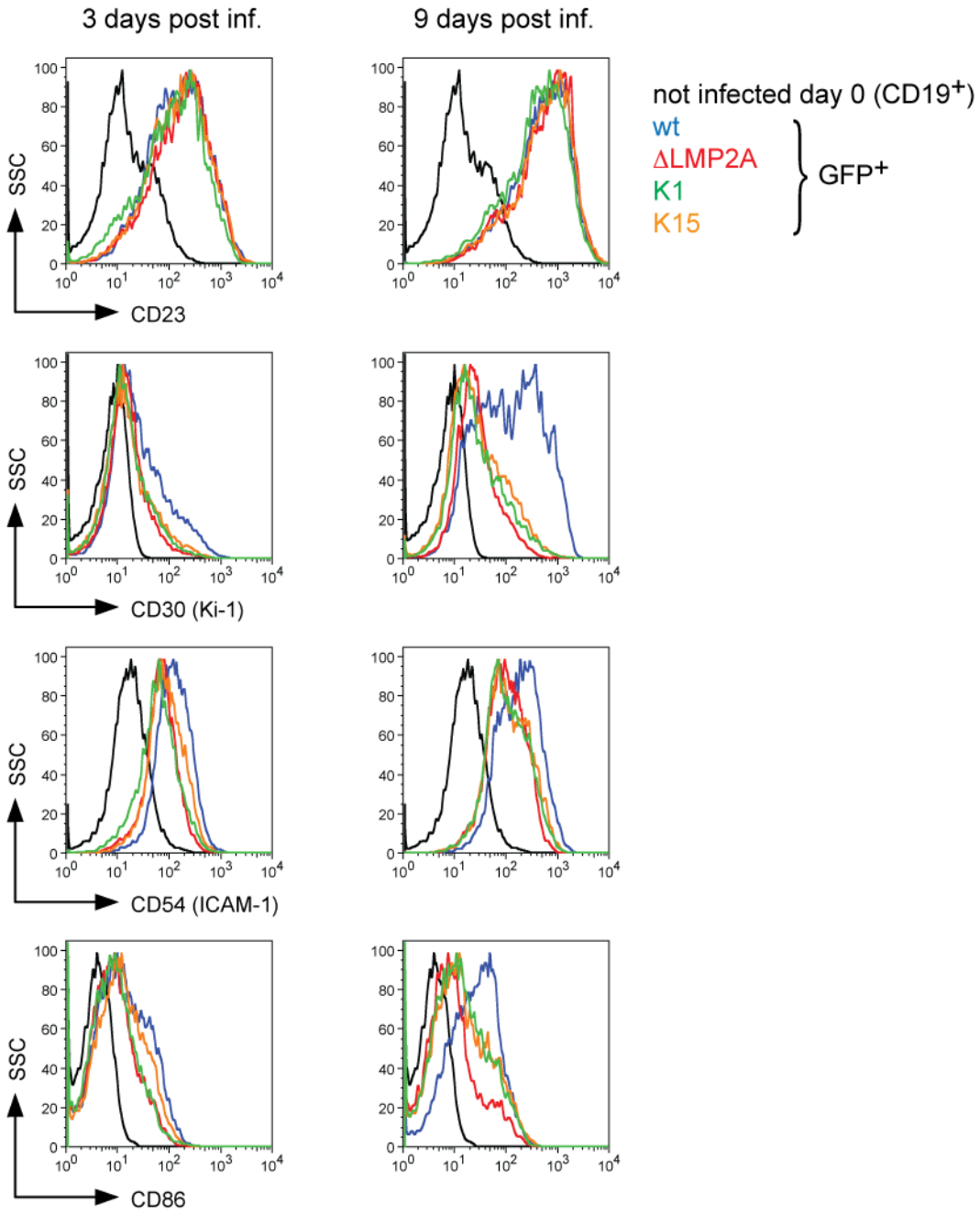


**Figure 5-21: Surface expression of B cell activation markers on B cells infected with wt EBV, ΔLMP2A EBV, K1 EBV, or K15 EBV strains.**
Infection of B cells with wt EBV induces the expression of B cell activation markers. The expression of CD23, CD30, CD54, or CD86 was analyzed by flow cytometry. 5 x $10^6$ B cells from adenoids were infected with wt EBV, ΔLMP2A EBV, K1 EBV, or K15 EBV strains or left uninfected. At the day of infection (day zero), cells were stained with a FITC-coupled antibody directed against the B cell marker CD19 as well as APC-coupled antibodies specific for the B cell activation markers CD23, CD30, CD54, and CD86 and analyzed by flow cytometry. Only $CD19^+$ cells were included in the analysis of day zero and compared to $GFP^+$, EBV infected cells at day three and nine p.i.. The experiment was repeated twice, and one representative experiment is shown.

Infection with all four EBV strains also increased expression of CD86. Again, wt EBV and ΔLMP2A EBV-infected cells showed the highest and lowest expression, respectively, nine days p.i.. K1 and K15 EBV infection induced intermediate CD86 expression levels suggesting a moderate effect of K1 and K15 on CD86 expression. Along with CD30, LMP1 supposedly activates CD86 expression explaining the general increase in CD86 expression upon EBV infection (Peters *et al.*, 2010).

Infection of pre-activated human peripheral blood B cells with KSHV did not alter the expression of CD23 and CD54 but, in contrast to what I observed, reduced the expression of CD86 (Rappocciolo *et al.*, 2008). The different results might be explained by the different experimental setups. Rappocciolo and colleagues used KSHV virus for B cell infection while I used EBV encoding the KSHV *K1* and *K15* genes expressed from a heterogeneous EBV promoter.

My experiments indicated that LMP2A has a clear role in upregulating CD30, CD54, and CD86. My experiments also suggested that K1 and K15 both slightly induce the surface expression of CD86 but not CD30 and CD54 (Figure 5-21).

#### *5.3.3.4 Cytokine production*

Infection with EBV induces B cell proliferation but also production of several cytokines, which are important for numerous effects, such as T cell activation (e.g. interleukin (IL)-2), induction of inflammation (e.g. IL-6 and IL-8), and B cell activation and immune suppression (e.g. IL-10) (Hornef *et al.*, 1995; McColl *et al.*, 1997; Wroblewski *et al.*, 2002). I investigated whether the infection of unsorted B cells with wt EBV, ΔLMP2A EBV, K1 EBV, and K15 EBV strains induced cytokines in the supernatant of infected B cells. To this end, 1 x $10^6$ unsorted B cells from adenoids were infected with wt EBV, ΔLMP2A EBV, K1 EBV, or K15 EBV strains with MOIs of 0.1 and 0.05 and cultured in 1ml medium. One day p.i., cells were supplied with fresh medium at a cell density of 1 x $10^6$ cells/ml. Eight days p.i., the number of transformed cells was determined, as described in Figure 5-12. Cell cultures, which contained equal numbers of transformed cells, were chosen for cytokine analysis to exclude variations in cytokine production due to different cell densities. B cell cultures, initially infected with wt EBV at an MOI of 0.05 or

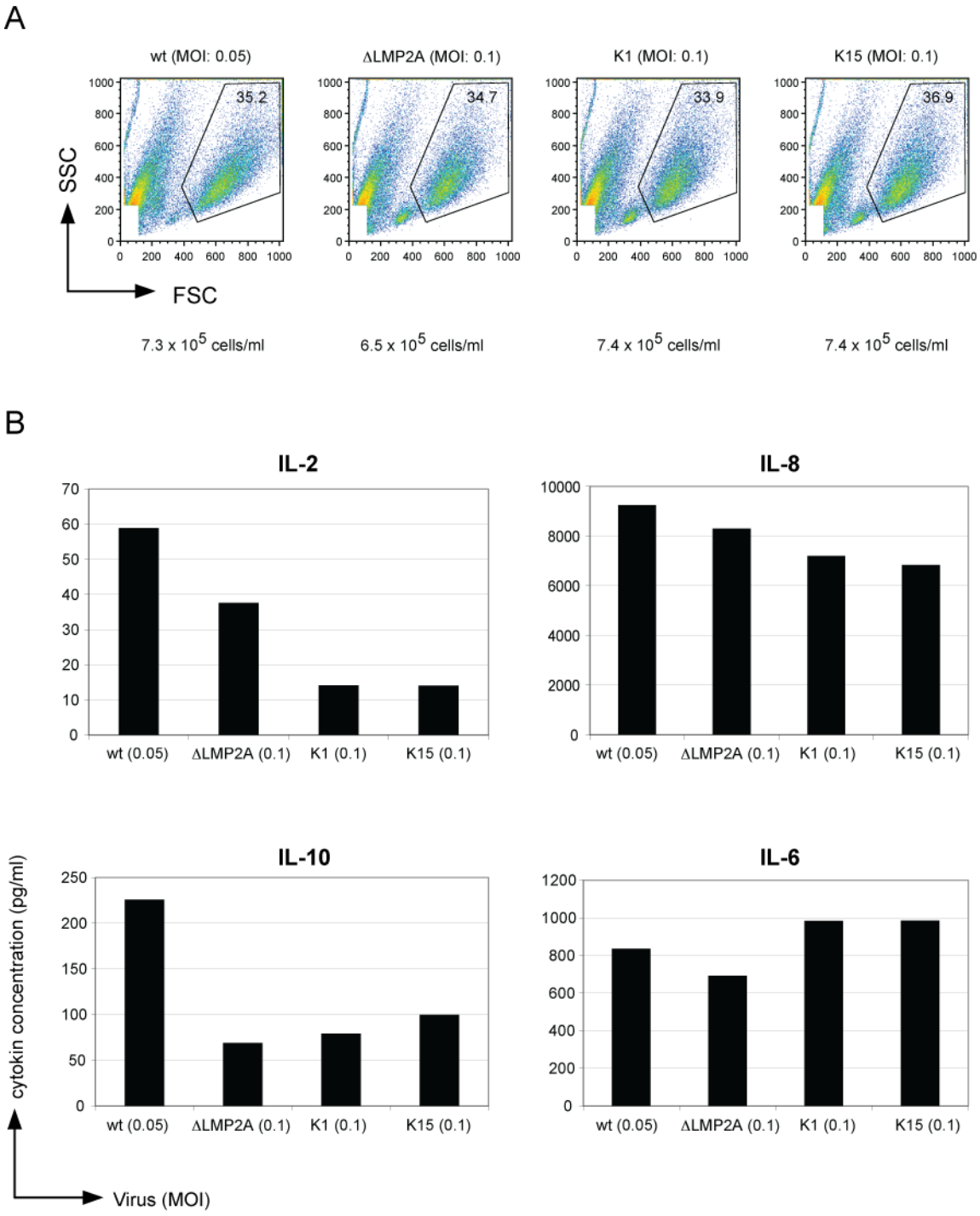


**Figure 5-22: Cytokine induction of B cells infected with four different EBV strains eight days p.i..**
Infection of B cells with wt, ΔLMP2A, K1, or K15 EBV induced cytokine production. 1 x $10^6$ B cells from adenoids were infected with wt EBV, ΔLMP2A EBV, K1 EBV, or K15 EBV strains at two different MOI (multiplicity of infection). A) Eight days p.i., the absolute number of cells in the LCL-gate was determined. B cell cultures of each virus strain were selected for an equal cell number. Cell cultures, containing cells that were infected at an MOI of 0.05 of wt EBV and an MOI of 0.1 of ΔLMP2A EBV, K1 EBV, and K15 EBV, were chosen for further cytokine expression analysis. B) Eight days p.i., the concentration of the cytokines IL-2, IL-6, IL-8, and IL-10 in the four B cell cultures was determined by FlowCytomix™ Multiplex analysis. The experiment was performed once. There was no major difference of IL-8 and IL-6 cytokine concentrations in supernatants of the different infected cells. The supernatant of wt EBV infected cells contained the highest concentrations of IL-2 and IL-10. The induction of IL-2 in ΔLMP2A EBV-infected cells was reduced by a factor of 1.5 and in K1 EBV and K15 EBV-infected B cells by a factor of 4.2

compared to wt EBV infected cells. The IL-10 concentration in the supernatant of cells infected with ΔLMP2A EBV, K1 EBV, and K15 EBV was reduced by a factor of 3.3, 2.9, and 2.3, respectively, compared to the supernatant obtained from wt EBV-infected cells. Thus, IL-2 and IL-10 expression might be induced by LMP2A but not K1 or K15 in B cells.

ΔLMP2A EBV, K1 EBV, and K15 EBV at an MOI of 0.1, had comparable cell densities (Figure 5-22 A). IL-2, IL-6, IL-8, and IL-10 concentrations in cell supernatants of these four EBV infections were determined using the FlowCytomix™ Multiplex Technology. There was no significant difference in IL-6 and IL-8 expression between cultures infected with the four EBV strains, which might be due to the induction of these cytokines by LMP1 (Eliopoulos *et al.*, 1999) (Figure 5-22 B).

The induction of IL-2 in ΔLMP2A EBV-infected cells was reduced by a factor of 1.5 and in K1 EBV and K15 EBV-infected B cells by a factor of 4.2 compared to wt EBV infected cells. The IL-10 concentration in the supernatant of cells infected with ΔLMP2A EBV, K1 EBV, and K15 EBV was reduced by a factor of 3.3, 2.9, and 2.3, respectively, compared to the supernatant obtained from wt EBV-infected cells. Accordingly, IL-2 and IL-10 expression might be induced by LMP2A but not K1 or K15 expression in B cells.

### 5.3.4 BCR signaling in the presence of LMP2A, K1, and K15

Hallmarks of BCR signaling are protein phosphorylation and an increase in cellular $Ca^{2+}$ concentration upon BCR stimulation. BCR cross-linking in LCLs, generated from wt EBV infection, induced protein phosphorylation but not $Ca^{2+}$-influx, whereas in ΔLMP2A LCLs, both processes were activated (Medele, 2010). Why LMP2A blocks $Ca^{2+}$-influx but not protein phosphorylation is not known. Stable transfection of BJAB cells with a K1 expression plasmid decreased the surface IgM expression suggesting a downregulation of BCR signaling (Lee *et al.*, 2000). Similarly, transient transfection of a K15 expression plasmid into BJAB cells and subsequent BCR cross-linking with an α-hIgM antibody reduced the $Ca^{2+}$-influx compared to vector transfected cells (Pietrek et al., 2010). Choi and colleagues transiently expressed a CD8-K15 chimera into BJAB cells, in which the cytoplasmic tail of K15 replaced the cytoplasmic tail of CD8. Cross-linking of the BCR with α-hIgM antibody slightly decreased tyrosine phosphorylation in Western blot analysis compared to cells, which express CD8-Δ missing the K15 cytoplasmic tail (Choi *et al.*, 2000).

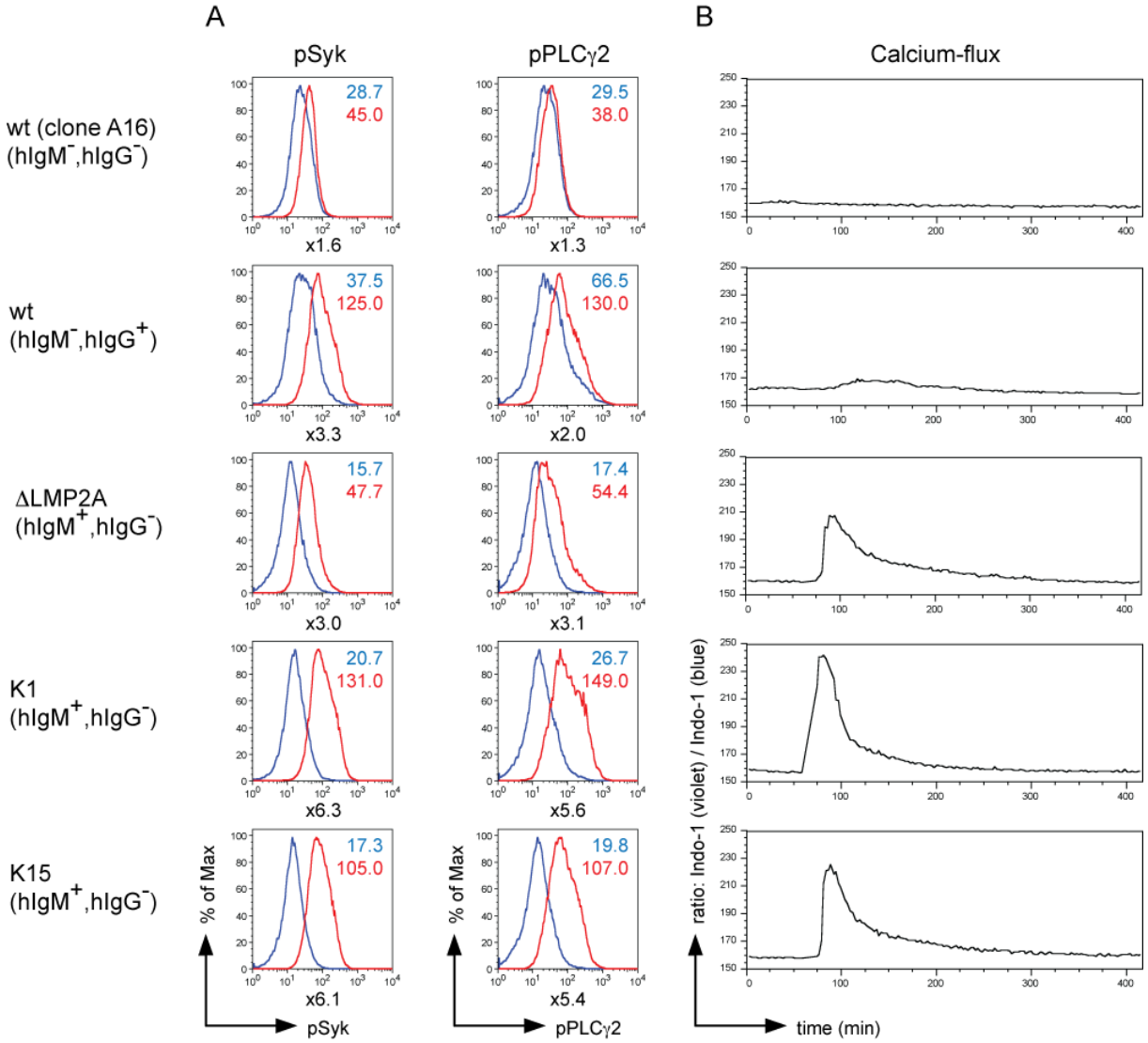


**Figure 5-23: The KSHV proteins K1 and K15 do not inhibit BCR signaling.**
Cross-linking with an α-hIgG/M antibody can induce BCR signaling and phosphorylation of signaling molecules, e.g. Syk and PLCγ2, or an influx of calcium into the cytoplasm. A) The increase of Syk and PLCγ2 phosphorylation after BCR stimulation was investigated in established LCLs, which were generated through infection of adenoid B cells with wt EBV, ΔLMP2A EBV, K1 EBV, or K15 EBV strains. An LCL clone, which was generated from infection with wt EBV and unable to express a BCR (clone A16), was included as negative control. The BCR of the four LCLs was cross-linked for 10min with 25µg/ml α-hIgG/M antibody or left untreated. Cells were fixed, permeabilized, and stained with phosphospecific α-pSyk-Alexa647 or with α-pPLCγ2-Alexa647 antibodies. Histograms of flow cytometry analysis are shown. Numbers next to the graphs display the mean fluorescent intensities for not cross-linked (blue) and cross-linked (red) cells. Numbers below the graphs show the fold increases in mean fluorescent intensity of the pSyk- and pPLCγ2-signals after BCR stimulation. BCR⁻ wt EBV-infected LCLs (clone A16) did not show an increase in Syk and PLCγ2 phosphorylation after antibody addition, as expected. In LCLs generated from wt (BCR⁺), ΔLMP2A EBV, K1 EBV, and K15 EBV strains, BCR cross-linking induced a significant increase in Syk and PLCγ2 phosphorylation indicating that neither LMP2A nor K1 and K15 inhibited phosphorylation of BCR signaling molecules. B) The same LCLs were loaded with 3µM Indo-1 AM, and the ratio of Indo-1 in the violet vs. blue channel (y-axis) was measured over time (x-axis). After one minute of base line measurement the BCR was cross-linked with 25µg/ml α-hIgG/A/M F(ab)$_2$-fragment. An influx of calcium into the cytoplasm shifts the Indo-1 emission to the violet channel increasing the violet/blue ration. BCR⁻ wt EBV-infected LCLs (clone A16) did not show an increase in cytoplasmic calcium levels after antibody mediated BCR cross-linking, as expected. LCLs generated from wt but not ΔLMP2A EBV strain showed

impaired calcium mobilization after BCR cross-link confining that LMP2A blocked BCR's calcium signaling. In contrast, BCR cross-linking induced calcium influx in LCLs generated with K1 EBV and K15 EBV strains suggesting that K1 and K15 proteins did not block BCR-mediated calcium signaling.

I infected unsorted cells with wt EBV, ΔLMP2A EBV, K1 EBV, and K15 EBV and generated LCLs, which expressed high levels of IgG (wt EBV infection) or IgM (ΔLMP2A EBV, K1 EBV and K15 EBV). I investigated whether K1 and K15 can block BCR signaling by a change in phosphorylated Syk (pSyk) and phosphorylated PLCγ2 (pPLCγ2) levels and an alteration in $Ca^{2+}$-influx. A wt EBV LCL, unable to express a BCR due to crippled mutations in the Ig genes (referred as clone A16 in Mancao *et al.*, 2005), was used as negative control for BCR cross-linking induced signaling. The BCR was either cross-linked with an α-hIgG/M antibody for 10min at 37°C or left untreated. Cells were fixed, permeabilized, stained with antibodies specific for pSyk or pPLCγ2, and analyzed by flow cytometry. BCR cross-linking increased pSyk and pPLCγ2 levels in all tested cell lines but the negative control cell line A16 indicating that LMP2A, K1, and K15 did not block BCR induced protein-phosphorylation.

The same LCLs were loaded with 3μM Indo-1 AM. Indo-1 is a fluorescent dye, which changes its emission wavelength from 475nm (blue) to 400nm (violet) upon calcium binding. An increase in cellular $Ca^{2+}$ can be measured by an increase in the violet/blue wavelength ratio. The baseline violet/blue ratio of Indo-1 loaded LCLs was measured for 1min. Subsequently, the BCR was cross-linked with an α-hIgG/A/M $F(ab')_2$ fragment and the $Ca^{2+}$-influx was measured by the change in the violet/blue ratio for 5min. The $Ca^{2+}$-influx was impaired in both wt EBV LCLs but not in ΔLMP2A, K1, and K15 EBV LCLs indicating that LMP2A but not K1 or K15 blocked BCR induced calcium signaling.

# 6 Discussion

## 6.1 Functionally impeded LMP2A:mCD69 and NP-mIgM mutant EBVs

EBV transforms primary human B cells *in vitro* to yield LCLs. This *in vitro* model is ideal to study viral genes and their functions in transforming B cells. LMP2A is not essential for transformation of primary human B cells that express a functional BCR (Longnecker et al., 1992; Longnecker et al., 1993; Speck et al., 1999). In contrast, $BCR^-$ B cells both, *in vivo* and *in vitro,* depend on LMP2A for their EBV-mediated transformation (Caldwell *et al.*, 1998; Caldwell *et al.*, 2000; Merchant *et al.*, 2000; Mancao *et al.*, 2005; Mancao & Hammerschmidt, 2007). B cells can loose their ability to express a functional BCR when they differentiate in a germinal center reaction and undergo somatic hypermutation, which introduces random mutations into the Ig genes. The purpose of this process is to improve the affinity of the BCRs to their cognate antigens, but, since somatic hypermutation is a random process, most of the mutations decrease BCR affinities or even disrupt the Ig genes. These B cells are incapable of expressing a functional, high affinity BCR and undergo apoptosis because they lack strong and necessary survival signals (Liu *et al.*, 1989; Kraus *et al.*, 2004).

Expression of LMP2A in a transgenic mouse enabled immature $BCR^-$ B cells to leave the bone marrow, maturate, and locate to secondary lymphoid organs in the periphery (Caldwell *et al.*, 1998; Caldwell *et al.*, 2000; Merchant *et al.*, 2000). This is a key finding, although, EBV is not known to infect immature B cells in the bone marrow *in vivo*. Therefore, we turned to mature B cells and sorted $BCR^-$ and $BCR^+$ B cell populations for infection experiments. wt EBV but not ΔLMP2A EBV infection rescued $BCR^-$ sorted GC B cells from apoptosis. Accordingly, human LCLs generated from *in vitro* wt EBV infection of naive B cells contained about 65% $BCR^+$ and 32% $BCR^-$ cells, whereas LCLs generated from ΔLMP2A EBV infection were always $BCR^+$ (Bechtel *et al.*, 2005; Chaganti *et al.*, 2005; Mancao *et al.*, 2005; Mancao & Hammerschmidt, 2007). These results led to the hypothesis that LMP2A is a constitutively active BCR mimic in this model (Mancao & Hammerschmidt, 2007).

LCLs that express an inducible LMP2A:mCD69 chimeric protein were used to compare LMP2A and BCR signaling in established LCLs (see section 1.3.4.3). Cross-linking of LMP2A:mCD69 with an α-mCD69 specific antibody or cross-linking of the endogenous BCR with an α-hIgG/M specific antibody demonstrated that both receptors can induce protein phosphorylation, $Ca^{2+}$-influx, and transcription of a similar set of genes (Medele, 2010). It thus appears that LMP2A continuously supplies the EBV-infected cell with necessary survival signals and ensures the differentiation process of EBV-infected naive B cell into memory B cells. Upon differentiation, viral gene expression shuts down preventing an immune response *in vivo* (see section 1.3.2).

During a germinal center reaction, it is uncertain at which stage of B cell differentiation and how long LMP2A or BCR support B cell survival. To address this important aspect, I established two new maxi-EBVs, which could provide the opportunity to vary LMP2A and BCR signaling strength in a dose and temporally controlled manner shortly after infection. Because a stable HEK293 virus producer cell line could not be generated with the previous CMV-LMP2A:mCD69 maxi-EBV (p3696), a new maxi-EBV, which expresses LMP2A:mCD69 (p3993) *in lieu* of LMP2A, was cloned. In this mutant EBV, the *LMP2A:mCD69* gene was inserted into the endogenous *LMP2A* locus and expressed from the LMP2A-promoter. LMP2A:mCD69 cross-linking with an α-mCD69 antibody was expected to activate LMP2A:mCD69 signaling. A second maxi-EBV was cloned, in which LMP2A was replaced by a murine IgM molecule that specifically binds the hapten NP. Addition of NP-coupled antigen complexes, which differ in complexation and affinity, should activate mIgM signaling to various degrees. High-titer HEK293 virus producer cell lines could be generated with both maxi-EBVs, and viral particles were used for infection experiments of $BCR^-$ B cells to study the effect of LMP2A:mCD69 and mIgM signaling during B cell proliferation.

I expected the expression levels to be critical for the inducibility and functionality of the LMP2A:mCD69 and NP-mIgM system. LMP2A:mCD69 signaling should be completely silent in the absence of cross-linking antibodies phenotypically resembling the ΔLMP2A genotype, but the surface expression level of LMP2A:mCD69 needs to be high enough to allow cross-linking in order to rescue the survival of $BCR^-$ B cells. Similarly, the NP-mIgM

expression levels had to be high enough to induce tonic signaling resembling the human $BCR^+$ phenotype in the absence of antigen but low enough to induce mIgM signaling upon antigen binding. Also, the timing of the expression of LMP2A:mCD69 and NP-mIgM after EBV infection was critical. Because signaling function of LMP2A:mCD69 and mIgM can only be compared if their expression kinetics are comparable, the same promoter had do be used. The first and simplest choice was the LMP2A promoter, which should express the transgenes similarly as the endogenous LMP2A in wt EBV-infected B cells. Several problems, which might be linked to the expression levels of LMP2A:mCD69 and NP-mIgM, emerged and are discussed in the following sections.

### 6.1.1 The LMP2A:mCD69 EBV

A clonal LCL, which encodes a CMV-promoter driven LMP2A:mCD69 (3696 LCL) and expresses negligible BCR levels, was already present in the lab. LMP2A:mCD69 expression levels were high enough to mimic tonic BCR signals rescuing the $BCR^-$ B cell from apoptosis. α-mCD69 antibody-mediated cross-linking also induced protein phosphorylation of downstream signal mediators demonstrating that the LMP2A:mCD69 construct is functional (Medele, 2010).

*Expression and functionality of the LMP2A promoter-driven LMP2A:mCD69 construct*

The expression level of the LMP2A promoter-driven LMP2A:mCD69 in established $BCR^+$ LCLs was lower by a factor about six as compared to $BCR^-$ CMV-LMP2A:mCD69 LCLs (Figure 5-5). Because an increase in Syk and PLCγ2 phosphorylation upon LMP2A:mCD69 cross-linking could only be observed in the CMV promoter-driven but not in the LMP2A promoter-driven LMP2A:mCD69 LCL, I assumed that the LMP2A promoter-driven LMP2A:mCD69 surface expression level was too low to support signaling upon cross-linking. It appears that the LMP2A promoter was too weak to ensure sufficient LMP2A:mCD69 expression or that the $BCR^+$ B cells did not depend on its expression and therefore downregulate the LMP2A promoter. To cope with this scenario, I sorted $BCR^-$ B cells from adenoids, infected them with (LMP2A promoter-driven) LMP2A:mCD69 EBV, and cultivated the cells on normal or α-mCD69 antibody coupled feeder cells. LMP2A:mCD69 EBV-infected $BCR^-$ B cells proliferated slowly on feeder cells, but antibody stimulation fully rescued their proliferative phenotype

suggesting that the $BCR^-$ B cells depend on survival signals from induced LMP2A:mCD69 signaling. In a parallel experiment, unsorted cells, which are mainly $BCR^+$ B cells, were infected with the same EBV strain for an internal control. Cultivation of these cells on antibody-coupled feeder cells increased their proliferation only slightly compared to normal, uncoupled feeder cells. My finding suggested that, in contrast to $BCR^-$ B cells, $BCR^+$ B cells express low levels of LMP2A:mCD69 insufficient to induce LMP2A:mCD69 signaling by α-mCD69 antibody cross-linking. However, the outgrowth experiment mostly fulfilled the requirements for an inducible LMP2A:mCD69 system in $BCR^-$ infected B cells: (i) Spontaneous LMP2A:mCD69 signaling was very low and therefore non-functional, but (ii) surface expression level of LMP2A:mCD69 was high enough to reconstitute the wt EBV phenotype upon antibody-mediated cross-linking.

In order to improve the experimental conditions, I replaced the LMP2A promoter by the CAG promoter in yet another maxi-EBV (p4252 maxi-EBV) to increase the expression of LMP2A:mCD69. Despite a number of attempts, no stable HEK293 virus producer cell lines could be generated presumably because transfected, $GFP^+$ HEK293 cells died shortly after p4252 maxi-EBV transfection and subsequent hygromycin selection. DNA sequencing confirmed the integrity of the hygromycin resistance gene. Because overexpression of the *LMP2A:mCD69* gene in HEK293 might negatively effect their survival, a "loxP - neomycin resistance gene - stop - loxP" cassette was introduced in a new maxi-EBV. In this p4489 maxi-EBV, LMP2A:mCD69 expression is conditionally abrogated, but, again, stable HEK293 virus producer cell lines could not be established. Most likely, a second site mutation was accidently introduced, which impaired genomic maintenance of this class of maxi-EBVs.

*An alternative approach to control LMP2A signaling*

Regulating protein stability would be an alternative approach to control signaling of LMP2A. Two different systems have been developed recently, which can regulate protein net lives at will (Banaszynski *et al.*, 2006; Haugwitz *et al.*, 2008; Neklesa *et al.*, 2011). The ProteoTuner™ system is based on a ligand-dependent destabilizing domain, which is fused to the protein of interest. In absence of the ligand Shield-1, the fusion protein is instable and constantly degraded, but the addition of the membrane-permeant

Shield-1 quickly stabilizes the protein and increases its half-life to functional levels. The steady-state levels of the fusion protein can be varied by the concentration of Shield-1. There are two main advantages of this system compared to the inducible LMP2A:mCD69: (i) It would permit to study signaling of wt LMP2A, which might be a critical aspect of its functionality, and (ii) the LMP2A-promoter in combination with Shield-1 should provide sufficient steady-state levels of LMP2A protein. This approach appears to be attractive to conditionally activate LMP2A signaling and to study its consequences.

### 6.1.2 The NP-mIgM EBV

B cells from the quasi-monoclonal (QM) mouse exclusively express the NP-specific IgM at their surface. *Ex vivo* studies with these primary cells demonstrated that the mIgM expression level was sufficient to induce an increase in protein phosphorylation upon adding $NP_{15}$-BSA, a multivalent antigen of NP-mIgM. B cell proliferation could be activated with $NP_{15}$-BSA in conjunction with $\alpha$-CD40 antibody confirming that the transgenic NP-mIgM molecule constitutes a functional BCR in murine B cells (Hokazono *et al.*, 2003).

*NP-mIgM protein expression in human LCLs*

The NP-specific mIgM is expressed from a single open reading frame (ORF) in the maxi-EBV p4090. A furin cleavage site and a 2A motif separate the cDNAs coding for Ig heavy and light chains. The 2A site induces ribosome skipping during translation releasing the first terminally processed amino acid chain. It encompasses most of the amino acids from the 2A motif, which are subsequently removed by furin cleavage at its recognition site located upstream of the N-terminus of the 2A peptide sequence (Figure 5-7). The mIgM ORF was under control of the endogenous LMP2A promoter, but LCLs generated with this NP-mIgM EBV did not express detectable levels of mIgM in flow cytometry analysis. Accordingly, the LMP2A-promoter was replaced by the much stronger CAG promoter. In LCLs, which were infected with the generated NP-mIgM EBV strain (p4254), expression of the single mIgM heavy and light chains could be assessed by Western blot analysis. The heavy chain band migrated somewhat slower in protein preparations from LCLs than a murine control cell line, which could be due to

incomplete furin cleavage or different posttranscriptional protein modification, e.g. glycosylation in human B cells. Tolar and colleagues fused the cyan fluorescent protein (CFP) or yellow fluorescent protein (YFP) to the C-termini of NP–specific mIgMs to conduct cytosolic FRET experiments. They observed mIgM clustering and tyrosine phosphorylation upon $NP_{18-26}$-BSA treatment in a murine B cell line (Tolar *et al.*, 2005) suggesting that the CFP- and YFP-coupled mIgMs were functional. From their results, it seems unlikely that 26 additional amino acids at the C-terminus of the µ heavy chain that stem from the 2A-domain and the furin cleavage site peptide compromise mIgM transport or antigen binding when not fully trimmed. The murine IgM has five glycosylation sites within the constant regions, which are glycosylated to different extents (Anderson *et al.*, 1983; Anderson *et al.*, 1985; Wang *et al.*, 2003). Glycosylation might protect the IgM from proteolysis (Dulis *et al.*, 1982), but it is not required for membrane-bound localization (Sibley & Wagner, 1981). Glycosylation sites can also be present in the variable regions influencing antigen binding (Wright *et al.*, 1991). Whether the NP-binding site encompasses glycosylated moieties is unknown. Human cells express a different N-acetyl glucosaminyltransferase that catalyzes a different type of glycosylation compared to mouse cells (Arnold *et al.*, 2007). This difference might explain variant glycosylations of Igs in different host cell lines, e.g. the TKµ murine pre-B cell line and human LCLs.

*NP-mIgM surface expression is downregulated in human LCLs*

Certain human clonal $BCR^+$ LCLs, established with the NP-mIgM mutant EBV, showed a high mIgM surface expression five weeks post infection, which was reduced by a factor of 30 in the following weeks of cultivation. 5-azacytidin treatment could restore the mIgM surface expression levels indicating that the reduced mIgM expression in established LCLs was due to methylation-dependent promoter silencing. This change was unexpected because mIgM expression was achieved from the CAG promoter, which is well known for strong and epigenetically stable activity in different cell types (Xu *et al.*, 2001; Weber & Cannon, 2007). Fang and colleagues infected mice with an adeno-associated virus that encodes a soluble rat IgG (rIgG) antibody specific for the Vascular Endothelial Growth Factor (VEGF). Equivalent to the NP-specific mIgM, the VEGF-specific rIgG was expressed under control of the CAG promoter and the cDNAs coding

for the heavy and light chains were separated by a furin and 2A site (Fang *et al.*, 2005). The authors observed a high rIgG titer 28 days post infection, which decreased by a factor of eight thereafter to nearly stable levels for four months. The reductions in Ig expression in this report and in my experiments suggest that the CAG promoter is unsuitable for Ig expression in B cells and prone to epigenetical repression. Baup *et al.* observed a transient down-regulation of CAG promoter activity in T cells. They ubiquitously expressed the green fluorescent protein (GFP) under control of this promoter in transgenic mice and monitored GFP expression during T cell development (Baup *et al.*, 2009). T cells mature from the $CD4^-/CD8^-$ double negative state to become $CD4^+/CD8^+$ double positive and reach the $CD4^+/CD8^-$ or $CD4^-/CD8^+$ single positive state, eventually. GFP was expressed in all T cell development states but $CD4^+/CD8^+$ double-positive cells indicating that the CAG promoter was transiently downregulated during T cell development. EBV infection drives the cell into a germinal center-like reaction leading to B cell differentiation. It is conceivable that EBV's induced B cell differentiation can also negatively influence the activity of the CAG promoter.

*Surface expression levels and signaling capacity of the NP-mIgM in QM mouse B cells and established human LCLs*

I compared the mIgM surface expression levels in LCLs established from the NP-mIgM EBV to QM mouse B cells. QM mouse B cells expressed a homogenous mIgM surface level, which was sufficient to bind $NP_{18}$-BSA, whereas most of the NP-mIgM LCLs expressed lower mIgM surface levels incapable of $NP_{18}$-BSA-binding (Figure 5-10). In comparison to IgG, the affinity of an IgM to its antigen is generally lower, which is compensated by the higher avidity of soluble IgMs, which have ten antigen binding sites due to their pentameric structure (Janeway *et al.*, 2001). The affinity describes the strength of a single bond, but the term avidity characterizes the combined strength of multiple bonds. Accordingly, the membrane-bound mIgM is a classical Ig molecule with two antigen-binding pockets, which needs to be expressed at a certain surface density to bind $NP_{18}$-BSA efficiently. Most likely, this level was not reached in NP-mIgM LCLs and $NP_{26}$-BSA stimulation did not induce Syk phosphorylation, as expected (Figure 5-11). In contrast, addition of the α-mIgM antibody b7-6 increased pSyk levels in NP-mIgM LCLs even at low mIgM surface levels. This b7-6 antibody is rat IgG1 subtype (Cambier *et al.*,

1986) suggesting that it has a higher affinity to the murine μ heavy chain than the antigen to its mIgM surface receptor. Additionally, the b7-6 antibody could span larger distances than $NP_{26}$-BSA clustering the mIgM even at low surface densities. The successful induction of Syk phosphorylation in NP-mIgM LCLs upon antibody-mediated cross-linking documented that a murine IgM is capable of signaling in a human B cell. So far, it was only shown that a human IgM is functional in murine B cells (Shaw *et al.*, 1990; Pleiman *et al.*, 1994; Grupp *et al.*, 1995; Zidovetzki *et al.*, 1998).

*NP-mIgM expression does not rescue human $BCR^-$ B cells from apoptosis*

As already discussed for the LMP2A:mCD69 construct, the established NP-mIgM LCLs were $BCR^+$ and thus independent of a basic expression levels of the mIgM for their survival. Infection of $BCR^-$ B cells with NP-mIgM EBV and cultivation on uncoupled or α-mIgM antibody b7-6 coupled feeder cells did not rescue these cells from apoptosis (Figure 5-15). It can be concluded that $BCR^-$ B cells express insufficient levels of mIgM, which cannot replace a functional human BCR. An alternative is that a murine IgM is incapable of substituting for human IgM. Because $BCR^-$ B cells, infected with NP-mIgM EBV did not survive, the surface expression level of mIgM in $BCR^+$ and $BCR^-$ human B cells could not be studied. Humanizing the constant regions of the mIgM heavy and light chains of the mIgM could possibly circumvent functional problems based on the species differences between the murine IgM and the human LCLs. Replacement of the CAG promoter by the human heavy chain promoter and Eμ enhancer might have increased mIgM expression to physiological levels.

The aim of this part of my PhD was to investigate the influence of graded LMP2A and BCR signaling on the survival and differentiation of $BCR^-$ B cells shortly after infection. Two EBV mutants, the LMP2A:mCD69 and NP-mIgM EBVs, were needed for this comparative study. Unfortunately, infection of $BCR^-$ B cells with NP-mIgM EBV could not rescue these cells from apoptosis under all conditions tested ($NP_{26}$-BSA antigen-addition or α-mIgM b7-6 antibody-stimulation). Thus, the planned experiments could not be pursued.

## 6.2 K1 and K15 can partially replace LMP2A functions

EBV and KSHV belong to the family of γ-herpes viruses. They both can induce tumors in infected epithelial and B cells. The EBV protein LMP2A was shown to act as a BCR mimic, and its expression can rescue $BCR^-$ B cells from apoptosis by providing necessary survival signals. BCR and LMP2A both contain an ITAM, which might be responsible for the induction of genuine BCR signaling cascades. LMP2A is constitutively active in contrast to the BCR, which is activated upon antigen binding. B cells, which receive a strong BCR signal in the absence of T helper cell-mediated activation of their CD40 receptor, undergo apoptosis to prevent their survival as auto-reactive B cells. To avert this scenario, EBV encodes LMP1, which is a constitutively active CD40 receptor mimic. Accordingly, the orchestrated work of LMP2A and LMP1 activates B cells, protects them from apoptosis, and induces their proliferation.

To date, it is unclear whether KSHV can also rescue $BCR^-$ B cells from apoptosis by providing necessary survival signals as LMP2A does. Two KSHV proteins are possible candidates for this task: K1 and K15. They are both transmembrane proteins and contain a cytoplasmic domain, which constantly activates certain signaling cascades. K1 contains an ITAM and was shown to activate Syk as well as the PI3K/Akt pathway similar to LMP2A (Wen & Damania, 2010), but K1 contains only one transmembrane domain and has a genomic location similar to EBV's LMP1. K15, in turn, has 12 transmembrane domains and a genomic location like LMP2A but lacks an ITAM domain. K15 does not activate Syk but engages TRAF signal mediators similar to LMP1, but K15 was shown to block BCR induced $Ca^{2+}$-influx like LMP2A (Damania, 2004; Pietrek *et al.*, 2010).

To investigate whether K1 or K15 of KSHV are functional homologs of EBV's LMP2A, the *LMP2A* gene was replaced by *K1* or *K15* in two mutant EBVs. LCLs that express K1 and K15 under control of the LMP2A-promoter were established by infecting adenoid B cells with both mutant viruses. Suitable antibodies to detect K1 and K15 protein were not available (discussed in section 5.3.2), but the expression of K1 and K15 mRNA in these LCLs was approved by qRT-PCR. The mRNA level of K1 was equivalent to the mRNA

level of LMP2A in LCLs generated from infection with wt EBV. The mRNA level of K15 was reduced by a factor of 2.6 compared to LMP2A in wt EBV LCLs.

*K1 and K15 can rescue BCR$^-$ B cells from apoptosis*

BCR$^-$ sorted B cells underwent apoptosis when they were infected with ΔLMP2A EBV, but infection with wt EBV, K1 EBV, or K15 EBV strains rescued them. The proliferation rate of K1 EBV-infected BCR$^-$ B cells was slightly higher than that of K15 EBV-infected cells but lower than wt EBV infected cells. Double infection of BCR$^-$ B cells with both, K1 and K15 mutant EBVs, did not enhance cellular proliferation suggesting that K1 and K15 have similar, non-complementing functions in B cells that did not act additively or synergistically. From these results, it can be concluded that K1 and K15 can both partially replace LMP2A's function by rescuing BCR$^-$ B cells from apoptosis.

Because LMP2A, K1, and K15 expression is controlled by the same promoter (the LMP2A-promoter), the kinetics of their expression are expected to be identical in EBV-infected cells. In fact, the expression levels of LMP2A, K1, and K15 are similar in established LCLs, as shown by qRT-PCR (Figure 5-17). Despite these similarities, the proliferation rate of K1 and K15 EBV-infected BCR$^-$ B cells was reduced compared to wt EBV-infected cells suggesting that the intensity or quality of signaling by K1 and K15 differ from LMP2A.

An important feature of BCR and LMP2A signaling is the activation and phosphorylation of Syk. It is the first signaling mediator that is recruited to the phosphorylated ITAMs of the BCR and LMP2A activating all subsequent signaling cascades. K1 but not K15 contain an ITAM and was shown to activate Syk (Wen & Damania, 2010). To analyze this situation, unsorted B cells were infected with ΔLMP2A, wt, K1, and K15 mutant EBVs and the pSyk levels were determined after two days. All infected cells had higher pSyk levels than uninfected cells. Cell that had been infected with K1 and K15 were equal and showed only slightly elevated levels of phosphorylated Syk compared to ΔLMP2A EBV-infected cells but did not reach the pSyk levels of wt EBV infected cells. This experiments suggested that the rescue of BCR$^-$ B cells cannot only result from Syk phosphorylation in K1 EBV- and K15 EBV-infected B cells. Because all infected cells, independently of the

mutant EBV strain used, had increased pSyk levels compared to uninfected cells and infected cells were mainly $BCR^+$ (unsorted), tonic BCR signaling might have increased the pSyk levels.

*K1 and K15 do not show a clear influence on B cell activation marker expression*

Infection of primary B cells with EBV induces the expression of B cell activation markers such as CD23, CD30, CD54, and CD86 (Young & Rickinson, 2004). It was tested whether their expression differs in primary B cells infected with ΔLMP2A EBV, K15 EBV, K1 EBV, or wt EBV three and nine days post infection. Expression of CD23, CD30, CD54 and CD86 was generally elevated in all infected B cells.

There was no difference in CD23 expression after infection with all four EBV strains, but CD30, CD54, and CD86 expression varied. Cells infected with ΔLMP2A EBV, K1 EBV, and K15 EBV had similar CD30 and CD54 levels, but CD86 levels of K1 and K15 infected B cells were in between ΔLMP2A and wt EBV infected cells (Figure 5-21). Expression of CD23 was shown to be activated by EBNA2, and several publications suggested that LMP1 expression correlates with an increase in CD30 and CD86 surface levels (Calender *et al.*, 1987; Wang *et al.*, 1987; Niedobitek, 1996; Peters *et al.*, 2010). Furthermore, CD30 expression correlates with increased CD54 levels (Uchihara *et al.*, 2006). EBNA2 and LMP1 are encoded in all four EBV strains used in this experiment explaining the general increase in CD23, CD30, CD54, and CD86 expression upon B cell infection. Nevertheless, LMP2A might influence CD30, CD54, and CD86 because wt EBV infected cells had highest levels of these three markers.

In my experiments, K1 did not strongly change expression of CD30, CD54, and CD86, which is in accordance to published data, in which stable expression of K1 in BJAB cells also did not show an influence on CD30, CD54, and CD86 expression (Lee *et al.*, 2000). Infection of activated human peripheral blood B cells with KSHV also did not change the expression of CD23 and CD54 but, in contrast to what I observed, decreased the expression of CD86 (Rappocciolo *et al.*, 2008). The different results might be explained by the different experimental setups. Rappocciolo and colleagues used KSHV virus in infection experiments, while I used EBV encoding the KSHV proteins K1 and K15. In the

publication by Rappocciolo *et al*., reduced CD86 expression was probably induced by an unidentified KSHV protein.

In essence, a clear influence of K1 and K15 on B cell activation marker expression was not observed.

*LMP2A but not K1 and K15 influence cytokine expression*

To further address the question how K1 and K15 can rescue $BCR^-$ B cells from apoptosis, a cytokine release assay was performed. Cytokines are small, secreted signaling molecules that are important for intercellular communication and chemotaxis and have immunomodulatory role. The concentration of the cytokines IL-2, IL-6, IL-8, and IL-10 in the supernatant of adenoid cell suspensions was determined eight days post infection with ΔLMP2A EBV, K1 EBV, K15 EBV, or wt EBV.

IL-6 and IL-8 concentrations were similar in all four tested supernatants. In general, IL-6 is expressed in B cells, macrophages and T cells and is important for B cell differentiation into plasma cells (Klein *et al.*, 2003). IL-6 expression was shown to be induced by EBV-infection (Tosato *et al.*, 1990; Yokoi *et al.*, 1990; Hornef *et al.*, 1995; Wroblewski *et al.*, 2002) and is a target of EBV-encoded miRNAs (Samanta & Takada, 2010). $KSHV^+$ PEL cell lines also show an NF-κB dependent upregulation of IL-6 (Keller *et al.*, 2000). Transgenic mice, which express K1 under control of the SV40 promoter, did not show a change in IL-6 mRNA levels in the B and T cell compartments compared to nontransgenic mice (Prakash *et al.*, 2002) excluding K1 as possible IL-6 activator. HeLa cells that were transiently transfected with K15 expression plasmids showed an increase in IL-6 mRNA levels probably mediated by upregulating NF-κB (Brinkmann *et al.*, 2003; Brinkmann *et al.*, 2007). It is worth mentioning that KSHV encodes a viral IL-6 homolog (vIL-6), which can takeover human IL-6's functions (hIL-6), but vIL-6 secretion is less tightly regulated (Wen & Damania, 2010).

Published data demonstrated that EBV infection induces IL-8 expression (Klein *et al.*, 1996), which is important for chemotactic attraction of several cell types to the site of infection, thereby, possibly enhancing the numbers of B cells that EBV can infected. BJAB

cells and HeLa cells that were transiently transfected with K1 and K15 expression plasmids, respectively, showed an increase in IL-8 mRNA and protein levels (Lee *et al.*, 2005; Brinkmann *et al.*, 2007; Pietrek *et al.*, 2010). Because IL-6 and IL-8 concentrations were similar in ΔLMP2A EBV, K1 EBV, K15 EBV, or wt EBV-infected B cell cultures, LMP2A, K1, or K15 might not have an impact on IL-6 and IL-8 secretion.

IL-2 and IL-10 concentrations were strongly reduced in ΔLMP2A EBV, K1 EBV, and K15 EBV-infected B cell cultures compared to wt EBV infections. IL-2 was shown to be increased in the serum of patients suffering from IM (Hornef *et al.*, 1995). It is secreted by activated T cells and stimulates T cell proliferation in an autocrine manner (Janeway *et al.*, 2001). IL-2 production of T cells can be inhibited by cyclosporine A, which was added to the medium during the whole experiment. Accordingly, the high amounts of IL-2 in wt EBV infected cell cultures might be secreted by infected B cells that express LMP2A suggesting that IL-2 might be a downstream target of LMP2A. It could be shown that EBV infected B cells express the IL-2 receptor (Stein *et al.*, 1985), and treatment of non-infected murine B cells with IL-2 and α-hIgM antibody induced proliferation (Nakanishi *et al.*, 1992). Accordingly, an increase in IL-2 levels in wt EBV-infected B cells, together with expression of LMP2A (mimicking the Ig stimulation), might enhance proliferation of infected B cells.

$EBV^+$ BL cells as well as LCLs express high levels of human IL-10 (hIL-10) (Hornef *et al.*, 1995; Klein *et al.*, 1996; Wroblewski *et al.*, 2002). It is under debate whether LMP1 induces the expression of hIL-10 or *vice versa* (Kis *et al.*, 2006; Lambert & Martinez, 2007). Recently, it was shown that EBV's viral miRNAs activate hIL-10 secretion in BL cells (Samanta & Takada, 2010). BJAB cells that were transiently transfected with a K1 expression plasmid showed an increase in IL-10 mRNA and protein levels compared to vector transfected cells (Lee *et al.*, 2005). EBV encodes also a viral IL-10 homolog (vIL-10). Both, human and vIL-10, inhibit the production of inflammatory cytokines, deactivate macrophages, reduce T cell proliferation, but enhance B cell maturation (Itoh & Hirohata, 1995). Human IL-10 but not vIL-10 activate T cell proliferation, increases the expression of MHC II molecules on B cells, and blocks IL-2 production by $CD4^+$ T cells (Slobedman *et al.*, 2009). Accordingly, there is a link between IL-2 and IL-10 expression,

which might explain why IL-2 and IL-10 were both found elevated in the cytokine release assays. In further experiments, it might be worth to investigate if and how LMP2A induces IL-2 and IL-10 expression.

*How could K1 and K15 rescue BCR$^-$ B cells from apoptosis – suggestions from literature*

The experiments discussed above could not explain how K1 and K15 rescue BCR$^-$ B cells from apoptosis, but published data suggest several possible mechanisms.

BJAB cells that expressed a CD8-K1 chimera, in which the C-terminus of K1 replaces the cytoplasmic part of CD8, showed an increase in PI3K and Akt phosphorylation (Tomlinson & Damania, 2004). Phosphorylation of Akt was shown to correlate with its activation (Kohn *et al.*, 1996) leading to the induction of several signaling pathways responsible for cell survival (Calamito *et al.*, 2009). It was demonstrated that mature BCR$^-$ B cells can be rescued from apoptosis by activating the PI3K pathway, which might transduce the genuine tonic BCR signal (Srinivasan *et al.*, 2009). Accordingly, K1 could rescue BCR$^-$ B cells from apoptosis by activating the PI3K/Akt pathway similar to the BCR rescuing BCR$^-$ B cells from apoptosis.

It is also conceivable that K1 and K15 reach this goal by activating NF-κB, which is important for B cell survival (Guo *et al.*, 2004; de Oliveira *et al.*, 2010). K1 activates NF-κB-responsive promoter elements in BC3 cells, which were derived from PEL and are KSHV-positive but EBV-negative (Arvanitakis *et al.*, 1996; Samaniego *et al.*, 2001). Transgenic mice expressing K1 displayed an increased NF-κB activity in B cells, which was ITAM-dependent and mediated by Lyn (Prakash *et al.*, 2002; Prakash *et al.*, 2005). In contrast, transient transfection of K1 into HEK293T cells decreased active NF-κB factors (Konrad *et al.*, 2009). The contradicting results may stem from the different cellular systems employed. Less is known about K15, but reporter assays in HEK293T cells demonstrated that it also induces NF-κB probably mediated by TRAF binding (Brinkmann *et al.*, 2003). Even though K1 and K15 might rescue BCR$^-$ B cells from apoptosis by activating NF-κB, B cells that were infected with K1 and K15 EBV strains also express LMP1. LMP1 strongly activates NF-κB (de Oliveira *et al.*, 2010) but is insufficient to rescue BCR$^-$ B cells from apoptosis in the absence of LMP2A (Figure 5-18).

It is questionable if K1 and K15 add to LMP1 induced NF-κB activation and if an increase in NF-κB activation improves B cell survival.

K1 and K15 could also inhibit apoptosis by alternative ways. K1-expressing BJAB cells were less sensitive to Fas-mediated apoptosis than vector transfected cells, which can be explained by K1's ability to bind to the Fas receptor interfering with binding of pro-apoptotic Fas (Wang *et al.*, 2007; Berkova *et al.*, 2009). K15 was shown to inhibit apoptosis in HeLa cells via binding to Hax-1, an inhibitor of the pro-apoptotic protein Bax (Sharp *et al.*, 2002).

*Does KSHV infect BCR$^-$ B cells?*

PEL and HL cells commonly originate from GC B cells, which carry hypermutated Ig genes but do not express surface Ig, a situation incapable with survival in clonal B cells. 80-90% of PEL cells and 100% of Ig$^-$ HL cells are EBV$^+$ coding for the BCR mimic LMP2A (Arguello *et al.*, 2003; Kuppers, 2009). However, there are reports of KSHV$^+$ PEL cases that are EBV$^-$ and BCR$^-$ (Ig κ$^-$ and Ig λ$^-$) (Said *et al.*, 1996; Carbone *et al.*, 1998) raising the question whether KSHV also codes for a BCR mimic.

Only recently, infection studies with primary cells from PBMCs or tonsils with KSHV have been performed. The infection rate of primary, non-stimulated B cells was very low, but chemical activated or tonsillar B cells (which contain a fraction of GC-activated B cells) showed a KSHV infection rate of 5-10% (Rappocciolo *et al.*, 2008; Hassman *et al.*, 2011; Myoung & Ganem, 2011). Hassman and colleagues infected tonsillar cell suspensions with KSHV and stained the cells with antibodies directed against the Ig λ and κ light chains two to three days post infection. Two third of the cells were λ$^+$ or κ$^+$ and one third λ$^-$ and κ$^-$. Since they did not find LANA transcripts in the λ$^-$ and κ$^-$ fraction as well as the κ$^+$ fraction, they concluded that KSHV exclusively infects λ$^+$ B cells (Hassman *et al.*, 2011). Myoung and colleagues observed an infection of tonsillar CD19$^+$ B cells and CD3$^+$ T cells with KSHV, but, unfortunately, did not determine expression levels of Ig λ$^-$ and κ$^-$ in the CD19$^+$ KSHV$^+$ fraction (Myoung & Ganem, 2011). Accordingly, there are no hints from infection studies with KSHV that show a susceptibility and survival of BCR$^-$ B cells upon KSHV infection. KSHV does not transform

$BCR^+$ B cells. Thus, it might be too optimistic to expect a rescue of $BCR^-$ B cells by KSHV *in vitro*.

*K1 and K15 do not block BCR signaling*

Several studies claimed that LMP2A blocks BCR signaling. Antibody-mediated BCR cross-linking induced $Ca^{2+}$-influx and protein phosphorylation in ΔLMP2A LCLs but not in wt LCLs (Fruehling & Longnecker, 1997; Dykstra *et al.*, 2001). Stephanie Medele from our group used phosphospecific flow cytometry to investigate whether LMP2A blocks BCR signaling. This method allows detection of phosphorylated signal mediators in single cells and is superior to conventional Western blot analysis. She could show that antibody-mediated BCR cross-linking increased the levels of e.g. phosphorylated Syk and PLCγ2 in wt LCLs, but she could not detect $Ca^{2+}$-influx in LMP2A expressing B cells (Medele, 2010). Studies using LCLs, which express the LMP2A:mCD69 chimeric protein, demonstrated that LMP2A can activate $Ca^{2+}$-signaling suggesting that LMP2A does not actively block BCR induced $Ca^{2+}$-influx. After depletion of the $Ca^{2+}$-stores, the cell needs a certain recovery time before it can react to a second BCR signal to raise cytosolic $Ca^{2+}$ concentrations. LMP2A is constitutively active, but the constantly triggered $Ca^{2+}$-influx might impede the recovery of the cell and, thereby, desensitizes the cells in regard to $Ca^{2+}$ signaling (Medele, 2010).

Clustering of the CD8-K1 chimera by α-CD8 antibody induced tyrosine phosphorylation and $Ca^{2+}$-influx in BJAB cells (Lee *et al.*, 1998). Antibody-mediated cross-linking of K1 in BJAB cells increases intracellular $Ca^{2+}$ levels as it was shown for LMP2A:mCD69 (Lee *et al.*, 2005) implying that K1 constitutively activates $Ca^{2+}$ signaling similar to LMP2A. BJAB cells, which transiently or stably expressed K15 or CD8-K15, showed a reduced $Ca^{2+}$-influx after antibody-mediated BCR cross-link (Choi *et al.*, 2000; Pietrek *et al.*, 2010) suggesting that K15 blocks BCR induced $Ca^{2+}$-signaling.

I compared the influence of LMP2A, K1, and K15 on BCR induced Syk and PLCγ2 phosphorylation as well as $Ca^{2+}$-influx. BCR cross-linking increased pSyk and pPLCγ2 levels in all tested cell lines but the negative control (Figure 5-23) indicating that LMP2A, K1, and K15 did not block BCR-induced protein-phosphorylation. The $Ca^{2+}$-

influx was impaired in wt EBV LCLs but not in ΔLMP2A, K1, and K15 EBV LCLs, demonstrating that LMP2A but not K1 and K15 block BCR-induced $Ca^{2+}$-signaling.

*Outlook*

My data demonstrated that the KSHV proteins K1 and K15 can partially replace the function of LMP2A and rescue $BCR^-$ B cells from apoptosis. Because basic Syk posphorylation levels of B cells infected with wt, ΔLMP2A, K1, or K15 EBV strains were similar, Syk might not be the key player in this process. Recently, it was published that mature $BCR^-$ B cells can be rescued from apoptosis via activated PI3K signaling (Srinivasan *et al.*, 2009). It is conceivable that LMP2A, K1, and/or K15 influence PI3K activity and, thereby, induce B cell survival. Accordingly, it should be tested if there is a difference in PI3K activity in B cells infected with ΔLMP2A EBV, K1 EBV, K15 EBV, and wt EBV.

Furthermore, a gene expression profile of primary B cells freshly infected with wt, ΔLMP2A, K1, and K15 EBV strains might provide an overview of genes differentially regulated by LMP2A, K1, and K15 in order to understand how K1 and K15 can rescue $BCR^-$ B cells from apoptosis.

# 7 Summary

Hodgkin-Reed Sternberg (HRS) cells are the genuine tumor cells of Hodgkin's lymphoma (HL). They are B cells by many criteria, but some do not express a BCR (Kuppers, 2009). BCR negative ($BCR^-$) B cells normally undergo apoptosis, but all $BCR^-$ HRS cells are infected with EBV, which encodes LMP2A. It is a constitutively active BCR mimic, provides the necessary survival signals *in vivo* (Caldwell *et al.*, 1998; Caldwell *et al.*, 2000; Merchant *et al.*, 2000), and recues $BCR^-$ B cells from apoptosis *in vitro* (Mancao *et al.*, 2005; Mancao & Hammerschmidt, 2007).

The aim of my project was to compare the effect of BCR and LMP2A signaling shortly after infection of primary B cells. Towards this end, I constructed mutant EBVs, in which the *LMP2A* gene was replaced by genes encoding either LMP2A:mCD69 or a NP-specific murine (m) IgM. The intention was to control the onset and strength of LMP2A and BCR signaling. The phenotype of primary B cells, infected with the conditional EBV mutants, was studied to reveal the contributions of LMP2A or BCR to cellular survival and proliferation control.

LMP2A:mCD69 EBV infected primary $BCR^-$ B cells proliferated and reconstituted the wt EBV phenotype when cultured on feeder cells and stimulated with $\alpha$-mCD69 antibodies indicating that an active LMP2A signal is necessary for the initial proliferation of $BCR^-$ B cells. In human B cells infected with the mutant EBV, NP-mIgM surface density was low. As a consequence, NP-antigen barely bound to surface mIgM, did not activate mIgM signaling, and NP-mIgM EBV-infected primary $BCR^-$ B cells did not proliferate when stimulated with $\alpha$-mIgM antibodies. As the NP-mIgM mutant EBV was not functional in my experiments, I could not compare its signaling to the LMP2A:mCD69 molecule.

Similar to EBV, KSHV can cause B cell lymphomas. The two KSHV proteins, K1 and K15, partially resemble LMP2A in structure and function (Damania, 2004; Brinkmann & Schulz, 2006), but it was not known whether they could rescue $BCR^-$ B cells from apoptosis like LMP2A. To address this question, I constructed two mutant EBV strains, which encode *K1* and *K15 in lieu* of *LMP2A*.

Infection of BCR$^-$ sorted B cells with K1 and K15 mutant EBV strains rescued them from apoptosis, but proliferation rates of K1 EBV and K15 EBV-infected B cells were lower than wt EBV-infected cells indicating that K1 and K15 can partially replace LMP2A's function. Double infection of BCR$^-$ B cells with both, K1 and K15 mutant EBV, suggested that the functions of K1 and K15 are similar and non-complementing. An influence of K1 and K15 on CD23, CD30, CD54, and CD86 B cell marker expression and cytokine induction was not apparent in primary B cells. Antibody-mediated BCR stimulation induced protein phosphorylation and calcium-signaling in the presence of K1 and K15 indicating that they do not block BCR signals as published previously (Lee *et al.*, 2000; Choi *et al.*, 2000; Pietrek *et al.*, 2010).

In my thesis, I could show that EBV and KSHV both encode proteins, which can rescue BCR$^-$ B cells from apoptosis, explaining how a subset of EBV- or KSHV-positive lymphoma B cells can survive without expressing a functional BCR.

# 8 Abbreviations

| | |
|---|---|
| Akt | serine/threonine protein kinase |
| AP-1 | activator protein 1 (transcription factor) |
| APC | antigen presenting cell |
| APS | ammonium persulfate |
| BAC | bacterial artificial chromosome |
| BCA | bathocuproin disulfonat |
| BCAP | B cell adaptor for PI3K |
| Bcl-2 | B cell lymphoma 2 protein |
| BCR | B cell receptor |
| BLNK | B cell linker protein |
| BSA | bovine serum albumin |
| Btk | Bruton's tyrosin kinase |
| $Ca^{2+}$ | calcium ion |
| CAG promoter | composite promoter explained in detail in section 5.2.1 |
| CaM | calmodulin |
| CD | cluster of differentiation |
| cDNA | complementary DNA |
| CFP | cyan fluorescent protein |
| Clk2 | CDC-like kinase 2 |
| CLP | common lymphoid progenitor |
| Cm | chloramphenicol |
| CMP | common myeloid progenitor |
| CMV | Cytomegalovirus |
| Cp | crossing point |
| CP | terminal carboxypeptidase |
| CRAC channel | calcium release-activated calcium channel |
| CsA | Ciclosporin A |
| CSR | class switch recombination |
| DAG | diacylglycerol |
| $ddH_2O$ | double-deionized water |
| DMSO | dimethyl sulfoxide |
| DNA | deoxyribonucleic acid |
| Dnmt1 | DNA methyltransferase 1 |
| DOC | deoxycholic acid |
| DOG | 2-deoxy-D-galactose |
| DTT | dithiothreitol |
| EBNA | EBV nuclear antigen |
| EBV | Epstein-Barr virus |
| ECL | enhanced chemiluminescence |
| *E. coli* | *Escherichia coli* |
| EDTA | ethylene diamine tetra-acetic acid |
| ER | endoplasmic reticulum |
| FACS | fluorescence-activated cell sorting |
| FITC | fluorescein isothiocyanate |
| FL | fluorescence channel |

| | |
|---|---|
| FR | family repeats |
| FRET | fluorescence resonance energy transfer |
| FSC | forward scatter |
| galK | galactokinase K |
| GFP | green fluorescent protein |
| GRU | green Raji unit |
| GTP | guanosine triphosphate |
| GC | germinal center |
| h | human |
| H or HC | heavy chain |
| HEK293 | human embryonic kidney cells |
| HIV | human immunodeficiency virus |
| HL | Hodgkin's lymphoma |
| HRP | horseradish peroxidase |
| HRS cells | Hodgkin's Reed-Sternberg cells |
| HSC | hematopoietic stem cells |
| Hyg | hygromycin |
| ICAM-1 | intercellular adhesion molecule 1 |
| inf. | infection |
| Ig | immunoglobulin |
| IL | interleukin |
| IM | infectious mononucleosis |
| $IP_3$ | inositol-trisphosphate |
| ITAM | immunoreceptor tyrosine-based activation motif |
| ITIM | immunoreceptor tyrosine-based inhibition motif |
| KSHV | Kaposi's sarcoma-associated herpes virus |
| L or LC | light chain |
| LANA | latency-associated nuclear antigen |
| LB | Luria broth |
| LCL | lymphoblastoid cell line |
| LFA | lymphocyte-function-associated antigen |
| LMP | latent membrane protein |
| LPS | lipopolysaccharide |
| m | murine |
| MAPK | mitogen-activated protein kinase |
| MCD | Multicentric Castleman's disease |
| miRNA | micro RNA |
| MOI | multiplicity of infection |
| NF-κB | nuclear factor-κB |
| MHC | major histocompatibility complex |
| NIP | 4-hydroxy-5iodo-3-nitrophenyl |
| NK cell | natural killer cell |
| NP | 4-hydroxy-3-nitrophenyl |
| OD | optical density |
| ORF | open reading frame |
| PAGE | polyacrylamide gel electrophoresis |
| PCR | polymerase chain reaction |
| PDK | phosphoinositide-dependent protein kinase |

| | |
|---|---|
| PE | phycoerythrin |
| PEI | polyethylene imine |
| PEL | Primary effusion lymphoma |
| p.i. | post infection |
| PI3K | phosphoinositide 3-kinase |
| $PIP_2$ | phosphatidylinositol 4,5-bisphosphate |
| $PIP_3$ | phosphatidylinositol (3,4,5)-trisphosphate |
| PKC | protein kinase C |
| PLCγ2 | phospholipase C γ2 |
| pPLCγ2 | phosphorylated phospholipase C γ2 |
| pSyk | phosphorylated spleen tyrosine kinase |
| PTLD | post transplant lymphoproliferative disorder |
| PTEN | phosphatase and tensin homolog |
| Ptk | protein-tyrosine kinase |
| QM mouse | quasi-monoclonal mouse |
| qRT-PCR | quantitative real-time PCR |
| RAG | recombination-activating genes |
| RNA | ribonucleic acid |
| SDS | sodium dodecyl sulfate |
| SH2 | SRC homology 2 |
| SLC | surrogate light chain |
| SHP-1 | protein tyrosine phosphatase-1 |
| SSC | sideward scatter |
| Syk | spleen tyrosine kinase |
| UV | ultra violet |
| TCR | T cell receptor |
| TEMED | tetramethylethylenediamine |
| TNF | tumor necrosis factor |
| TPA | tetradecanoylphorbol acetate |
| TR | terminal repeat |
| TRAF | tumor necrosis factor receptor-associated factor |
| v | viral |
| VEGF | vascular endothelial growth factor |
| v-FLIP | viral Fas-associated death-domain like IL-1 β-convertase enzyme inhibitory protein |
| v-IRF3 | viral interferon regulatory factor 3 |
| wt | wild type |
| YFP | yellow fluorescent protein |
| $^-$ | positive |
| $^+$ | negative |
| Δ | delta (deleted) |

<u>aminoacids</u>

| | |
|---|---|
| A | alanine |
| D | aspartic acid |
| E | glutamic acid |
| G | glycine |
| I | isoleucine |

| | |
|---|---|
| K | lysine |
| L | leucine |
| N | asparagine |
| P | proline |
| Q | glutamine |
| R | arginine |
| S | serine |
| T | threonine |
| V | valine |

<u>units</u>

| | |
|---|---|
| kDa | kilo Dalton |
| F | Farad |
| x g | g-force |
| h | hour |
| l | liter |
| min | minute |
| Ω | ohm |
| rpm | revolutions per minute |
| s | second |
| V | volt |
| °C | degree Celsius |

# 9 References

**Ali A K, Saito S, Shibata S, Takada K and Kanda T. 2009.** Distinctive effects of the Epstein-Barr virus family of repeats on viral latent gene promoter activity and B-lymphocyte transformation. *J Virol*, **83**:9163-9174.

**Altmann M and Hammerschmidt W. 2005.** Epstein-Barr virus provides a new paradigm: a requirement for the immediate inhibition of apoptosis. *PLoS Biol*, **3**:e404.

**Anderson D R, Atkinson P H and Grimes W J. 1985.** Major carbohydrate structures at five glycosylation sites on murine IgM determined by high resolution 1H-NMR spectroscopy. *Arch Biochem Biophys*, **243**:605-618.

**Anderson D R, Samaraweera P and Grimes W J. 1983.** Incomplete glycosylation of Asn 563 in mouse immunoglobulin M. *Biochem Biophys Res Commun*, **116**:771-776.

**Anderton E, Yee J, Smith P, Crook T, White R E and Allday M J. 2008.** Two Epstein-Barr virus (EBV) oncoproteins cooperate to repress expression of the proapoptotic tumour-suppressor Bim: clues to the pathogenesis of Burkitt's lymphoma. *Oncogene*, **27**:421-433.

**Arguello M, Sgarbanti M, Hernandez E, Mamane Y, Sharma S, Servant M, Lin R and Hiscott J. 2003.** Disruption of the B-cell specific transcriptional program in HHV-8 associated primary effusion lymphoma cell lines. *Oncogene*, **22**:964-973.

**Arnold J N, Wormald M R, Sim R B, Rudd P M and Dwek R A. 2007.** The impact of glycosylation on the biological function and structure of human immunoglobulins. *Annu Rev Immunol*, **25**:21-50.

**Arvanitakis L, Mesri E A, Nador R G, Said J W, Asch A S, Knowles D M and Cesarman E. 1996.** Establishment and characterization of a primary effusion (body cavity-based) lymphoma cell line (BC-3) harboring kaposi's sarcoma-associated herpesvirus (KSHV/HHV-8) in the absence of Epstein-Barr virus. *Blood*, **88**:2648-2654.

**Babcock G J, Decker L L, Volk M and Thorley-Lawson D A. 1998.** EBV persistence in memory B cells in vivo. *Immunity*, **9**:395-404.

**Baer R, Bankier A T, Biggin M D, Deininger P L, Farrell P J, Gibson T J, Hatfull G, Hudson G S, Satchwell S C, Seguin C and et al. 1984.** DNA sequence and expression of the B95-8 Epstein-Barr virus genome. *Nature*, **310**:207-211.

**Banaszynski L A, Chen L C, Maynard-Smith L A, Ooi A G and Wandless T J. 2006.** A rapid, reversible, and tunable method to regulate protein function in living cells using synthetic small molecules. *Cell*, **126**:995-1004.

**Banchereau J, de Paoli P, Valle A, Garcia E and Rousset F. 1991.** Long-term human B cell lines dependent on interleukin-4 and antibody to CD40. *Science*, **251**:70-72.

**Batten M, Groom J, Cachero T G, Qian F, Schneider P, Tschopp J, Browning J L and Mackay F. 2000.** BAFF mediates survival of peripheral immature B lymphocytes. *J Exp Med*, **192**:1453-1466.

**Baup D, Moser M, Schurmans S and Leo O. 2009.** Developmental regulation of the composite CAG promoter activity in the murine T lymphocyte cell lineage. *Genesis*, **47**:799-804.

**Bechtel D, Kurth J, Unkel C and Kuppers R. 2005.** Transformation of BCR-deficient germinal-center B cells by EBV supports a major role of the virus in the pathogenesis of Hodgkin and posttransplantation lymphomas. *Blood*, **106**:4345-4350.

**Berkova Z, Wang S, Wise J F, Maeng H, Ji Y and Samaniego F. 2009.** Mechanism of Fas signaling regulation by human herpesvirus 8 K1 oncoprotein. *J Natl Cancer Inst*, **101**:399-411.

**Bird A G, McLachlan S M and Britton S. 1981.** Cyclosporin A promotes spontaneous outgrowth in vitro of Epstein-Barr virus-induced B-cell lines. *Nature*, **289**:300-301.

**Bradley J R and Pober J S. 2001.** Tumor necrosis factor receptor-associated factors (TRAFs). *Oncogene*, **20**:6482-6491.

**Brinkmann M M, Glenn M, Rainbow L, Kieser A, Henke-Gendo C and Schulz T F. 2003.** Activation of mitogen-activated protein kinase and NF-kappaB pathways by a Kaposi's sarcoma-associated herpesvirus K15 membrane protein. *J Virol*, **77**:9346-9358.

**Brinkmann M M, Pietrek M, Dittrich-Breiholz O, Kracht M and Schulz T F. 2007.** Modulation of host gene expression by the K15 protein of Kaposi's sarcoma-associated herpesvirus. *J Virol*, **81**:42-58.

**Brinkmann M M and Schulz T F. 2006.** Regulation of intracellular signalling by the terminal membrane proteins of members of the Gammaherpesvirinae. *J Gen Virol*, **87**:1047-1074.

**Britton S and Palacios R. 1982.** Cyclosporin A--usefulness, risks and mechanism of action. *Immunol Rev*, **65**:5-22.

**Bryant P and Ploegh H. 2004.** Class II MHC peptide loading by the professionals. *Curr Opin Immunol*, **16**:96-102.

**Calamito M, Juntilla M M, Thomas M, Northrup D L, Rathmell J, Birnbaum M J, Koretzky G and Allman D. 2009.** Akt1 and Akt2 promote peripheral B-cell maturation and survival. *Blood*, **115**:4043-4050.

**Caldwell R G, Brown R C and Longnecker R. 2000.** Epstein-Barr virus LMP2A-induced B-cell survival in two unique classes of EmuLMP2A transgenic mice. *J Virol*, **74**:1101-1113.

**Caldwell R G, Wilson J B, Anderson S J and Longnecker R. 1998.** Epstein-Barr virus LMP2A drives B cell development and survival in the absence of normal B cell receptor signals. *Immunity*, **9**:405-411.

**Calender A, Billaud M, Aubry J P, Banchereau J, Vuillaume M and Lenoir G M. 1987.** Epstein-Barr virus (EBV) induces expression of B-cell activation markers on in vitro infection of EBV-negative B-lymphoma cells. *Proc Natl Acad Sci U S A*, **84**:8060-8064.

**Cambier J C, Gauld S B, Merrell K T and Vilen B J. 2007.** B-cell anergy: from transgenic models to naturally occurring anergic B cells? *Nat Rev Immunol*, **7**:633-643.

**Cambier J C, Heusser C H and Julius M H. 1986.** Abortive activation of B lymphocytes by monoclonal anti-immunoglobulin antibodies. *J Immunol*, **136**:3140-3146.

**Cancro M P. 2009.** Signalling crosstalk in B cells: managing worth and need. *Nat Rev Immunol*, **9**:657-661.

**Carbone A, Cilia A M, Gloghini A, Capello D, Todesco M, Quattrone S, Volpe R and Gaidano G. 1998.** Establishment and characterization of EBV-positive and EBV-

negative primary effusion lymphoma cell lines harbouring human herpesvirus type-8. *Br J Haematol*, **102**:1081-1089.

**Cascalho M, Ma A, Lee S, Masat L and Wabl M**. **1996.** A quasi-monoclonal mouse. *Science*, **272**:1649-1652.

**Cascalho M, Wong J and Wabl M**. **1997.** VH gene replacement in hyperselected B cells of the quasimonoclonal mouse. *J Immunol*, **159**:5795-5801.

**Chaganti S, Bell A I, Pastor N B, Milner A E, Drayson M, Gordon J and Rickinson A B**. **2005.** Epstein-Barr virus infection in vitro can rescue germinal center B cells with inactivated immunoglobulin genes. *Blood*, **106**:4249-4252.

**Chandran B**. **2010.** Early events in Kaposi's sarcoma-associated herpesvirus infection of target cells. *J Virol*, **84**:2188-2199.

**Chandriani S and Ganem D**. **2010.** Array-based transcript profiling and limiting-dilution reverse transcription-PCR analysis identify additional latent genes in Kaposi's sarcoma-associated herpesvirus. *J Virol*, **84**:5565-5573.

**Cho N H, Choi Y K and Choi J K**. **2008.** Multi-transmembrane protein K15 of Kaposi's sarcoma-associated herpesvirus targets Lyn kinase in the membrane raft and induces NFAT/AP1 activities. *Exp Mol Med*, **40**:565-573.

**Choi J K, Lee B S, Shim S N, Li M and Jung J U**. **2000.** Identification of the novel K15 gene at the rightmost end of the Kaposi's sarcoma-associated herpesvirus genome. *J Virol*, **74**:436-446.

**Choi T, Huang M, Gorman C and Jaenisch R**. **1991.** A generic intron increases gene expression in transgenic mice. *Mol Cell Biol*, **11**:3070-3074.

**Christman J K**. **2002.** 5-Azacytidine and 5-aza-2'-deoxycytidine as inhibitors of DNA methylation: mechanistic studies and their implications for cancer therapy. *Oncogene*, **21**:5483-5495.

**Damania B**. **2004.** Oncogenic gamma-herpesviruses: comparison of viral proteins involved in tumorigenesis. *Nat Rev Microbiol*, **2**:656-668.

**de Felipe P, Luke G A, Hughes L E, Gani D, Halpin C and Ryan M D**. **2006.** E unum pluribus: multiple proteins from a self-processing polyprotein. *Trends Biotechnol*, **24**:68-75.

**de Oliveira D E, Ballon G and Cesarman E**. **2010.** NF-kappaB signaling modulation by EBV and KSHV. *Trends Microbiol*, **18**:248-257.

**Delecluse H J, Hilsendegen T, Pich D, Zeidler R and Hammerschmidt W**. **1998.** Propagation and recovery of intact, infectious Epstein-Barr virus from prokaryotic to human cells. *Proc Natl Acad Sci U S A*, **95**:8245-8250.

**Delgado P, Cubelos B, Calleja E, Martinez-Martin N, Cipres A, Merida I, Bellas C, Bustelo X R and Alarcon B**. **2009.** Essential function for the GTPase TC21 in homeostatic antigen receptor signaling. *Nat Immunol*, **10**:880-888.

**Dulis B H, Kloppel T M, Grey H M and Kubo R T**. **1982.** Regulation of catabolism of IgM heavy chains in a B lymphoma cell line. *J Biol Chem*, **257**:4369-4374.

**Dykstra M L, Longnecker R and Pierce S K**. **2001.** Epstein-Barr virus coopts lipid rafts to block the signaling and antigen transport functions of the BCR. *Immunity*, **14**:57-67.

**Eliopoulos A G, Gallagher N J, Blake S M, Dawson C W and Young L S**. **1999.** Activation of the p38 mitogen-activated protein kinase pathway by Epstein-Barr virus-encoded latent membrane protein 1 coregulates interleukin-6 and interleukin-8 production. *J Biol Chem*, **274**:16085-16096.

**Engels N, Wollscheid B and Wienands J**. **2001.** Association of SLP-65/BLNK with the B cell antigen receptor through a non-ITAM tyrosine of Ig-alpha. *Eur J Immunol*, **31**:2126-2134.

**Fang J, Qian J J, Yi S, Harding T C, Tu G H, VanRoey M and Jooss K**. **2005.** Stable antibody expression at therapeutic levels using the 2A peptide. *Nat Biotechnol*, **23**:584-590.

**Fang J, Yi S, Simmons A, Tu G H, Nguyen M, Harding T C, VanRoey M and Jooss K**. **2007.** An antibody delivery system for regulated expression of therapeutic levels of monoclonal antibodies in vivo. *Mol Ther*, **15**:1153-1159.

**Feske S**. **2007.** Calcium signalling in lymphocyte activation and disease. *Nat Rev Immunol*, **7**:690-702.

**Fruehling S and Longnecker R**. **1997.** The immunoreceptor tyrosine-based activation motif of Epstein-Barr virus LMP2A is essential for blocking BCR-mediated signal transduction. *Virology*, **235**:241-251.

**Fruehling S, Swart R, Dolwick K M, Kremmer E and Longnecker R**. **1998.** Tyrosine 112 of latent membrane protein 2A is essential for protein tyrosine kinase loading and regulation of Epstein-Barr virus latency. *J Virol*, **72**:7796-7806.

**Gillies S D, Morrison S L, Oi V T and Tonegawa S**. **1983.** A tissue-specific transcription enhancer element is located in the major intron of a rearranged immunoglobulin heavy chain gene. *Cell*, **33**:717-728.

**Glenn M, Rainbow L, Aurade F, Davison A and Schulz T F**. **1999.** Identification of a spliced gene from Kaposi's sarcoma-associated herpesvirus encoding a protein with similarities to latent membrane proteins 1 and 2A of Epstein-Barr virus. *J Virol*, **73**:6953-6963.

**Graham F L, Smiley J, Russell W C and Nairn R**. **1977.** Characteristics of a human cell line transformed by DNA from human adenovirus type 5. *J Gen Virol*, **36**:59-74.

**Grossmann C, Podgrabinska S, Skobe M and Ganem D**. **2006.** Activation of NF-kappaB by the latent vFLIP gene of Kaposi's sarcoma-associated herpesvirus is required for the spindle shape of virus-infected endothelial cells and contributes to their proinflammatory phenotype. *J Virol*, **80**:7179-7185.

**Grupp S A, Mitchell R N, Schreiber K L, McKean D J and Abbas A K**. **1995.** Molecular mechanisms that control expression of the B lymphocyte antigen receptor complex. *J Exp Med*, **181**:161-168.

**Guo B, Su T T and Rawlings D J**. **2004.** Protein kinase C family functions in B-cell activation. *Curr Opin Immunol*, **16**:367-373.

**Hammerschmidt W**. **2011.** What keeps the power on in lymphomas? *Blood*, **117**:1777-1778.

**Hammerschmidt W and Sugden B**. **2004.** Epstein-Barr virus sustains Burkitt's lymphomas and Hodgkin's disease. *Trends Mol Med*, **10**:331-336.

**Harwood N E and Batista F D**. **2010.** Early events in B cell activation. *Annu Rev Immunol*, **28**:185-210.

**Hassman L M, Ellison T J and Kedes D H**. **2011.** KSHV infects a subset of human tonsillar B cells, driving proliferation and plasmablast differentiation. *J Clin Invest*, **121**:752-768.

**Haugwitz M, Nourzaie O, Gandlur S and Sagawa H**. **2008.** ProteoTuner: a novel system with rapid kinetics enables reversible control of protein levels in cells and organisms. *Biotechniques*, **44**:432-433.

**Hettich E, Janz A, Zeidler R, Pich D, Hellebrand E, Weissflog B, Moosmann A and Hammerschmidt W. 2006.** Genetic design of an optimized packaging cell line for gene vectors transducing human B cells. *Gene Ther*, **13**:844-856.

**Higuchi R, Fockler C, Dollinger G and Watson R. 1993.** Kinetic PCR analysis: real-time monitoring of DNA amplification reactions. *Biotechnology (N Y)*, **11**:1026-1030.

**Hislop A D, Taylor G S, Sauce D and Rickinson A B. 2007.** Cellular responses to viral infection in humans: lessons from Epstein-Barr virus. *Annu Rev Immunol*, **25**:587-617.

**Hogan P G, Lewis R S and Rao A. 2010.** Molecular basis of calcium signaling in lymphocytes: STIM and ORAI. *Annu Rev Immunol*, **28**:491-533.

**Hokazono Y, Adachi T, Wabl M, Tada N, Amagasa T and Tsubata T. 2003.** Inhibitory coreceptors activated by antigens but not by anti-Ig heavy chain antibodies install requirement of costimulation through CD40 for survival and proliferation of B cells. *J Immunol*, **171**:1835-1843.

**Hornef M W, Wagner H J, Kruse A and Kirchner H. 1995.** Cytokine production in a whole-blood assay after Epstein-Barr virus infection in vivo. *Clin Diagn Lab Immunol*, **2**:209-213.

**Ikeda M, Ikeda A, Longan L C and Longnecker R. 2000.** The Epstein-Barr virus latent membrane protein 2A PY motif recruits WW domain-containing ubiquitin-protein ligases. *Virology*, **268**:178-191.

**Itoh K and Hirohata S. 1995.** The role of IL-10 in human B cell activation, proliferation, and differentiation. *J Immunol*, **154**:4341-4350.

**Jackson S M, Harp N, Patel D, Wulf J, Spaeth E D, Dike U K, James J A and Capra J D. 2009.** Key developmental transitions in human germinal center B cells are revealed by differential CD45RB expression. *Blood*, **113**:3999-4007.

**Janeway C A, Travers P, Walport M and Shlomchik M J. 2001.** Immunobiology. *Garland science, New York*, **5th edition**.

**Jenner R G and Boshoff C. 2002.** The molecular pathology of Kaposi's sarcoma-associated herpesvirus. *Biochim Biophys Acta*, **1602**:1-22.

**Katzman R B and Longnecker R. 2004.** LMP2A does not require palmitoylation to localize to buoyant complexes or for function. *J Virol*, **78**:10878-10887.

**Keller S A, Schattner E J and Cesarman E. 2000.** Inhibition of NF-kappaB induces apoptosis of KSHV-infected primary effusion lymphoma cells. *Blood*, **96**:2537-2542.

**Kelly M E and Chan A C. 2000.** Regulation of B cell function by linker proteins. *Curr Opin Immunol*, **12**:267-275.

**Keyna U, Beck-Engeser G B, Jongstra J, Applequist S E and Jack H M. 1995.** Surrogate light chain-dependent selection of Ig heavy chain V regions. *J Immunol*, **155**:5536-5542.

**Kis L L, Takahara M, Nagy N, Klein G and Klein E. 2006.** IL-10 can induce the expression of EBV-encoded latent membrane protein-1 (LMP-1) in the absence of EBNA-2 in B lymphocytes and in Burkitt lymphoma- and NK lymphoma-derived cell lines. *Blood*, **107**:2928-2935.

**Kit S, Dubbs D R, Piekarski L J and Hsu T C. 1963.** Deletion of Thymidine Kinase Activity from L Cells Resistant to Bromodeoxyuridine. *Exp Cell Res*, **31**:297-312.

**Klein B, Tarte K, Jourdan M, Mathouk K, Moreaux J, Jourdan E, Legouffe E, De Vos J and Rossi J F. 2003.** Survival and proliferation factors of normal and malignant plasma cells. *Int J Hematol*, **78**:106-113.

**Klein S C, Kube D, Abts H, Diehl V and Tesch H**. **1996.** Promotion of IL8, IL10, TNF alpha and TNF beta production by EBV infection. *Leuk Res*, **20**:633-636.

**Kohn A D, Takeuchi F and Roth R A**. **1996.** Akt, a pleckstrin homology domain containing kinase, is activated primarily by phosphorylation. *J Biol Chem*, **271**:21920-21926.

**Konrad A, Wies E, Thurau M, Marquardt G, Naschberger E, Hentschel S, Jochmann R, Schulz T F, Erfle H, Brors B, Lausen B, Neipel F and Sturzl M**. **2009.** A systems biology approach to identify the combination effects of human herpesvirus 8 genes on NF-kappaB activation. *J Virol*, **83**:2563-2574.

**Krauer K G, Burgess A, Buck M, Flanagan J, Sculley T B and Gabrielli B**. **2004.** The EBNA-3 gene family proteins disrupt the G2/M checkpoint. *Oncogene*, **23**:1342-1353.

**Kraus M, Alimzhanov M B, Rajewsky N and Rajewsky K**. **2004.** Survival of resting mature B lymphocytes depends on BCR signaling via the Igalpha/beta heterodimer. *Cell*, **117**:787-800.

**Kulathu Y, Grothe G and Reth M**. **2009.** Autoinhibition and adapter function of Syk. *Immunol Rev*, **232**:286-299.

**Kuppers R**. **2009.** The biology of Hodgkin's lymphoma. *Nat Rev Cancer*, **9**:15-27.

**Kurosaki T**. **2011.** Regulation of BCR signaling. *Mol Immunol*, **48**:1287-1291.

**Kurosaki T, Shinohara H and Baba Y**. **2009.** B cell signaling and fate decision. *Annu Rev Immunol*, **28**:21-55.

**Lagunoff M, Majeti R, Weiss A and Ganem D**. **1999.** Deregulated signal transduction by the K1 gene product of Kaposi's sarcoma-associated herpesvirus. *Proc Natl Acad Sci U S A*, **96**:5704-5709.

**Lam K P, Kuhn R and Rajewsky K**. **1997.** In vivo ablation of surface immunoglobulin on mature B cells by inducible gene targeting results in rapid cell death. *Cell*, **90**:1073-1083.

**Lambert S L and Martinez O M**. **2007.** Latent membrane protein 1 of EBV activates phosphatidylinositol 3-kinase to induce production of IL-10. *J Immunol*, **179**:8225-8234.

**Lee B S, Alvarez X, Ishido S, Lackner A A and Jung J U**. **2000.** Inhibition of intracellular transport of B cell antigen receptor complexes by Kaposi's sarcoma-associated herpesvirus K1. *J Exp Med*, **192**:11-21.

**Lee B S, Connole M, Tang Z, Harris N L and Jung J U**. **2003.** Structural analysis of the Kaposi's sarcoma-associated herpesvirus K1 protein. *J Virol*, **77**:8072-8086.

**Lee B S, Lee S H, Feng P, Chang H, Cho N H and Jung J U**. **2005.** Characterization of the Kaposi's sarcoma-associated herpesvirus K1 signalosome. *J Virol*, **79**:12173-12184.

**Lee H, Guo J, Li M, Choi J K, DeMaria M, Rosenzweig M and Jung J U**. **1998.** Identification of an immunoreceptor tyrosine-based activation motif of K1 transforming protein of Kaposi's sarcoma-associated herpesvirus. *Mol Cell Biol*, **18**:5219-5228.

**Li M, Lee H, Yoon D W, Albrecht J C, Fleckenstein B, Neipel F and Jung J U**. **1997.** Kaposi's sarcoma-associated herpesvirus encodes a functional cyclin. *J Virol*, **71**:1984-1991.

**Lim C S, Seet B T, Ingham R J, Gish G, Matskova L, Winberg G, Ernberg I and Pawson T**. **2007.** The K15 protein of Kaposi's sarcoma-associated herpesvirus recruits

the endocytic regulator intersectin 2 through a selective SH3 domain interaction. *Biochemistry*, **46**:9874-9885.

**Ling P D, Peng R S, Nakajima A, Yu J H, Tan J, Moses S M, Yang W H, Zhao B, Kieff E, Bloch K D and Bloch D B. 2005.** Mediation of Epstein-Barr virus EBNA-LP transcriptional coactivation by Sp100. *EMBO J*, **24**:3565-3575.

**Liu Y J, Joshua D E, Williams G T, Smith C A, Gordon J and MacLennan I C. 1989.** Mechanism of antigen-driven selection in germinal centres. *Nature*, **342**:929-931.

**Longnecker R, Miller C L, Miao X Q, Marchini A and Kieff E. 1992.** The only domain which distinguishes Epstein-Barr virus latent membrane protein 2A (LMP2A) from LMP2B is dispensable for lymphocyte infection and growth transformation in vitro; LMP2A is therefore nonessential. *J Virol*, **66**:6461-6469.

**Longnecker R, Miller C L, Miao X Q, Tomkinson B and Kieff E. 1993.** The last seven transmembrane and carboxy-terminal cytoplasmic domains of Epstein-Barr virus latent membrane protein 2 (LMP2) are dispensable for lymphocyte infection and growth transformation in vitro. *J Virol*, **67**:2006-2013.

**Lu J, Verma S C, Cai Q and Robertson E S. 2011.** The Single RBP-J{kappa} Site within the LANA Promoter Is Crucial for Establishing Kaposi's Sarcoma-Associated Herpesvirus Latency during Primary Infection. *J Virol*, **85**:6148-6161.

**Mancao C, Altmann M, Jungnickel B and Hammerschmidt W. 2005.** Rescue of "crippled" germinal center B cells from apoptosis by Epstein-Barr virus. *Blood*, **106**:4339-4344.

**Mancao C and Hammerschmidt W. 2007.** Epstein-Barr virus latent membrane protein 2A is a B-cell receptor mimic and essential for B-cell survival. *Blood*, **110**:3715-3721.

**Manning B D and Cantley L C. 2007.** AKT/PKB signaling: navigating downstream. *Cell*, **129**:1261-1274.

**Matskova L, Ernberg I, Pawson T and Winberg G. 2001.** C-terminal domain of the Epstein-Barr virus LMP2A membrane protein contains a clustering signal. *J Virol*, **75**:10941-10949.

**McColl S R, Roberge C J, Larochelle B and Gosselin J. 1997.** EBV induces the production and release of IL-8 and macrophage inflammatory protein-1 alpha in human neutrophils. *J Immunol*, **159**:6164-6168.

**Medele S. 2010.** Das Latente Membranprotein 2A des Epstein-Barr Virus und der humane B-Zell-Rezeptor
- Ein Vergleich -. *PhD Thesis, LMU Munich*.

**Merchant M, Caldwell R G and Longnecker R. 2000.** The LMP2A ITAM is essential for providing B cells with development and survival signals in vivo. *J Virol*, **74**:9115-9124.

**Mesri E A, Cesarman E and Boshoff C. 2010.** Kaposi's sarcoma and its associated herpesvirus. *Nat Rev Cancer*, **10**:707-719.

**Miller G, Shope T, Lisco H, Stitt D and Lipman M. 1972.** Epstein-Barr virus: transformation, cytopathic changes, and viral antigens in squirrel monkey and marmoset leukocytes. *Proc Natl Acad Sci U S A*, **69**:383-387.

**Miyazaki J, Takaki S, Araki K, Tashiro F, Tominaga A, Takatsu K and Yamamura K. 1989.** Expression vector system based on the chicken beta-actin promoter directs efficient production of interleukin-5. *Gene*, **79**:269-277.

**Mocsai A, Ruland J and Tybulewicz V L. 2010.** The SYK tyrosine kinase: a crucial player in diverse biological functions. *Nat Rev Immunol*, **10**:387-402.

**Myoung J and Ganem D. 2011.** Infection of primary human tonsillar lymphoid cells by KSHV reveals frequent but abortive infection of T cells. *Virology*, **413**:1-11.

**Nagasawa T. 2006.** Microenvironmental niches in the bone marrow required for B-cell development. *Nat Rev Immunol*, **6**:107-116.

**Nakanishi K, Hirose S, Yoshimoto T, Ishizashi H, Hiroishi K, Tanaka T, Kono T, Miyasaka M, Taniguchi T and Higashino K. 1992.** Role and regulation of interleukin (IL)-2 receptor alpha and beta chains in IL-2-driven B-cell growth. *Proc Natl Acad Sci U S A*, **89**:3551-3555.

**Nakayama K. 1997.** Furin: a mammalian subtilisin/Kex2p-like endoprotease involved in processing of a wide variety of precursor proteins. *Biochem J*, **327 ( Pt 3)**:625-635.

**Neklesa T K, Tae H S, Schneekloth A R, Stulberg M J, Corson T W, Sundberg T B, Raina K, Holley S A and Crews C M. 2011.** Small-molecule hydrophobic tagging-induced degradation of HaloTag fusion proteins. *Nat Chem Biol*, **7**:538-543.

**Niedobitek G. 1996.** The role of Epstein-Barr virus in the pathogenesis of Hodgkin's disease. *Ann Oncol*, **7 Suppl 4**:11-17.

**Nitschke L and Tsubata T. 2004.** Molecular interactions regulate BCR signal inhibition by CD22 and CD72. *Trends Immunol*, **25**:543-550.

**Niwa H, Yamamura K and Miyazaki J. 1991.** Efficient selection for high-expression transfectants with a novel eukaryotic vector. *Gene*, **108**:193-199.

**Niwa M, Rose S D and Berget S M. 1990.** In vitro polyadenylation is stimulated by the presence of an upstream intron. *Genes Dev*, **4**:1552-1559.

**Park S J, Seo M D, Lee S K, Ikeda M, Longnecker R and Lee B J. 2005.** Expression and characterization of N-terminal domain of Epstein-Barr virus latent membrane protein 2A in Escherichia coli. *Protein Expr Purif*, **41**:9-17.

**Peltz G A, Trounstine M L and Moore K W. 1988.** Cloned and expressed human Fc receptor for IgG mediates anti-CD3-dependent lymphoproliferation. *J Immunol*, **141**:1891-1896.

**Peters A L, Stunz L L, Meyerholz D K, Mohan C and Bishop G A. 2010.** Latent membrane protein 1, the EBV-encoded oncogenic mimic of CD40, accelerates autoimmunity in B6.Sle1 mice. *J Immunol*, **185**:4053-4062.

**Pierce S K and Liu W. 2010.** The tipping points in the initiation of B cell signalling: how small changes make big differences. *Nat Rev Immunol*, **10**:767-777.

**Pietrek M, Brinkmann M M, Glowacka I, Enlund A, Havemeier A, Dittrich-Breiholz O, Kracht M, Lewitzky M, Saksela K, Feller S M and Schulz T F. 2010.** Role of the Kaposi's sarcoma-associated herpesvirus K15 SH3 binding site in inflammatory signaling and B-cell activation. *J Virol*, **84**:8231-8240.

**Pleiman C M, Chien N C and Cambier J C. 1994.** Point mutations define a mIgM transmembrane region motif that determines intersubunit signal transduction in the antigen receptor. *J Immunol*, **152**:2837-2844.

**Poole L J, Zong J C, Ciufo D M, Alcendor D J, Cannon J S, Ambinder R, Orenstein J M, Reitz M S and Hayward G S. 1999.** Comparison of genetic variability at multiple loci across the genomes of the major subtypes of Kaposi's sarcoma-associated herpesvirus reveals evidence for recombination and for two distinct types of open reading frame K15 alleles at the right-hand end. *J Virol*, **73**:6646-6660.

**Prakash O, Swamy O R, Peng X, Tang Z Y, Li L, Larson J E, Cohen J C, Gill J, Farr G, Wang S and Samaniego F. 2005.** Activation of Src kinase Lyn by the Kaposi

sarcoma-associated herpesvirus K1 protein: implications for lymphomagenesis. *Blood*, **105**:3987-3994.

**Prakash O, Tang Z Y, Peng X, Coleman R, Gill J, Farr G and Samaniego F. 2002.** Tumorigenesis and aberrant signaling in transgenic mice expressing the human herpesvirus-8 K1 gene. *J Natl Cancer Inst*, **94**:926-935.

**Pulvertaft J V. 1964.** Cytology of Burkitt's Tumour (African Lymphoma). *Lancet*, **1**:238-240.

**Rappocciolo G, Hensler H R, Jais M, Reinhart T A, Pegu A, Jenkins F J and Rinaldo C R. 2008.** Human herpesvirus 8 infects and replicates in primary cultures of activated B lymphocytes through DC-SIGN. *J Virol*, **82**:4793-4806.

**Reth M. 1989.** Antigen receptor tail clue. *Nature*, **338**:383-384.

**Reznik S E and Fricker L D. 2001.** Carboxypeptidases from A to z: implications in embryonic development and Wnt binding. *Cell Mol Life Sci*, **58**:1790-1804.

**Rivas C, Thlick A E, Parravicini C, Moore P S and Chang Y. 2001.** Kaposi's sarcoma-associated herpesvirus LANA2 is a B-cell-specific latent viral protein that inhibits p53. *J Virol*, **75**:429-438.

**Rovedo M and Longnecker R. 2007.** Epstein-barr virus latent membrane protein 2B (LMP2B) modulates LMP2A activity. *J Virol*, **81**:84-94.

**Ryan M D, King A M and Thomas G P. 1991.** Cleavage of foot-and-mouth disease virus polyprotein is mediated by residues located within a 19 amino acid sequence. *J Gen Virol*, **72 ( Pt 11)**:2727-2732.

**Said J W, Tasaka T, Takeuchi S, Asou H, de Vos S, Cesarman E, Knowles D M and Koeffler H P. 1996.** Primary effusion lymphoma in women: report of two cases of Kaposi's sarcoma herpes virus-associated effusion-based lymphoma in human immunodeficiency virus-negative women. *Blood*, **88**:3124-3128.

**Samaniego F, Pati S, Karp J E, Prakash O and Bose D. 2001.** Human herpesvirus 8 K1-associated nuclear factor-kappa B-dependent promoter activity: role in Kaposi's sarcoma inflammation? *J Natl Cancer Inst Monogr*:15-23.

**Samanta M and Takada K. 2010.** Modulation of innate immunity system by Epstein-Barr virus-encoded non-coding RNA and oncogenesis. *Cancer Sci*, **101**:29-35.

**Sanford K K, Earle W R and Likely G D. 1948.** The growth in vitro of single isolated tissue cells. *J Natl Cancer Inst*, **9**:229-246.

**Sharp T V, Wang H W, Koumi A, Hollyman D, Endo Y, Ye H, Du M Q and Boshoff C. 2002.** K15 protein of Kaposi's sarcoma-associated herpesvirus is latently expressed and binds to HAX-1, a protein with antiapoptotic function. *J Virol*, **76**:802-816.

**Shaw A C, Mitchell R N, Weaver Y K, Campos-Torres J, Abbas A K and Leder P. 1990.** Mutations of immunoglobulin transmembrane and cytoplasmic domains: effects on intracellular signaling and antigen presentation. *Cell*, **63**:381-392.

**Shulman M J, Heusser C, Filkin C and Kohler G. 1982.** Mutations affecting the structure and function of immunoglobulin M. *Mol Cell Biol*, **2**:1033-1043.

**Sibley C H and Wagner R A. 1981.** Glycosylation is not required for membrane localization or secretion of IgM in a mouse B cell lymphoma. *J Immunol*, **126**:1868-1873.

**Slobedman B, Barry P A, Spencer J V, Avdic S and Abendroth A. 2009.** Virus-encoded homologs of cellular interleukin-10 and their control of host immune function. *J Virol*, **83**:9618-9629.

**Speck P, Kline K A, Cheresh P and Longnecker R. 1999.** Epstein-Barr virus lacking latent membrane protein 2 immortalizes B cells with efficiency indistinguishable from that of wild-type virus. *J Gen Virol*, **80 ( Pt 8)**:2193-2203.

**Srinivasan L, Sasaki Y, Calado D P, Zhang B, Paik J H, DePinho R A, Kutok J L, Kearney J F, Otipoby K L and Rajewsky K. 2009.** PI3 kinase signals BCR-dependent mature B cell survival. *Cell*, **139**:573-586.

**Stein H, Mason D Y, Gerdes J, O'Connor N, Wainscoat J, Pallesen G, Gatter K, Falini B, Delsol G, Lemke H and et al. 1985.** The expression of the Hodgkin's disease associated antigen Ki-1 in reactive and neoplastic lymphoid tissue: evidence that Reed-Sternberg cells and histiocytic malignancies are derived from activated lymphoid cells. *Blood*, **66**:848-858.

**Stuart S G, Trounstine M L, Vaux D J, Koch T, Martens C L, Mellman I and Moore K W. 1987.** Isolation and expression of cDNA clones encoding a human receptor for IgG (Fc gamma RII). *J Exp Med*, **166**:1668-1684.

**Sugimoto M, Tahara H, Ide T and Furuichi Y. 2004.** Steps involved in immortalization and tumorigenesis in human B-lymphoblastoid cell lines transformed by Epstein-Barr virus. *Cancer Res*, **64**:3361-3364.

**Takada K. 1984.** Cross-linking of cell surface immunoglobulins induces Epstein-Barr virus in Burkitt lymphoma lines. *Int J Cancer*, **33**:27-32.

**Thorley-Lawson D A. 2001.** Epstein-Barr virus: exploiting the immune system. *Nat Rev Immunol*, **1**:75-82.

**Thorley-Lawson D A and Allday M J. 2008.** The curious case of the tumour virus: 50 years of Burkitt's lymphoma. *Nat Rev Microbiol*, **6**:913-924.

**Tolar P, Sohn H W and Pierce S K. 2005.** The initiation of antigen-induced B cell antigen receptor signaling viewed in living cells by fluorescence resonance energy transfer. *Nat Immunol*, **6**:1168-1176.

**Tolar P, Sohn H W and Pierce S K. 2008.** Viewing the antigen-induced initiation of B-cell activation in living cells. *Immunol Rev*, **221**:64-76.

**Tomlinson C C and Damania B. 2004.** The K1 protein of Kaposi's sarcoma-associated herpesvirus activates the Akt signaling pathway. *J Virol*, **78**:1918-1927.

**Tosato G, Tanner J, Jones K D, Revel M and Pike S E. 1990.** Identification of interleukin-6 as an autocrine growth factor for Epstein-Barr virus-immortalized B cells. *J Virol*, **64**:3033-3041.

**Tovey M G, Lenoir G and Begon-Lours J. 1978.** Activation of latent Epstein-Barr virus by antibody to human IgM. *Nature*, **276**:270-272.

**Treanor B, Depoil D, Gonzalez-Granja A, Barral P, Weber M, Dushek O, Bruckbauer A and Batista F D. 2010.** The membrane skeleton controls diffusion dynamics and signaling through the B cell receptor. *Immunity*, **32**:187-199.

**Tsurumi T, Fujita M and Kudoh A. 2005.** Latent and lytic Epstein-Barr virus replication strategies. *Rev Med Virol*, **15**:3-15.

**Uchihara J N, Matsuda T, Okudaira T, Ishikawa C, Masuda M, Horie R, Watanabe T, Ohta T, Takasu N and Mori N. 2006.** Transactivation of the ICAM-1 gene by CD30 in Hodgkin's lymphoma. *Int J Cancer*, **118**:1098-1107.

**Vancha A R, Govindaraju S, Parsa K V, Jasti M, Gonzalez-Garcia M and Ballestero R P. 2004.** Use of polyethyleneimine polymer in cell culture as attachment factor and lipofection enhancer. *BMC Biotechnol*, **4**:23.

**Vereide D T and Sugden B. 2011.** Lymphomas differ in their dependence on Epstein-Barr virus. *Blood*, **117**:1977-1985.

**Wang F, Gregory C D, Rowe M, Rickinson A B, Wang D, Birkenbach M, Kikutani H, Kishimoto T and Kieff E. 1987.** Epstein-Barr virus nuclear antigen 2 specifically induces expression of the B-cell activation antigen CD23. *Proc Natl Acad Sci U S A*, **84**:3452-3456.

**Wang F, Nakouzi A, Angeletti R H and Casadevall A. 2003.** Site-specific characterization of the N-linked oligosaccharides of a murine immunoglobulin M by high-performance liquid chromatography/electrospray mass spectrometry. *Anal Biochem*, **314**:266-280.

**Wang H, Grzywacz B, Sukovich D, McCullar V, Cao Q, Lee A B, Blazar B R, Cornfield D N, Miller J S and Verneris M R. 2007.** The unexpected effect of cyclosporin A on CD56+CD16- and CD56+CD16+ natural killer cell subpopulations. *Blood*, **110**:1530-1539.

**Wang S, Maeng H, Young D P, Prakash O, Fayad L E, Younes A and Samaniego F. 2007.** K1 protein of human herpesvirus 8 suppresses lymphoma cell Fas-mediated apoptosis. *Blood*, **109**:2174-2182.

**Warming S.** BAC Recombineering using the modified DH10B strain SW102 and a galK positive/counterselection cassette.

**Warming S, Costantino N, Court D L, Jenkins N A and Copeland N G. 2005.** Simple and highly efficient BAC recombineering using galK selection. *Nucleic Acids Res*, **33**:e36.

**Weber E L and Cannon P M. 2007.** Promoter choice for retroviral vectors: transcriptional strength versus trans-activation potential. *Hum Gene Ther*, **18**:849-860.

**Wen K W and Damania B. 2010.** Kaposi sarcoma-associated herpesvirus (KSHV): molecular biology and oncogenesis. *Cancer Lett*, **289**:140-150.

**Wies E, Hahn A S, Schmidt K, Viebahn C, Rohland N, Lux A, Schellhorn T, Holzer A, Jung J U and Neipel F. 2009.** The Kaposi's Sarcoma-associated Herpesvirus-encoded vIRF-3 Inhibits Cellular IRF-5. *J Biol Chem*, **284**:8525-8538.

**Wright A, Tao M H, Kabat E A and Morrison S L. 1991.** Antibody variable region glycosylation: position effects on antigen binding and carbohydrate structure. *EMBO J*, **10**:2717-2723.

**Wroblewski J M, Copple A, Batson L P, Landers C D and Yannelli J R. 2002.** Cell surface phenotyping and cytokine production of Epstein-Barr Virus (EBV)-transformed lymphoblastoid cell lines (LCLs). *J Immunol Methods*, **264**:19-28.

**Xu Z L, Mizuguchi H, Ishii-Watabe A, Uchida E, Mayumi T and Hayakawa T. 2001.** Optimization of transcriptional regulatory elements for constructing plasmid vectors. *Gene*, **272**:149-156.

**Yokoi T, Miyawaki T, Yachie A, Kato K, Kasahara Y and Taniguchi N. 1990.** Epstein-Barr virus-immortalized B cells produce IL-6 as an autocrine growth factor. *Immunology*, **70**:100-105.

**Young L S and Rickinson A B. 2004.** Epstein-Barr virus: 40 years on. *Nat Rev Cancer*, **4**:757-768.

**Zidovetzki R, Rost B and Pecht I. 1998.** Role of transmembrane domains in the functions of B- and T-cell receptors. *Immunol Lett*, **64**:97-107.

# 10 Acknowledgements

Ich möchte mich bei allen bedanken, die mich während meiner Doktorarbeit unterstützt haben. Dabei geht mein besonderer Dank an:

**Prof. Dr. Wolfgang Hammerschmidt** für die fachliche Unterstützung und das Vertrauen, daß auch eine schwierige Doktorarbeit gut zu Ende zu bringen ist.

**Prof. Dr. Dirk Eick** für die offizielle Betreuung meiner Doktorarbeit seitens der Universität und für die aufmunternden Worte im Thesis Committee.

**Prof. Dr. Hans-Martin Jäck** und **Edith Roth** der Universität Erlangen für die umfangreiche, fachliche Unterstützung des Immunglobulin-Projektes und die vielen wissenschaftlichen Diskussionen.

**Stephanie Medele** für ihre Motivation, zahlreiche persönliche und fachliche Diskussionen, die reibungslose Zusammenarbeit und den Spaß im Mädels-Labor.

Des weiteren danke ich **Christine Göbel** für die vielen persönlichen Gespräche und die Hilfe auf den letzten Metern, **Dagmar Pich** für das fachsimpeln und rumtüfteln am FACS Aria, meiner Arbeitsgruppe (**Markus K., Anne, Martin, Eri, Montse, Romana, Markus P**.) für die tolle Atmosphäre, die wissenschaftlichen Diskussionen im Kuschel-Seminar und die stete Hilfsbereitschaft.

Ich danke meiner **Familie** für ihre Unterstützung und besonders **Roland** … ohne dich hätte ich es nie so weit geschafft! Danke!